ABSTRACT

HOSSEINI GHASEMABADIAN, PAYAM . Transport of Organic Compounds through Piping Materials. (Under the direction of Dr. Mohammad Pour-Ghaz and Dr. Detlef Knappe).

Piping materials such as pipes and rubber gaskets are an integral component of water and wastewater conveyance system. They may be subject to contamination exposure during their service life especially when located in the areas with contaminated soil and/or groundwater. Depending on the type of contamination they are exposed to, a range of species can come in contact with the outer surface of pipe or gasket and penetrate such materials leading to long-term durability issues and contamination of water flowing through the pipe.

A large number of water contamination incidents reported in the US have been caused by gross spillage of gasoline or leakage from underground storage tanks in the gas stations or improper release of chlorinated solvents mainly used in dry cleaning operations resulting in the prevalence of petroleum-based products and chlorinated organic solvents in the contaminated areas.

In the first part of this work, rigid PVC (u-PVC) pipe was selected based on its higher resistance to aromatic and chlorinated hydrocarbons than other types of polymer-based pipe materials. Also, three types of gaskets i.e. chloroprene rubber (CR), nitrile rubber (NBR), and fluoroelastomer rubber (FKM) were chosen to study their degradation in the presence of benzene and tertrachloroethylene (PCE). Second part is concerned with the measurement and modeling of the diffusion of (liquid) benzene and PCE in saturated cement paste while the third part of the work is on the quantification of benzene and PCE vapors transport in unsaturated cement paste.

The results of the first part indicate that Williams-Landel-Ferry (WLF) method was successful in estimating the degradation of PVC pipe and rubber gaskets; a modification was made to consider the effect of contamination level of water with respect to benzene or PCE. It was also

shown that FKM performed the least mechanical properties degradation followed by NBR and CR gaskets. Also, severe swelling of CR once exposed to benzene demonstrates that volume stability of gasket materials is another important factor needs to be taken into account as it may cause water leakage due to the displacement at pipeline joints leading to further contamination of the water inside the pipe.

In the second part, the results reveal that the effective diffusivity (D_e) of VOCs in saturated cement paste decreases as water to cement ratio (w/c) decreases because of the reduced porosity and increased tortuosity of the pore network as well as increased ionic strength of the pore solution. Increasing the ionic strength of the pore solution lowers the solubility limit of VOCs in the pore solution and decreases the free diffusion coefficient of VOCs in the pore solution. Also, among the models employed to estimate D_e of benzene and PCE in saturated cement paste, modified Archie's model and phenomenological models can predict the effective diffusivity of VOCs with high accuracy.

Finally, the results of third part show that D_e of VOCs in unsaturated cement paste is significantly affected by the relative humidity (RH) of the environment the cement-based materials are exposed to; the effect of RH on reducing transport rate is larger than that of w/c ratio and VOCs size. In addition, the effect of VOCs' size on their effective diffusivity in unsaturated cement paste became more pronounced as RH drops. Also, by further modification of commonly used composite models (parallel and serial) based on a conceptual model of cement-based matrices, an alternative composite (AC) model was proposed to better predict the values of D_e of benzene and PCE in unsaturated cement paste samples as compared to the parallel and series models. The modified form of Archie's model for unsaturated porous media was shown to best predict D_e than other widely utilized empirical models.

© Copyright 2020 by Payam Hosseini Ghasemabadian

All Rights Reserved

Transport of Organic Compounds through Piping Materials

by
Payam Hosseini Ghasemabadian

A dissertation submitted to the Graduate Faculty of
North Carolina State University
in partial fulfillment of the
requirements for the Degree of
Doctor of Philosophy

Civil Engineering

Raleigh, North Carolina
2020

APPROVED BY:

_____	_____
Mohammad Pour-Ghaz Co-chair of Advisory Committee	Detlef Knappe Co-chair of Advisory Committee
_____	_____
Mohammed Gabr	Milad Abolhasani

DEDICATION

To my beloved parents and my exceptional sister. I could not have done this without your unwavering support.

BIOGRAPHY

Payam was born in Tehran, Iran on September 21, 1987. In 2010, he obtained his B.Sc. in Civil Engineering from Sharif University of Technology (SUT), Tehran, Iran. During his undergraduate studies at SUT, he actively participated in many research studies concerning advanced topics in the field of cement science such as developing low environmental impact supplementary cementitious materials, internal curing of concrete, recycled concretes, modification of cement-based matrices at nanoscale, and rheological properties of fresh cementitious binders, majority of which was supervised by Dr. Alireza Khaloo.

In 2013, he obtained his master's degree in Road and Pavement Engineering from SUT. During his master's studies, he investigated the effect of travel time of concrete mixers on the mechanical performance and durability of nano-modified concrete mixtures under the supervision of Dr. Manouchehr Vaziri. Right after his graduation, in 2013, he joined ASIHE university as a lecturer and the director of the Concrete Technology and Construction Materials Laboratories where he worked until June 2016. Thereafter, in 2016, he moved to the United Stated to pursue his Ph.D. studies at North Carolina State University (NC State) under the supervision of Dr. Mohammad Pour-Ghaz. His research at NC State, while co-advised by Dr. Detlef Knappe, mainly focused on the durability of piping materials including concrete and plastic pipes and rubber gaskets exposed to contaminated water with Volatile Organic Compounds (VOCs). During his Ph.D. work, he proposed a modified model for predicting the tensile strength degradation of PVC pipe and rubber gaskets located in areas contaminated with aromatic and chlorinated hydrocarbons (benzene and tetrachloroethylene, respectively). In addition, he quantified the diffusivity of such contaminants in cement-based matrices and proposed new models to predict the effective diffusivity of VOCs in saturated and unsaturated cementitious media.

ACKNOWLEDGMENTS

Firstly, I would like to thank my advisor Dr. Mohammad Pour-Ghaz for providing me with the opportunity to pursue my Ph.D. studies at NC State and his continuous support during this journey. It has been a great learning experience working with him during my research. I would also like to thank Dr. Detlef Knappe as my co-advisor for his guidance and invaluable help with my project. Furthermore, special gratitude is extended to the other members of my Ph.D. committee, Dr. Mohammed Gabr and Dr. Milad Abolhasani for their insightful advice, availability, and willingness to help. I would also like to thank Amie McElroy for her great contribution to my research.

I would like to express my appreciation to Dr. Gregory Lucier, Mr. Jerry Atkinson, and Mr. Johnathan McEntire at Constructed Facilities Laboratory (CFL) for their unfailing technical support and collaboration. I had really great time at CFL communicating with you gentlemen. Also, I am thankful for having many good friends at CFL, their collaboration, motivation, and the fun time we had together.

I would also like to express my deepest love and appreciation to my parents, Aliakbar Hosseini Ghasemabadian and Tayebeh Esmaeilpour, and my amazing sister and best friend, Pardis for their eternal love, encouragement, and whole-hearted support throughout all the years of my education. Last but not least, I am grateful for my friends here in the US or back home in Iran, Reza Rashetnia, Maryam Delavar Rafiee, Amir Dezfooliyan, Armita Mohammadian, Farid Alborzi, Atefeh Zamani, Hamed Mousavi, Danny Smyl,, Fransisco Jativa, Guillermo Gonzalez-Berrios, Sung Park, Hyunjun Choi, Amir Ghanbari, Farshad Saberi Movahed, Hadi Eshraghi, Madjid Delkash, San Bawi, Sam Brohaugh, Amirhossein Mazrooei, Kioumars Afshari, Zahra Faeli, Sultan Alhomair, Ashkan Nafisi, Arash Bozorgi, Hussam Abu Nimeh, Omar Khalaf Alla,

Hamid Jahanbakhsh, Alireza Farrokhi, Sanaz Pourfarzad, Farshid Adeli, Siavash Vahidi, Mohammad Hossein Hajikarimi, Mohammad Pourjafari, Mohammad Asadi, Abbas Booshehrian, Ali Asadabadi, Hossein Dormohammadi, Nima Gholizadeh, Reza Hosseinpourpia, Mahmoud Fakoorpoor, Pegah Ghasemi, Mojtaba Sardarmehni, and Mohammad Hossein Mobini, for their friendship and unstinting support.

TABLE OF CONTENTS

LIST OF TABLES

LIST OF FIGURES

Chapter 1

Introduction

1.1 Problem statement

Soil and groundwater can be contaminated by various sources among which contamination caused by operations in gas stations and dry cleaning facilities are frequently encountered in the water contamination incidents. Such contaminations cause release of aromatic and chlorinated hydrocarbons into the soil; which can later dissolve in the groundwater.

Since subsurface utilities including water, wastewater, and stormwater pipeline and drainage systems may be exposed to the contamination happening in the soil or groundwater, contaminants can reach pipeline and diffuse into the pipe and gasket materials. This brings about two major issues: environmental and structural. Diffusion of toxic chemicals through piping materials can contaminate the water being conveyed by the pipeline and may cause matrix degradation in polymeric pipes and rubber gaskets.

To date, no study has been dedicated to assessing the effect of contaminated water on degradation of polymeric pipes and rubber gaskets. Most of the research works have been focused on measuring the diffusion of penetrants into the piping materials. As such, this study addresses mechanical stability issue by quantifying the impact of two major water contaminants i.e. benzene and PCE on the tensile strength of PVC pipe and three types of rubber gaskets including chloroprene rubber (CR, neoprene), Acrylonitrile (nitrile) butadiene rubber (NBR), and fluoroelastomer rubber (FKM). Benzene and PCE are among the most toxic and prevalent species

in water contamination incidences in the US. Accelerated aging methodology was adopted to develop a model for predicting tensile strength degradation of each piping material at a temperature of interest selected as 20 ^{o}C in this work. Since the diffusion of organic compounds such as benzene and PCE can degrade the polymeric structure of PVC pipe, measuring the rate of thickness loss due to the penetration of such contaminants is of great importance. Thickness loss for polymeric pipes is defined as the depth of swollen layer in pipe wall assumed to reduce the load bearing capacity of pipe because the swollen section cannot bear any load due to its polymeric matrix degradation. To measure the thickness of swollen layer, visual methods by light microscopy are being used. To avoid such tests that requires high precision and careful sample preparation, a new simplistic model was introduced to predict the rate of swollen thickness loss utilizing the model developed for tensile strength degradation of PVC exposed to benzene or PCE.

Concrete pipes are commonly used in culverts and drainage and sewer systems. As stated above, concrete pipe may also encounter the pollution in its surroundings leading to the diffusion of contaminants such as benzene and PCE through the pipe wall and contamination of water inside. Since highly volatile contaminants like Volatile Organic Compounds (VOCs) are capable of diffusing into the piping materials in the forms of vapor and liquid, studying the diffusion mechanisms of such chemicals in concrete materials would enable us to estimate the effective diffusivity of VOCs (benzene and PCE herein) in concrete as a piping material.

When it comes to quantifying the transport of VOCs in cement-based materials, only commercial building materials such as concrete blocks at their dry state (equilibrated at very low RHs generally $\leq$ 40%) have been assessed in the previous literature. This implies that concrete blocks tested were at very low relative humidity and only VOCs vapor diffusion was examined. However, in case of concrete pipes, as they convey water and/or can be located near or under water

table, the relative humidity within the pipe wall would be higher than that the building materials are usually exposed to. Thus, due to a lack of a systematic and extensive research on this topic, an effort was made in this study to first measure the effective diffusivity of VOCs in the forms of vapor and liquid in saturated and unsaturated cement paste which is the most porous part of concrete materials. Furthermore, some widely used empirical models for porous media were adopted to estimate the effective diffusion coefficient of VOCs in saturated and unsaturated cement paste samples and they were further modified to better represent the VOCs transport in cement-based materials. The models would allow us to predict the effective diffusivity without performing the diffusion test which is an elaborate and time-consuming test especially in case of saturated cementitious materials. In addition to the empirical models, new models were introduced based on the results of parametric study carried out and composite theory utilizing pore structure characteristics of the cement-based materials.

1.2 Objectives and organization

The following are the objectives of the current study:

1. Developing a model to predict tensile strength degradation of PVC and rubber gaskets exposed to water contaminated with benzene or PCE. This objective is addressed in Chapter 2.
2. Quantifying the effective diffusivity of benzene and PCE in saturated and unsaturated cement paste. This objective is addressed in Chapters 3 and 4.
3. Modification of existing empirical models for saturated and unsaturated porous media to be applicable for VOCs diffusion case and developing new models which allow us to

account for the parameters affecting VOCs diffusion in cementitious media. This objective is addressed in Chapters 3 and 4.

This thesis is organized in five chapters. Chapter 1 is the introduction and motivation for this study. Chapter 2 discusses the objective 1. Objectives 2 and 3 are discussed in Chapters 3 and 4. Chapter 5 is the final chapter, presenting the summary and concluding remarks.

Chapter 2

A Degradation Model for the Tensile Strength of PVC and Rubber Gasket Materials Exposed to Benzene and PCE Saturated Aqueous Solutions

2.1 Abstract

In this study, a tensile strength degradation model is developed for PVC pipe and three rubber gasket materials commonly used in stormwater drains and wet utilities; the degradation model considers exposure to a single contaminant at its saturation level. The contaminant considered included benzene and tetrachloroethylene (PCE) due to their prevalence. The materials considered are unplasticized Polyvinyl chloride (u-PVC) utilized as the pipe material and three types of rubber gaskets: Polychloroprene (Neoprene-CR), Acrylonitrile (nitrile) butadiene rubber (Buna-N), and fluoroelastomer rubber (FKM - Grade A Viton^{TM}). First, the degradation rates of these materials are experimentally quantified using accelerated testing; then using the experimental results and Williams-Landel-Ferry (WLF) method a degradation model is developed. Finally, a simplified method is introduced to relate the tensile strength degradation of PVC to the penetration rate of the contaminants.

2.2 Introduction

On some transportation projects soil and groundwater contaminated with petroleum and solvents are encountered in the right of way. Potential sources of the contamination include underground storage tanks, dry cleaning facilities, old unlined landfills, or abandoned industrial and agricultural operations with practices leading to soil and/or groundwater contamination. In such instances, installation of subsurface utilities, such as drainage pipes, can be potentially problematic since the effects of the contaminations on the integrity and durability of the subsurface drainage pipes and gaskets is largely unknown. Specifically, with regards to plastic pipes and gaskets, their degradation rate is mainly a function of two variables: the type of contamination and the physicochemical properties of the gasket and pipe materials.

Among different types of contaminants, petroleum-based products and chlorinated organic solvents are the most common in the US [1-3]. The largest number of contamination incidents reported is related to contamination by petroleum-based products (about 89%), followed by TCE (Trichloroethene) and PCE (Tetrachloroethylene) from dry cleaning solvents (about 5%) [1, 2]. All these contaminants have detrimental effects on plastic pipes and rubber gaskets because of their fast diffusion and their ability to degrade the polymeric structure of the materials and cause chain succession, leading to structural and serviceability issues [4]. In the present study, benzene and PCE are chosen to represent the two classes of contaminants; they are also the most common contaminants from each group.

The majority of the polymeric (plastic) pipes utilized in the US water pipeline system consist of unplasticized or rigid polyvinyl chloride (u-PVC), polyethylene (PE), and polybutylene (PB) pipes [5]. Since in the presence of aromatic and chlorinated hydrocarbons PVC pipes perform better than other types of polymer-based piping materials such as PE and PB pipes [4, 5], they are

the most commonly used pipes in the US since 1970s [5, 6]. PVC is an amorphous thermoplastic with very limited flexibility of the polymer chains [4, 5] and as a result are generally thought to be essentially impermeable to environmental organic contaminants, although permeation through PVC pipes can be expected in heavily contaminated situations over long periods of exposure [7, 8]. Therefore, in the present study u-PVC materials are used.

According to previous studies [9], gasket materials are approximately 5 to 100 times more permeable to organic chemicals as compared to pipe materials. Therefore, considering permeability and degradation of gasket materials is of great importance. The commonly used gasket materials in distribution and drainage systems are ethylene propylene diene monomer (EPDM), chloroprene rubber (CR; neoprene), styrene-butadiene rubber (SBR), nitrile rubber (NBR), fluoroelastomer rubber (FKM), and isoprene (IR) [10]. A given type is selected depending on the contamination condition of the piping system installation site [10]. SBR and CR gaskets are typically used for water distribution pipes whereas NBR and FKM gaskets are used for pipes conveying hydrocarbons and petroleum products or when hydrocarbon-resistant gaskets are required for water distribution [10]. In the present study, therefore, Polychloroprene (Neoprene-CR), Acrylonitrile (nitrile) butadiene rubber (Buna-N), and fluoroelastomer rubber (FKM - Grade A Viton^{TM}) are chosen to assess their degradation in the presence of contaminants.

In addition to experimental testing using accelerated aging, the data from accelerated aging experiment are used for the development of a degradation model in terms of percentage reduction in the tensile strength of the materials.

2.3 Experimental methods

2.3.1 PVC pipe specimens

Dog-bone shaped specimens were prepared from a green PVC pressure pipe segment (Figure 2.1). All specimens were cut from an 8-inch diameter pipe conforming to ANSI/AWWA C900 with a dimension ratio (DR) of 18 (which is equivalent to the pressure class of 235 psi). Since the pipe wall thickness was 0.55", Type III ASTM D 638 specimens were cut from the pipe segment.

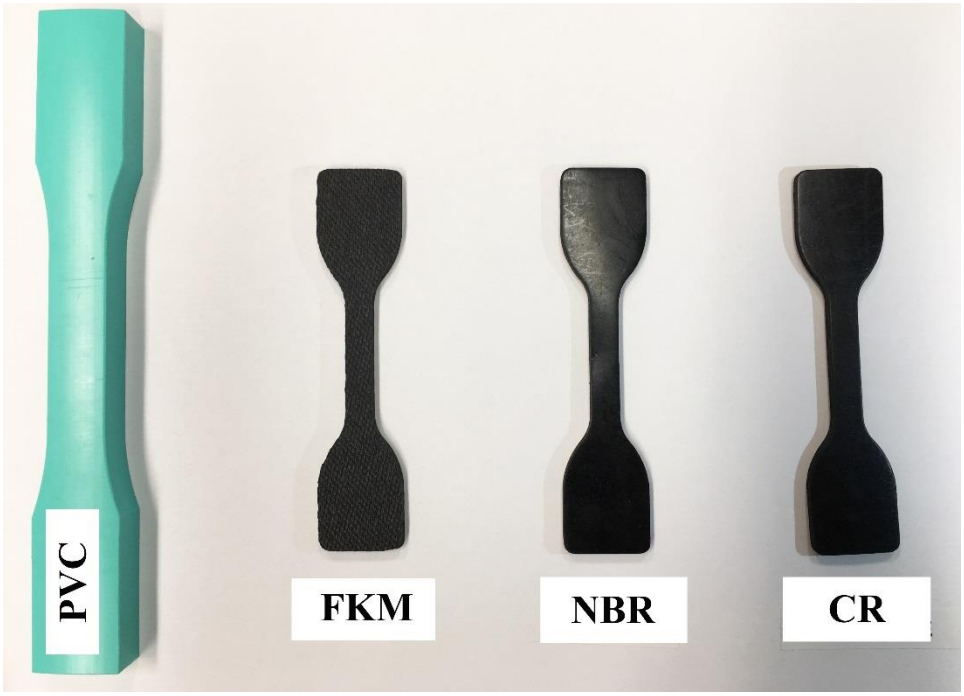

Figure 2.1 PVC and rubber gasket samples prepared for the experimental part.

2.3.2 Rubber gasket specimens

Rubber gasket specimens were cut from commercially available rubber sheets (i.e., CR, NBR, and FKM) using a press die with the dimensions specified for Type C dumbbell specimens per ASTM D 412 (Figure 2.1). The thickness of sheets was 0.125".

2.3.3 Accelerated aging

Accelerated aging was achieved by conditioning the specimens in saturated solution of contaminants (benzene or PCE) at elevated temperatures. Three different aging temperatures were considered; that is 68 ^{o}F (20 ^{o}C), 104 ^{o}F (40 ^{o}C), and 140 ^{o}F (60 ^{o}C). Since the glass transition of u-PVC and boiling temperature of benzene are approximately 176 ^{o}F (80 ^{o}C) [11, 12], the maximum aging temperature was set to 140 ^{o}F (60 ^{o}C) to avoid both structural change of PVC specimens due to elevated temperature and boiling of VOCs in the aqueous solutions. Both of these effects may impact the tensile strength degradation results. Moreover, the minimum temperature (reference temperature) was set to 68 ^{o}F (20 ^{o}C) as an average in-service temperature. The third aging temperature is the average of the minimum and maximum temperatures i.e., 104 ^{o}F (40 ^{o}C). Samples were placed in packer bottles and aged up to 7 months. Saturated aqueous solutions of benzene and PCE were prepared by adding 10-20 times more than the saturation level of corresponding chemical to maintain the saturation level during the aging. Bottles were monitored to check the availability of contaminants (benzene or PCE) every 14 days and more chemicals were added, if needed, to maintain the saturation level. To prepare the benzene- or PCE-saturated aqueous solutions, deionized water and analytical grade benzene or PCE were utilized to avoid contamination by other chemicals and substances. After preparing headspace-free bottles and sealing them using a commercially available chemical- and heat-resistant sealant, the bottles were then put in water tanks with controlled temperatures (104 ^{o}F and 140 ^{o}F) until the specified testing times. At each testing time, the samples were removed from the bottles and then placed in a laboratory oven set at 104 ^{o}F (40 ^{o}C) to dry. Depending on the sample type and aging duration, drying up to 48 hours was considered. Samples were considered “dry” when less than 0.1% change in their mass over an hour was measured. Mechanical properties of the aged and unaged PVC and

rubber gasket specimens were measured according to ASTM D 638 and ASTM D 412, respectively. The loading rate for all samples was set at 2 in/min (50 mm/min).

2.4 Degradation modeling

To develop degradation models, Arrhenius and Williams-Landel-Ferry (WLF) methods have widely been previously utilized [13]. The application of Arrhenius methodology requires first calculation of the degradation rate. As such, a unique relationship would be difficult to obtain to model the property change over time. WLF technique, on the other hand, can be adopted to achieve a specific relationship for the property loss/gain as a function of time. WLF model utilizes time-temperature superposition master curve where these are built by combining the results of mechanical test at specified ages and temperatures. The shift factor for each tensile strength degradation isotherm (at a temperature different from the reference temperature) is calculated and then used to convert the age of each data point of any specific isotherm to the equivalent age at the reference temperature. In other words, the age corresponding to each data point on any specific isotherm (t) is shifted to the equivalent age calculated through the multiplication of that age (t) by the shift factor obtained for the isotherm of interest ($t.a_T$). Finally, by successive shifts of isotherms, a master curve at the reference temperature is constructed. The WLF Equation 2.1 [13] is used to calculate the shift factor for each isotherm as follows:

$$\log(a_T) = \frac{c_1\,(T - T_o)}{c_2 + (T - T_o)} \tag{2.1}$$

where a_T is the shift factor of the curve of the measured tensile strength at each specific temperature (T) over time, T_o is reference temperature (taken as fixed at 68 ^oF in this study), and c_1 and c_2 are two coefficients dependent upon the material type.

All data measured at temperatures higher than reference temperature (T_o) over time, are shifted in time. The master curve at the reference temperature is then constructed by fitting a curve to all data including shifted (at temperatures other than reference) and reference temperature data. Using the obtained master curve, one can predict how long it will take to reach a specified strength loss (property degradation) limit which in turn can be translated into the service life of the material aging naturally under the exposure media. Figure 2.2 schematically illustrates WLF method using the actual data obtained in this study.

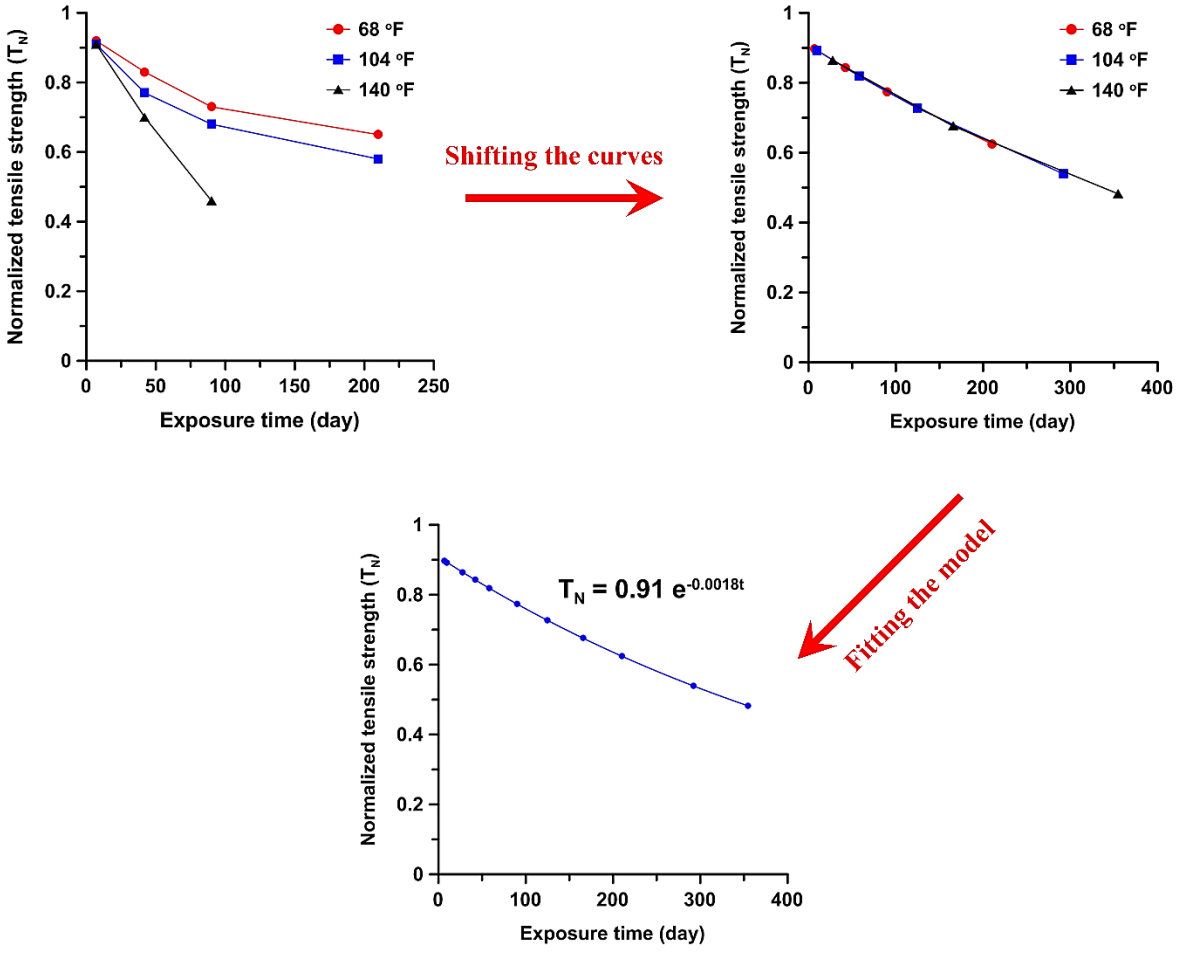

Figure 2.2 The process of obtaining the degradation models for the materials used in this study.

It should be noted that in developing the model, the tensile strength of samples for each material of interest was normalized with respect to its unaged (original unconditioned) tensile strength. This was done in order to negate the effect of unaged strength on the models and make the models' components e.g., degradation rates (i.e., b) comparable. The actual measurements are provided in Tables A1 to A4 (Appendix A). The normalized tensile strength (T_N) at each aging time and temperature was then used for modeling purposes. Moreover, to find the shift factors for each aging temperature, root-mean-square error or RSME function (Equation 2.2) was minimized to obtain the best fit.

$$RSME = \sqrt{\frac{\sum_{i=1}^{n}(P_i - T_N)^2}{n}} \tag{2.2}$$

where P_i is the predicted data based on the degradation function (exponential here) and shifted time, and *n* is the number of data collected for each specific material at all aging temperatures and durations.

2.5 Experimental results

Tables 2.1 to 2.4 present the results of tension test performed on PVC and rubber gasket materials before and after aging. As can be seen in Tables 2.1 to 2.3, overall benzene is more detrimental to plastic and rubber materials as compared to PCE since larger reductions of tensile strength in exposure to benzene is measured for all materials. Among rubber gasket samples, FKM performed the best in both exposure media i.e. benzene- and PCE-saturated aqueous solution

Based on Tables 2.1 to 2.3, after 30 weeks of exposure at 68 ^{o}F to PCE-saturated aqueous solution, the reduction in tensile strength of CR, NBR, and FKM are 35%, 29%, and 25%, respectively, whereas these materials experienced 50%, 47%, and 38% decrease when exposed to

benzene-saturated solutions after the same exposure period at 68 ^{o}F. Moreover, as presented in Table 2.4, tensile strength of PVC was degraded by about 13% and 26% after 30 weeks of exposure at 68 ^{o}F to PCE- and benzene-saturated aqueous solutions, respectively. In this respect, higher tensile strength reduction of rubber and plastic materials due to the exposure to benzene-saturated solution can be attributed to the higher penetration rate of benzene molecules than that of PCE since the swelling and therefore change in mechanical properties of these materials is caused by plasticizing effect of penetrants (Benzene and PCE) [4, 14]. This behavior of penetrants is related to their molecular size and weight as well as shape symmetry [15, 16]. Accordingly, in addition to being symmetrical, as benzene molecules are smaller and lighter than PCE ones [17], their penetration into the rubber and plastic materials would be faster than that of PCE, which makes them more aggressive to the polymeric structure. This issue was also experimentally observed for CR and NBR samples. As can be seen in Figure 2.3 depicting a photograph of CR after 13 weeks of exposure to benzene-saturated aqueous solution, the CR specimen experienced a severe swelling due to which the tension test could not be carried out on CR and NBR samples after 13 weeks at an elevated temperature of 140 ^{o}F. This large swelling can adversely affect gaskets' serviceability as it causes displacement at pipeline joints and therefore, leaks would be expected.

Table 2.1 Normalized tensile strength of aged CR gasket specimens.

Exposure media	Aging temperature (°F)	Aging duration (week)	Normalized tensile strength (%)
PCE-saturated aqueous solution	68	1	92 ± 5
		6	83 ± 6
		13	73 ± 5
		30	65 ± 8
	104	1	94 ± 0
		6	77 ± 7
		13	68 ± 1
		30	58 ± 5
	140	1	91 ± 1
		6	70 ± 3
		13	46 ± 4
		30	NA
Benzene-saturated aqueous solution	68	1	88 ± 1
		6	77 ± 3
		13	70 ± 5
		30	50 ± 3
	104	1	86 ± 1
		6	65 ± 4
		13	48 ± 2
		30	36 ± 8
	140	1	80 ± 4
		6	58 ± 4
		13	NA
		30	NA

Table 2.2 Normalized tensile strength of aged NBR gasket specimens.

Exposure media	Aging temperature (°F)	Aging duration (week)	Normalized tensile strength (%)
PCE-saturated aqueous solution	68	1	91 ± 8
		6	88 ± 6
		13	76 ± 0
		30	71 ± 4
	104	1	86 ± 2
		6	79 ± 6
		13	67 ± 2
		30	62 ± 4
	140	1	80 ± 7
		6	76 ± 1
		13	63 ± 3
		30	NA
Benzene-saturated aqueous solution	68	1	76 ± 1
		6	71 ± 5
		13	62 ± 1
		30	53 ± 4
	104	1	71 ± 5
		6	68 ± 5
		13	57 ± 3
		30	49 ± 1
	140	1	70 ± 4
		6	64 ± 0
		13	NA
		30	NA

Table 2.3 Normalized tensile strength of aged FKM gasket specimens.

Exposure media	Aging temperature (°F)	Aging duration (week)	Normalized tensile strength (%)
PCE-saturated aqueous solution	68	1	92 ± 6
		6	87 ± 6
		13	77 ± 3
		30	75 ± 3
	104	1	92 ± 6
		6	86 ± 2
		13	74 ± 3
		30	72 ± 4
	140	1	89 ± 7
		6	84 ± 6
		13	71 ± 2
		30	NA
Benzene-saturated aqueous solution	68	1	90 ± 5
		6	85 ± 7
		13	69 ± 2
		30	62 ± 4
	104	1	87 ± 2
		6	82 ± 2
		13	63 ± 6
		30	54 ± 3
	140	1	83 ± 6
		6	80 ± 2
		13	50 ± 4
		30	NA

Table 2.4 Normalized tensile strength of aged PVC specimens.

Exposure media	Aging temperature (°F)	Aging duration (week)	Normalized tensile strength (%)
PCE-saturated aqueous solution	68	1	96 ± 1
		6	96 ± 3
		13	93 ± 1
		30	87 ± 4
	104	1	95 ± 1
		6	92 ± 2
		13	90 ± 2
		30	83 ± 3
	140	1	95 ± 2
		6	90 ± 1
		13	88 ± 0
		25	78 ± 0
Benzene-saturated aqueous solution	68	1	96 ± 1
		6	92 ± 1
		13	90 ± 0
		30	74 ± 4
	104	1	93 ± 1
		6	90 ± 1
		13	74 ± 1
		30	21 ± 3
	140	1	92 ± 1
		6	87 ± 1
		13	39 ± 9
		30	NA

Figure 2.3 Severe swelling of CR sample after 13 weeks of exposure to benzene solution at 140 °F (Top: Unaged sample, Bottom: Swollen sample because of aging). Note: CR = chloroprene rubber.

2.6 Model development

In this section the models developed for tensile strength degradation of PVC and rubber gaskets due to the exposure to benzene and PCE are presented. Then, by utilizing the model obtained for PVC, a simplified method is proposed to estimate the penetration rate of contaminant of interest (i.e. benzene and PCE) into the PVC samples exposed to contaminated aqueous media at the saturation level.

2.6.1 Tensile strength degradation model

Following the process summarized above (Figure 2.2) a model is developed with the magnitude of the model coefficients being a function of the type of material and the exposure solution. The model coefficients are presented in Table 2.5, and these coefficients are used in the exponential function shown in Equation 2.3. Note that the exponential model was considered as it is the best fit model for the degradation of polymeric materials [13].

$$T_N = ae^{-bt} \tag{2.3}$$

where the T_N is the remaining tensile strength of material as a percentage of the initial tensile strength, a and b are coefficients reported in Table 2.5 and t (> 0) is time in days (@ 68 ^{o}F). Note that b determines the tensile strength degradation rate.

Table 2.5 Tensile strength degradation models for PVC pipe and rubber gasket materials exposed to contaminated water.

Material type	Exposure media	Model coefficients	
		a	b
CR	PCE-saturated	0.91	0.0018
	Benzene-saturated	0.86	0.0025
NBR	PCE-saturated	0.87	0.0010
	Benzene-saturated	0.73	0.0016
FKM	PCE-saturated	0.90	0.0010
	Benzene-saturated	0.89	0.0019
PVC	PCE-saturated	0.96	0.0003
	Benzene-saturated	1.00	0.0015

According to the model parameters presented in Table 2.5, it takes approximately 72 months for PVC to lose 50% of its strength while exposed to the saturated aqueous solution of PCE, whereas, it takes 16 months for 50% strength reduction when PVC is exposed to benzene solution. These data show the severity of loss of mechanical stability of PVC pipes when exposed to saturated aqueous environment.

Among the rubber gasket samples tested herein, and based on model parameters shown in Table 2.5, FKM performs the best followed by NBR and CR. The degradation rate of tensile strength of FKM is higher than that of NBR when exposed to saturated aqueous solution of benzene while FKM shows the same degradation rate as estimated under the of PCE exposure. However, the degradation rates of CR exposed to PCE- and benzene-saturated aqueous solutions are both higher than those of NBR and FKM.

It should be mentioned that the initial (i.e. unaged) tensile strength of FKM is higher than that of NBR which in turn leads to higher remaining strength of FKM than NBR even for long-term exposure to saturated PCE solution. Regarding this issue, to examine whether the unaged

tensile strength of gasket materials affects their rate of degradation, Spearman's correlation analysis was performed. Note that since the degradation rates and unaged tensile strengths data do not have normal distribution due to their limited number, a nonparametric correlation analysis i.e., Spearman's correlation was selected as there is no requirement of normality of the data. According to Table 2.6, as the p-value of correlation between unaged tensile strength and degradation rates in benzene and PCE is 0.667 and 0.333, respectively, such correlations are not significant at the 5% level which is a common significance level in engineering applications. Accordingly, there is no significant correlation between the unaged tensile strength and its degradation rates in different contaminated media evaluated in this study.

Table 2.6 Correlation matrix among unaged tensile strength and tensile strength degradation rates.

Variable		Unaged tensile strength	Degradation rate (in benzene)	Degradation rate (in PCE)
Unaged tensile strength	Correlation coefficient	1.000	-0.500	-0.866
	p-value	0.000	0.667	0.333
Degradation rate (in benzene)	Correlation coefficient	-0.500	1.000	0.866
	p-value	0.667	0.000	0.333
Degradation rate (in PCE)	Correlation coefficient	-0.866	0.866	1.000
	p-value	0.333	0.333	0.000

2.6.2 Proposed modification of the tensile strength degradation model for lower concentrations than the saturation level

The model developed here, Equation 2.3, is based on the saturated aqueous solutions of benzene and PCE (i.e., 1790 and 206 mg/L concentrations, respectively). However, these concentrations are seldom encountered in the field except in the close proximity to a nonaqueous phase liquid (NAPL) which might be caused by the gross spillage of pure chemicals [18]. In practice even 20%

saturation level of these chemicals is considered to be a high level of pollution in groundwater [18]. Therefore, the proposed models are conservative for the field applications and need to be modified to better represent field situations.

The strength (contaminant concentration) of aqueous solutions has a great influence on diffusion rates of solvents through plastics and rubbers [18]. The sorption rate decreases as the level of saturation of contaminant reduces. For instance, in the case of PVC exposure to benzene solutions, significant sorption could be observed for the 100 and 80% aqueous saturation levels whereas the percent weight gains for 60%, 40%, and 20% saturated aqueous solutions were below 2% after eight months of exposure [18]. In addition, sorption at the 20% saturated aqueous level was found to be statistically similar to that of the control experiment in deionized water [18].

In the case of rubber gasket materials, the gravimetric sorption of volatile organic compounds (VOCs) such as benzene or PCE can be estimated using linear, Freundlich, and Langmuir models [19, 20]. As the degradation of structure of polymers and elastomeric rubbers can be related to the absorption of penetrating chemicals and changes in the molecular structure of such materials, the drop in the tensile strength can be related to the penetrants' absorption extents [21, 22]. Since the absorption of chemicals is concentration-dependent according to the sorption isotherms [19, 22], the degradation of tensile strength of polymers and rubbers can then be assumed to be dependent on saturation level of the contaminant of interest.

Equation 2.4 introduces a modified model for the tensile strength degradation of the materials tested by applying a function (β) to the exponent of Equation 2.3 to account for the saturation level of exposure media. Note that β is applied to the exponent of tensile strength degradation models to avoid altering the assumed form of degradation models i.e. exponential

function yet showing a reduction in the extent of tensile strength degradation by decreasing the saturation level of the water contaminants.

Two different functions can be considered for (β): Linear and nonlinear. The linear function is simply the concentration of the contaminant over the saturation level. For example, in the case of exposure to benzene at a concentration of 179 mg/L, β = 179/1790 = 0.10. In the nonlinear approach the function β is calculated using Equation 2.5. The nonlinear approach is more conservative than the linear approach at low concentrations (less than 20%) which is the case for the majority of contaminated groundwater sites; at high concentration the value of β also rapidly approaches 1.0. It should be noted that Equation 2.5 is similar at low concentration to widely used models of sorption isotherms for polymers. Figure 2.4 shows both linear and nonlinear β functions ($0 < \beta \leq 1$).

$$T_N{}' = ae^{-b\beta t} \tag{2.4}$$

$$\beta = \text{Ln}\left(\frac{\frac{S}{100}}{1-\frac{S}{100}}\right) \tag{2.5}$$

where $T_N{}'$ is the modified normalized tensile strength and S is the saturation level of contaminant of interest in the aqueous exposure media in percent.

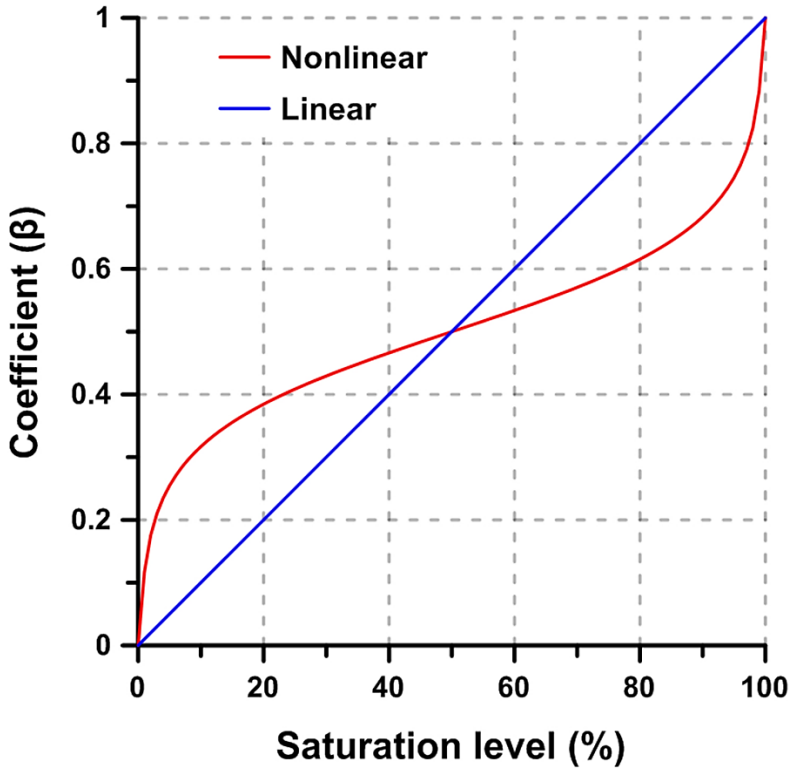

Figure 2.4 Conceptual models for the calculation of saturation dependence constant factor (β).

2.6.3 Contaminant penetration rate for PVC

The degradation of molecular structure of polymers due to the penetration of chemicals can be related to their loss of mechanical properties (e.g., tensile strength). As such, Mao et al. [23] proposed a microscopic visualization technique to estimate the penetration rates of organic solvents through PVC pipe samples. This method was applied to PVC as it was shown that the penetration of organic solvents into the PVC' structure can develop a moving front (case II diffusion) whose depth can be later measured by light microscopy over a specific exposure duration. The main reason for the presence of front is the change in the chemical structure of the polymer as the chemical penetrant reacts with the structure. Since PVC is an amorphous glassy polymer with very limited flexibility of the polymer chains, the sorption of organic compounds

such as benzene and PCE may cause swelling or plasticization reducing the polymer segmental relaxation times from very large (glassy behavior) to very short (rubbery behavior) and develops a sharp interface separating the inner glassy core from the outer rubbery layer which can later be visually detected through light microscopy [14, 23].

Assuming that the swollen layer cannot bear any load due the degradation of its polymeric structure, a simplified model is proposed to estimate the thickness of swollen layer based on the loss of tensile strength during the exposure. Afterwards, a relationship can be drawn between the thickness of swollen layer (i.e., penetration depth) and exposure time to calculate the penetration rate of contaminant of interest.

According to Mao et al. [22], the penetration depth or the thickness of swollen layer (L) can be obtained by Equation 2.6 as follows:

$$L = kt^n \tag{2.6}$$

where k is the penetration rate of the organic compounds, t is the time at which penetration depths are measured, and n is a constant value ranging from 0.5 to 1 depending on the ratio of the relaxation rate of the polymer to the diffusion rate of the organic penetrant [22-24]. In Fickian or Case I diffusion the rate of diffusion is much less than that of polymer relaxation [25]. Therefore, as we are dealing with dilute aqueous solutions of benzene and PCE in the current study, a value of 0.5 was chosen for n corresponding to Fickian diffusion. By plotting the penetration depth vs. square root of time a linear relationship would be obtained which gives the penetration depth as a constant value (k).

To calculate the penetration depth, the affected cross-sectional area of PVC due to the penetration of organic compounds can be schematically presented in Figure 2.5.

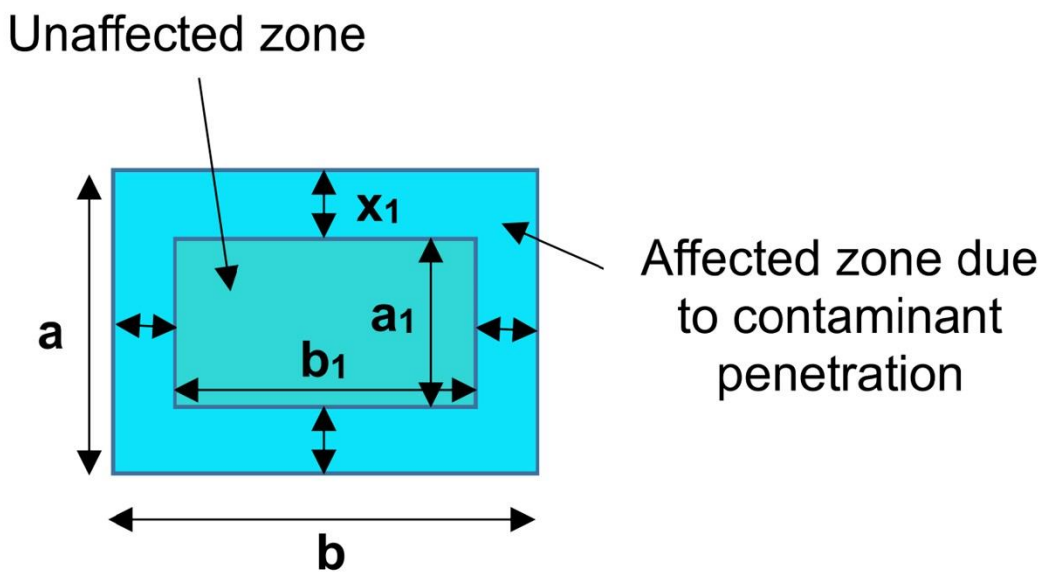

Figure 2.5 Conceptual model for the degradation of PVC sample at time t_1 of exposure.

According to Figure 2.5, for a rectangular cross section of PVC sample used in this study, the initial (time zero of exposure i.e. having unaged sample) intact cross-sectional area of the specimen can be obtained from Equation 2.7:

$$A_o = a \times b \tag{2.7}$$

Considering that the affected area cannot sustain any tensile load and the penetration (x_i) is uniform on each side of sample over the diffusion process, T_{N1} (normalized tensile strength at time t_1 of exposure) can be computed using Equation 2.8:

$$T_{N1} = \frac{A_1}{A_o} = \frac{a_1 \times b_1}{a \times b} = \frac{(a - 2x_1)(b - 2x_1)}{ab} \tag{2.8}$$

where A_1 is the intact area after the exposure time of t_1.

By rearranging the Equation 2.8 into Equation 2.9:

$$4{x_1}^2 - 2(a+b)x_1 + (1 - T_{N1})ab = 0 \quad (2.9)$$

Solving the quadratic equation (Equation 2.9) and finding its roots yields Equation 2.10:

$$x_1 = \frac{a + b \pm \sqrt{(a-b)^2 + 4abT_{N1}}}{4} \quad (2.10)$$

Only one of the roots of Equation 2.10 provides a reasonable result (another root is not physically permissible since it is close to the original dimension of the cross section). Now, by utilizing the model developed for tensile strength degradation of PVC exposed to saturated solution of benzene and PCE (i.e. calculating T_{Ni}), penetration depth (x_i) corresponding to that T_N can be attained. Finally, by plotting penetration depth (in) vs. square root of time (day) and fitting a linear regression line, the penetration rate of contaminant of interest would be calculated. The results of model fitting are shown in Figure 2.6 and the penetration rates of benzene and PCE for the case of benzene- and PCE-saturated aqueous solutions are presented in Table 2.7. In addition, the penetration rate of benzene calculated by Mao et al. [22] for the pure solvent as an exposure media is provided for comparison.

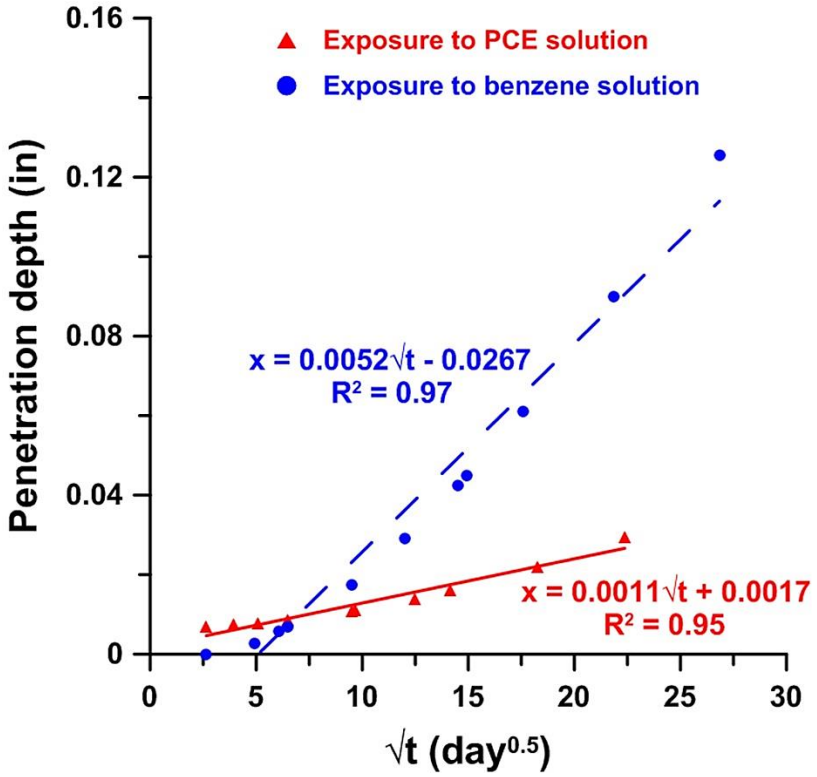

Figure 2.6 Linear regression models to calculate penetration rate of organic compounds.

Table 2.7 Penetration rates obtained based on the proposed conceptual model for PVC.

Penetrant type	Exposure medium	Penetration rate (in/day$^{0.5}$)
PCE	Saturated aqueous solution	0.0011
Benzene	Saturated aqueous solution	0.0052
Benzene	Pure solvent	0.0346 [22]

As shown in Table 2.7, the penetration rates of benzene through PVC pipe sample exposed to the saturated aqueous solutions of benzene is approximately five times higher than that of PCE. Also, the penetration of benzene when the exposure media is pure solvent is roughly seven times faster than such penetration while PVC is exposed to the saturated aqueous solution of benzene. This implies the severity of degradation of PVC pipe when a given spillage incident is very close to the pipe surface or there is no groundwater to dilute the organic compound. It should be noted

that this method cannot provide exact diffusion coefficient due to the multiple assumptions made to develop the model. It can however provide some measure of diffusion rate for comparison.

2.7 Concluding remarks

This paper proposes a methodology to model the tensile strength degradation of PVC and rubber gasket materials exposed to benzene and PCE saturated solutions. Also, the application of such models for predicting the penetration rates of benzene and PCE solutes was evaluated. The followings are summery and concluding remarks based on the results obtained in this study:

(i) The degradation of tensile strength of polymer (PVC) and elastomers (CR, NBR, FKM) was modeled using accelerated aging and WLF time-temperature superposition method.

(ii) PVC shows a good resistance against the penetration of benzene and PCE; based on the prediction of the model developed in this study, PVC takes 16 and 72 months to lose 50% of its initial tensile strength when exposed to benzene- and PCE-saturated solutions, respectively.

(iii) FKM was the most resistant rubber gasket followed by NBR and CR. However, as CR experiences a severe swelling after long-term exposure (or accelerated exposure at higher temperature), it may not be a viable option for use in pipeline system when there is a possibility of such chemical contamination.

(iv) The models developed in this study for predicting tensile strength loss of polymer and rubber used in this study provide estimates for contaminant-saturated solution and a modification was proposed to account for the effect of lower concentrations of contaminants.

(v) As demonstrated herein, the tensile strength test can be used as a rapid method to

estimate the rate of penetration of organic solvent into the polymers.

(vi) In the present paper, the gasket materials were not subjected to loading during the exposure. Laboratory simulation of simultaneous three-dimensional loading and exposure to contaminants is a rather challenging task. In the absence of such testing scheme, findings herein provide insight onto the degradation rate of gaskets. Further investigations regarding the effect of simultaneous loading and exposure to contaminants is warranted for future study.

Chapter 3

Diffusion of Benzene and Tetrachloroethylene through Saturated Cement Paste

3.1 Abstract

Diffusion of highly Volatile Organic Compounds (VOCs) through buried concrete elements, such as pipes and culverts, can occur if these elements come in contact with contaminated groundwater or soil. Among the various VOCs, benzene and tetrachloroethylene (PCE), found respectively in petroleum-based products and dry-cleaning solvents, are the most common contaminants. This paper aims at measuring the effective diffusion coefficients of benzene and PCE in cement paste with three different water to cement (w/c) ratios of 0.30, 0.40, and 0.60. The rates of VOCs diffusion in the forms of gas (i.e., vapor) and liquid (i.e., solubilized in water) were measured. The free diffusion coefficients of benzene and PCE in simulated pore solution were also measured and used for in empirical models.

The results show that VOCs diffusion coefficient decreases with the decrease of w/c because of reduced porosity and increased tortuosity of the pore network as well as increased ionic strength of the pore solution. The increased ionic strength of pore solution reduced the solubility limit of VOCs in the pore solution and decreased the free diffusion coefficient of VOCs in the pore solution. Work herein introduces models as well as the use of formation factor to estimate the VOCs diffusion coefficient through saturated cement paste. Among the empirical models and those proposed in this study, phenomenological models that include major factors affecting the diffusivity of VOCs in saturated cement-based materials provided the most accurate estimates.

3.2 Introduction

Concrete pipes are integral part of underground infrastructure and are used in storm water drains, sewer systems, and culverts because of their superior durability and mechanical performance at a relatively low cost [26]. Underground structures may be exposed to contaminated soil or groundwater. Among different types of contaminants, petroleum-based products (mostly result of leakage from underground storage tanks in fuel stations) and chlorinated organic solvents (commonly found in dry cleaners' locations) are the common in the US [1-3]. The vast majority of contamination incidents reported in the US is related to the contamination by petroleum-based products (about 89%), followed by trichloroethene (TCE) and tetrachloroethylene (PCE) from dry cleaning solvents (about 5%) [1, 2]. Transport of Volatile Organic Compounds (VOCs), such as benzene, TCE, and PCE that exist in petroleum-based products and chlorinated organic solvents through concrete is a major concern for owners and operators of underground infrastructure because of their well-documented health risks.

The transport of VOCs through concrete can occur through two main scenarios: (1) VOCs in gaseous form coming in contact with concrete, and (2) concrete coming in contact with groundwater containing dissolved VOCs. In the present work, we only consider saturated cement paste since underground concrete materials are commonly saturated because concrete pipes and other elements often carry water inside or are placed under water table (Figure 3.1). As such, VOCs need to diffuse through the pore liquid. We therefore refer to the first diffusion scenario as vapor-liquid diffusion and to the latter as liquid-liquid diffusion.

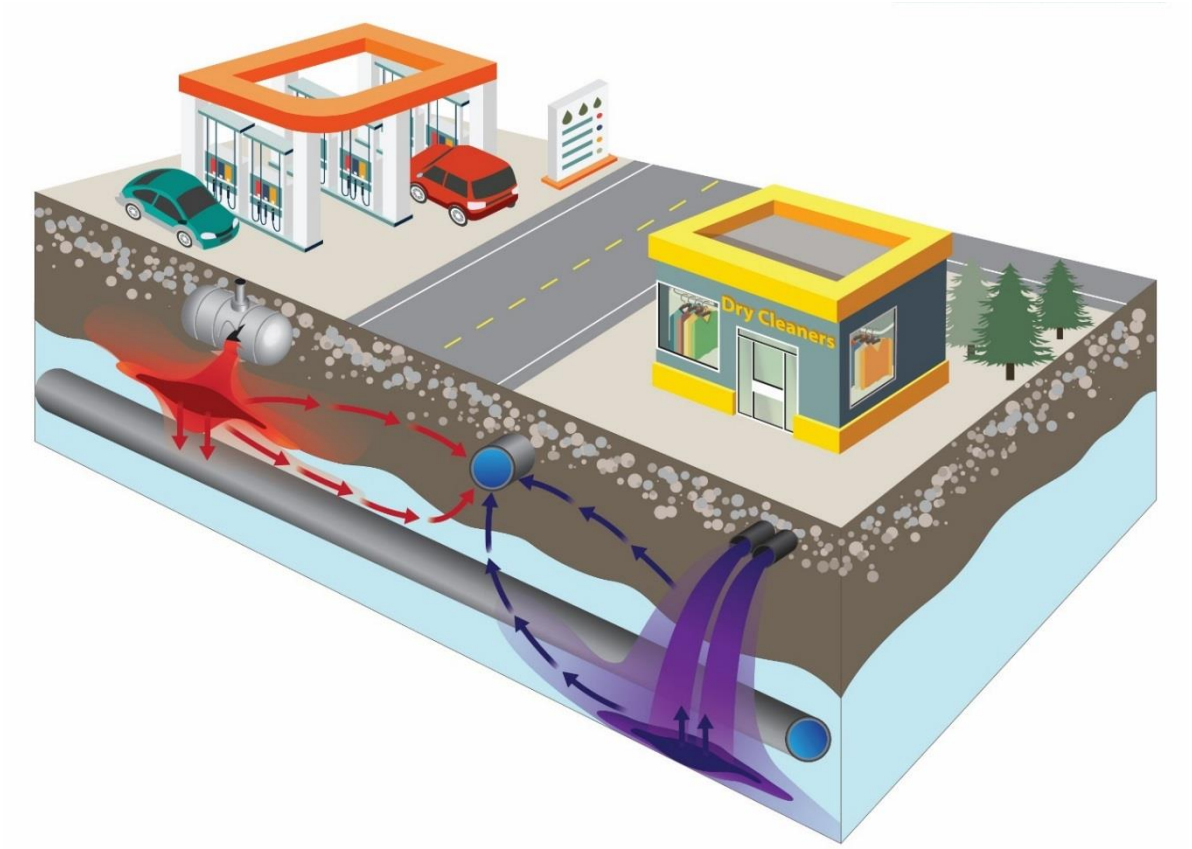

Figure 3.1 Water-solubilized liquid and vapor VOCs diffusion through saturated concrete pipe.

Very limited studies have measured the coefficient of VOCs diffusion through, broadly speaking, cement-based materials [27-30]. The majority of the existing literature are dedicated to the transport of VOCs in unsaturated or dry building materials such as ceiling tiles, anhydrite screed, gypsum board, solid (conventional) and aerated concrete with specialty formulation. According to the results reported in literature, the diffusion coefficient of octane was obtained as 1.04×10^{-7} m^2/s and 7.61×10^{-7} m^2/s for conventional and aerated concretes, respectively, at 45% RH and a temperature of 24 ^oC [27]. Moreover, the diffusion coefficient of ethyl acetate for these materials was measured as 0.51×10^{-7} m^2/s and 5.66×10^{-7} m^2/s, respectively [27]. There is no information was presented regarding the mixture design of the aforementioned cement-based

materials, as they were commercial products selected from the construction market. In Goreham and Lake study [30], the transport of two aromatic hydrocarbons (benzene and ethylbenzene) and one type of chlorinated hydrocarbon (trichloroethylene or TCE) through saturated cement-treated soil was measured. The cement-treated soil was a mixture of cement, water and soil with a cement content of 15% by mass of dry soil and three water to cement (w/c) ratios of 1.0, 1.5, and 2.0. In addition, the simultaneous diffusion of benzene, ethylbenzene, and TCE as well as the diffusion of TCE (alone) were measured. The diffusion coefficient of benzene, ethylbenzene, and TCE varied in a range of 2.25-3.00 $\times 10^{-10}$ m^2/s, 2.00-3.00 $\times 10^{-10}$ m^2/s, and 2.00-3.00 $\times 10^{-10}$ m^2/s, respectively, for various soil-cement samples. In addition, the diffusion coefficient of TCE when it was the sole contaminant was 21% and 33% higher in soil-cement samples with a w/c of 1.0 and 1.5, respectively, compared to its diffusion coefficient in a mixture of VOCs. The cement-based materials used in these reported studies are non-structural portland cement-based material that are used in construction of subsurface utilities and the measurement cannot be used to estimate the rate of diffusion of VOC's in structural concrete.

The main objective of the research herein is to quantify the transport of two types of VOCs (benzene and PCE) through saturated cement paste in the forms of vapor-liquid and liquid-liquid diffusion by measuring their effective diffusion coefficients. Also an attempt is made to calculate the effective diffusion coefficient of VOCs for cement pastes with various w/c ratios by using paste' pore structure parameters (porosity, tortuosity, and formation factor) and the coefficient of free (liquid) diffusion of VOCs in the simulated pore solutions. Measurements and models of the present work provide data and methods that can be used to estimate diffusivity of VOC's through saturated structural concrete.

3.3 Materials and Method

3.3.1 Specimen preparation

Cement paste mixtures with w/c of 0.30, 0.40, and 0.60 were made. Portland cement Type I/II conforming to ASTM C 150 and tap water were used for sample preparation. Cylindrical cement paste samples of 63.5 mm × 250 mm were made and seal-cured for two years to ensure a high degree of hydration and to minimize further change of pore structure during diffusion testing. Thermogravimetry test was performed at a rate of 10 ^{o}/min up to 1000 ^{o}C on cement paste samples (two replicates at each w/c) to quantify the degree of hydration (DOH) of cement particles at the age of two years per Equation 3.1.

$$DOH = \frac{w_b}{w_{b,\infty}} \times 100 \quad (3.1)$$

where w_b and $w_{b,\infty}$ are chemically bound water (g/g of ignited weight) at the age of interest and the ultimate chemically bound water corresponding to full hydration of cement particles regarded as 0.23 g per 1 g of cement, respectively [31].

DOH of cement pastes was measured as 81%, 92%, and 99% for w/c of 0.30, 0.40, and 0.60, respectively indicating that the samples are hydrated close to their theoretical limit based on Powers' model [32]. Therefore, minimal (if any) further changes in the microstructure is anticipated during the diffusion test.

To prepare cement paste samples for diffusion test, discs of 5 to 9 mm in thickness were cut from cylindrical samples and circumferentially coated with a hydrocarbon-resistant epoxy. Afterwards, cement paste discs were put in a sealed container to allow epoxy to be fully cured at room temperature of 22 ± 1 ^{o}C for a week before starting a diffusion test. Before the start of the

test, coated cement paste discs were vacuum saturated for 24 hours in deaired water to ensure all air pockets in the sample are removed.

3.3.2 Total permeable porosity

Total permeable porosity of cement pastes (φ) was measured according to the method by Bu et al. [33]. Vacuum saturation is used to saturate the cement paste samples, then the samples were dried in an electric oven set at 110 ± 5 ^{o}C for 24-48 h until achieving a weight change of less than 0.1%/h (m_{OD}). After drying, samples were placed in a desiccator filled with deaired water and saturated under vacuum for 4 h after which time the vacuum was turned off and the samples were kept in water for an additional time of 20 ± 2 h. Subsequently, the samples were removed from the desiccator and their surfaces were wiped with a saturated paper towels to render the samples at saturated surface dry (SSD) condition (m_{SSD}). Finally, the weight of the cement paste sample in water was measured and recorded (m_{SSB}). The volume ratio of total permeable porosity (φ) was determined using Equation 3.2. Three replicates were used, and the average result was reported for each cement paste mixture.

$$\varphi = \frac{m_{SSD} - m_{OD}}{m_{SSD} - m_{SSB}} \tag{3.2}$$

3.3.3 Simulated pore solution

Simulated pore solution for each w/c was prepared using the National Institute of Science and Technology model [34]. Input to the model include the samples' DOH (Table 3.1), their curing method (sealed herein), and the total alkalis content of the cement (Na_2O and K_2O as 0.35% and 0.77% by the mass of cement). NIST model only gives the composition of the ions dominating the

pore solution: Na^+, K^+, OH^-. To avoid leaching of calcium hydroxide from cement paste samples during liquid-liquid diffusion test, the calculated concentrations of Na^+, K^+, OH^- were added to saturated calcium hydroxide solution. The ionic compositions of the simulated pore solutions are shown in Table 3.1. These are utilized in diffusion tests to measure the effective and free diffusion coefficients of VOCs (D_e and D_o, respectively). To prepare the simulated pore solutions, ASTM type II water and reagent grade of NaOH, KOH, and $Ca(OH)_2$ were used.

Table 3.1 Ionic compositions and ionic strength of the simulated pore solutions used in the diffusion tests.

w/c	DOH (%)	Na^+ (M)	K^+ (M)	Ca^{2+} (M)	OH^- (M)	Ionic strength (M)
0.3	81	0.74	1.08	0.02	1.86	1.88
0.4	92	0.45	0.65	0.02	1.14	1.16
0.6	99	0.23	0.33	0.02	0.60	0.62

3.3.4 Diffusion measurements

A set of diffusion cells was designed and manufactured so that both vapor-liquid and liquid-liquid diffusions could be measured. Figure 3.2 shows the diffusion cell developed for this study.

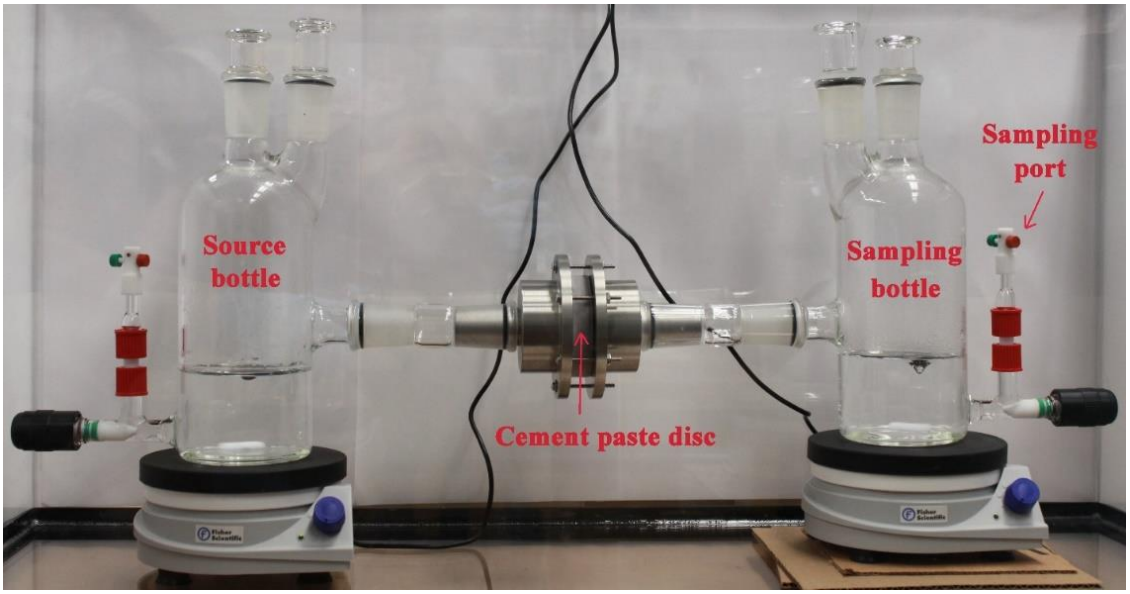

Figure 3.2 In-house diffusion cell for measuring VOCs transport through cement paste samples.

In this diffusion cell, the cement paste sample is sandwiched between two stainless steel plates which are then connected to the source and sampling bottles. The aqueous solution in the source bottle (upstream) is always kept at saturation by adding pure phase benzene or PCE in excess of their solubility limit.

In the vapor-liquid diffusion test, the liquid in the bottles do not come in contact with the sample. To avoid degradation of hydrocarbons by bacterial growth, both upstream and downstream (sampling) bottles consisted of acidified deionized distilled water (ASTM type II water) with maleic and ascorbic acids (5 and 0.625 g/L, respectively), following EPA method 524.3 [35].

In the liquid-liquid diffusion tests, both bottles were filled with the simulated pore solution since sample comes in contact the liquid. In this case acidification was not used since the high pH of the simulated pore solutions does not allow bacterial growth [36, 37].

Saturated VOC solutions used in diffusion tests were prepared by adding VOCs of interest in excess of solubility limit and water to a glass flask; the solutions were stirred with a magnetic

stirrer for two days to ensure complete dissolution. This was performed to avoid losing time at the start of the test and start the test with upstream at C_o (the saturation concentration of VOCs in each specific aqueous solution). During vapor-liquid diffusion process, VOCs already exit in the source solution would evaporate into the headspace in the bottle and then be partitioned between the air and the pore solution of the saturated sample in which the VOCs diffusion happens. In case of liquid-liquid diffusion, VOCs dissolved in the source bottle can directly diffuse the cement paste sample and reach the downstream bottle. To ensure that upstream was kept at saturation, additional VOCs was added to the upstream cell at the start of test and the amount of additional VOCs was continuously monitored. The diffusion cells were placed in a temperature-controlled chamber set at 25 ^{o}C to minimize the effect of temperature on the diffusion test results. Further details of VOCs vapor and liquid diffusion tests are provided in Appendix B.

At various exposure times, samples were taken from the downstream bottle to quantify the mass of diffused VOCs using the following procedure. Using Hamilton gastight® syringes, at each specified sampling time, two samples of 500 μL and 900 μL for benzene and PCE diffusion experiments, respectively, were taken from the downstream bottle and then diluted in a ratio of 1:42.7 with deionized distilled water (ASTM type II water) previously acidified with ascorbic and maleic acids (with the same concentrations used for acidifying the solutions in the bottles in the VOCs vapor diffusion test) for preserving the samples. Next, second dilution was performed using 300 μL and 1000 μL samples from the first diluted benzene and PCE vials, respectively, in a ratio of 1:42.7 with deionized distilled water. The samples were then kept in a refrigerator at a temperature of 4 ^{o}C until the measurement of the concentration of hydrocarbon of interest was performed using a Gas Chromatography–Mass Spectrometry (GC-MS). Finally, the diffused mass

of benzene or PCE through the cement paste samples were utilized to calculate the effective diffusion coefficient of VOCs.

3.3.5 VOCs solubility in the simulated pore solution

To measure the solubility of VOCs in the simulated pore solutions, 60-mL amber vials were first filled with the pore solutions simulated in the laboratory (PS1, PS2, and PS3) and then pure benzene and PCE were added to the vials at a volume of 1.0 mL and 0.5 mL, respectively. These volumes ensure that there is enough VOCs to saturate the pore solutions. All vials were headspace free and capped with a Teflon®-lined closure. The vials were kept in a chamber with controlled temperature (25 ^{o}C) for three days to allow VOCs to freely dissolve in the simulated pore solutions. Then, samples of 200 µL and 700 µL were taken from each vial (two replicates) for benzene and PCE, respectively, using Hamilton gastight® syringes and tested with GC-MS. In addition, the solubility of benzene and PCE in pure water was measured.

3.3.6 Diffusion coefficient estimation and modeling

3.3.6.1 Estimation of the effective diffusion coefficient

The measured concentrations in the sampling bottle over a period of 3-4 weeks were used to calculate the effective diffusion coefficient of cement paste samples using Fick's second law and assuming 1-D diffusion. A numerical scheme based on centered finite difference method with explicit formulations was developed in MATLAB to calculate the effective diffusion coefficients for vapor-liquid and liquid-liquid scenarios using Equation 3.3.

$$\varphi \frac{\partial C(x,t)}{\partial t} = D_e \frac{\partial^2 C(x,t)}{\partial x^2} \quad (3.3)$$

$C(x,0) = 0,\ 0 < x \leq L$ (Initial condition)
$C(0,t) = C_o, 0 \leq t$ (Boundary condition)

where C(x,t) is the concentration within the sample (mg/m^3) estimated by sampling from downstream solution; φ is the volume ratio of total permeable porosity; t is the sampling time (s); x is the distance within the sample in the diffusion direction (m); L is the sample thickness (m); D_e is the effective diffusion coefficient of VOCs in cementitious media (m^2/s), and C_o is the fixed concentration for benzene or PCE in the upstream which equals their solubility limit in the case of liquid-liquid diffusion or was obtained through Henry's law constant (HLC) for vapor-liquid diffusion using Equation 3.4:

$$H\ (dimensionless) = \frac{c_g}{c_a} \quad (3.4)$$

where H is the water-air partitioning coefficient for a dilute aqueous solution of hydrocarbon of interest, c_g and c_a are the concentrations of hydrocarbon in gas and aqueous phases, respectively. Since the concentrations of benzene and PCE are low at their solubility (case of dilute solution i.e., their concentrations are much below 10 g/L [38]), HLC is a good approximation to relate the concentrations of VOCs vapor in the source and sampling bottles to the concentrations of hydrocarbon of interest in the cement paste pore solution at both sides of the sample i.e., C_o at x = 0 and C at x = L (more details can be found in Appendix B).

For VOCs vapor to diffuse through saturated cement pastes, the vapor first needs to dissolve into the pore solution. Pore solution composition in cement-based materials depends on many factors such as the cement chemistry, w/c, and age. Hence, the solubility of VOCs in each specific pore solution differs and depends on the chemical composition of the pore solution. The

solubility of benzene and PCE in the pore solution of cement paste samples with various w/c ratios were experimentally measured (section 3.3.5).

In the calculation of the effective diffusion coefficient, the sorption of benzene and PCE by cement paste is assumed to be negligible since cement pastes contain negligible organic materials [39].

3.3.6.2 Free diffusion coefficient of VOCs in the simulated pore solution

The free diffusion coefficient of VOCs (D_o) in the cement paste pore solutions has not previously been reported in the literature; measurements were performed in this study using the diffusion cell and a perforated Teflon® disc of 3 mm in thickness (Figure 3.3). Teflon® was selected as the medium since no interaction between Teflon and benzene, and PCE or pore solution ions is anticipated. The values of D_o for various pore solutions corresponding to w/c of 0.30, 0.40, and 0.60 were measured; the same method that was used to measure the diffused mass of VOCs through cement paste samples (section 3.3.4). The diffusion coefficient of VOCs for Teflon® disc (D_T) was calculated using experimental measurement data. Afterwards, Equation 3.5 was used to compute D_o.

$$D_o = \frac{D_T}{\varphi} \tag{3.5}$$

where D_o is the coefficient of free diffusion of VOCs of interest, D_T is the effective diffusion coefficient for the Teflon® disc, and φ is the porosity of the Teflon® disc. Since the perforated pores in the Teflon® disc are non-tortuous (i.e., straight), $\tau = 1$. Equation 3.5 essentially represents models provided in section 3.3.6.3.1 with $\tau = 1$. The porosity of the Teflon discs (φ) equals 2.1%.

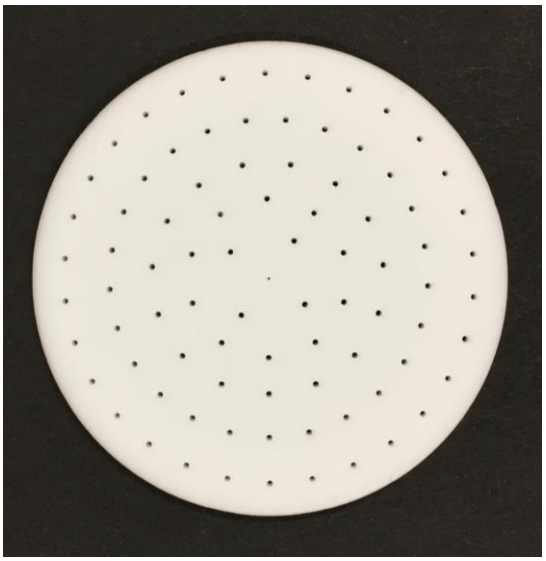

Figure 3.3 Perforated Teflon® disc with capillaries (800 μm in diameter) for measuring D_o.

3.3.6.3 Model-based estimation of the effective diffusivity

Performing measurements of VOC mass diffusion to estimate diffusivity is a time consuming and elaborated process. As such, introducing model-based methods to estimate the effective diffusivity of VOC through cement-based materials is of interest. In this section, a few empirical models, which have been previously developed by others [40-45], are used to calculate the effective diffusivity. In addition, models are introduced to better capture the effect of other factors on the diffusivity of VOCs in cement-based materials that are not included in the previously proposed models.

3.3.6.3.1 Models based on pore structure parameters

Previously, models have been developed that relate the effective diffusion coefficient of a diffusing species to their free diffusion coefficient (D_o) in an infinitely diluted aqueous solution; these models use pore structure parameters of the porous medium. Table 3.2 shows models commonly

used to evaluate the effect of the pore structure of porous media such as soil, rocks, and cement-based materials on the diffusion coefficient of diffusing species. In Table 3.2, the modified Archie's model (first row) requires the total permeable porosity, while other models utilize tortuosity as well. The models that use tortuosity differ only in the exponent of tortuosity term and therefore one approach is to consider this value as an unknown, n, to be calculated for the benzene and PCE diffusion cases, to be estimated using for example a best fit approach (modified tortuosity-based model).

Table 3.2 Empirical effective diffusivity models for cement paste using pore structure parameters and free diffusion coefficient in aqueous media (D_o).

Reference	Model	Pore structure parameter	Fitting parameter(s)
Archie [40] & Winsauer et al. [41] & Grathwohl [42]	$D_e = A\varphi^c D_o$	φ	A, c
Wyllie and Spangler [43]	$D_e = \frac{\varphi}{\tau^{0.5}} D_o$	φ & τ	-
Dogu and Smith [44]	$D_e = \frac{\varphi}{\tau} D_o$	φ & τ	-
Yang et al. [45]	$D_e = \frac{\varphi}{\tau^2} D_o$	φ & τ	-
Modified tortuosity-based model	$D_e = \frac{\varphi}{\tau^n} D_o$	φ & τ	n

φ: Volume ratio of total permeable porosity,
τ: Tortuosity
Do: Coefficient of free diffusion of VOCs in aqueous media

To use the models in Table 3.2, total permeable porosity, tortuosity, and free diffusion coefficient of VOCs in the simulated pore solutions need to be obtained. Procedures to quantify the former two (φ and D_o) are discussed in sections 3.3.2 and 3.3.6.2, respectively.

To calculate tortuosity (τ), electrical resistivity of cement paste samples and their pore solution were utilized according to Equation 3.6 [46, 47].

$$\rho_{cp} = \frac{\tau^2}{\varphi}\,\rho_o \tag{3.6}$$

where ρ_{cp} is the bulk resistivity of the cement paste (Ω.m), τ is the electrical-based tortuosity, and ρ_o is the resistivity of cement paste pore solution (Ω.m) which is theoretically estimated employing the NIST model [34]. Further details of calculating tortuosity based on the electrical method is provided in Appendix C.

3.3.6.3.2 Model based on Formation Factor (F) concept

Formation factor (F) is a microstructure-based parameter used to characterize the pore structure of a porous material and is dependent on pore size distribution, tortuosity and connectivity [40, 48, 49]. The factor F is quantified by the ratio of resistivity of a bulk material fully saturated with the pore fluid (ρ) and the resistivity of the pore fluid (ρ_o), per Equation 3.7 [40]:

$$F = \frac{\rho}{\rho_o} \tag{3.7}$$

According to the Nernst-Einstein relationship, F is equal to the ratio of the effective diffusivity of an ionic species through a porous medium (D_e) to the free diffusion coefficient of the ion of interest in the pore fluid (D_o) [50]. As a result, the effective diffusion coefficient for a porous matrix can be estimated by the calculation of F and the free diffusion coefficient of ionic species (D_o) in its pore fluid, Equation 3.8.

$$F = \frac{D_o}{D_e} \rightarrow D_e = \frac{D_o}{F} \tag{3.8}$$

Equation 3.8 was originally introduced for an ionic species; here we assess if this equation (FF model here after) can also be applicable to the case of nonpolar hydrocarbons such as benzene and PCE.

3.3.6.3.3 Phenomenological model

Effective diffusion coefficient (D_e) of VOCs in cement pastes is affected by the contributing factors. These factors are introduced to explain the VOCs diffusion process through cementitious materials (sections 3.4.3 and 3.4.4) and be able to predict the effective diffusivity (D_e) using parameters obtained through existing models such as NIST, literature, and some less elaborate experiments (e.g. measurements of DOH, porosity, and bulk electrical resistivity of cement-based samples). Models are proposed and introduced in section 3.4.5. The predicted values of D_e obtained using the new models are then compared with the experimental data.

3.4. Results and discussion

3.4.1 Pore structure parameters

Electrical resistivity of the cement pastes and their corresponding simulated pore solutions, and their total permeable porosity are presented in Table 3.3. Tortuosity values of cement paste matrices are calculated according to Equation C1 (Appendix C) and are shown in Table 3.4. The values of electrical resistivity, pore solution resistivity, and total permeable porosity from Table 3.3 are used herein.

The formation factor (F) for cement pastes with various w/c was calculated by inserting the values of bulk electrical resistivity of cement samples and the estimated resistivity of corresponding pore solutions (see Appendix C) into Equation 3.7. The results are shown in Table

3.4; in this case, and by decreasing w/c, the bulk electrical resistivity of cement paste increases and the resistivity of the pore solution decreases indicating that the pore structure becomes more tortuous and finer. As such, the formation factor increases with decreasing w/c.

Table 3.3 Electrical resistivity of the cement paste samples (ρ_{cp}) and the simulated pore solutions (ρ_o), and total permeable porosity.

w/c	ρ_{cp} (Ω.m)	ρ_o (Ω.m)	φ
0.30	58.63	0.032	0.246
0.40	30.64	0.048	0.323
0.60	21.41	0.085	0.417

Table 3.4 Pore structure parameters for the cement paste with various w/c ratios employed in this study.

w/c	τ	F[1] (-)
0.30	21.23	1832
0.40	14.36	638
0.60	10.25	252

[1] Calculated based on the resistivity of cement pastes and their simulated pore solution and employing Equation 3.7.

3.4.2 Solubility of benzene and PCE in the simulated pore solution

The measured solubility limit of VOCs in simulated pore solution with different ionic strength are shown in Figure 3.4. The solubility of benzene and PCE in pure water was measured as 1921 ± 144 mg/L and 222 ± 21. The average of measured values is within 7-8% of the solubility limits for benzene and PCE in pure water at 25 ^oC estimated using the US Environmental Protection Agency EPI Suite program (EPIWEB 4.1 shows 1790 mg/L and 206 mg/L, respectively.) The solubility limit of the hydrocarbons decreases as the ionic strength of the pore solution increases indicating that increasing salt concentration in aqueous solutions results in lowering the solubility of benzene and PCE due to the salting-out effect. Through such effect, the solubility of a nonelectrolyte (non-polar hydrocarbons such as benzene and PCE) in water is decreased when ions are added [51]. The

reduction in the solubility of PCE is more than that of benzene. For instance, at the highest ionic strength (1.88 M), the reduction in the benzene solubility is 70% while this value is 87% for PCE. The reason for this observation can be related to the larger size of PCE molecule as compared to that of benzene (kinetic diameter of 6.60 Å vs 5.85 Å). The salting-out effect is greater for solutes with a larger molecular size since they are more sensitive to the increase in cohesive energy in water caused by the salts consisting of small ions that enhance the structuring of aqueous phases [52].

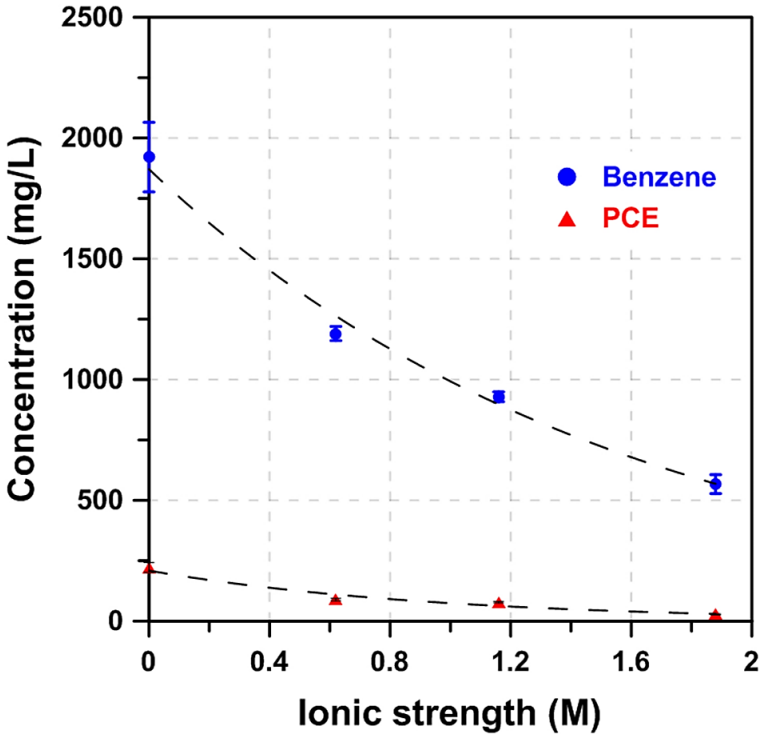

Figure 3.4 Effect of ionic strength of the cement pore solution on the solubility of benzene and PCE (The trendlines are added for visualization purposes).

3.4.3 Free diffusion coefficient (D_o)

The results of VOCs concentration measurements through the diffusion tests are provided in Figure 3.5.

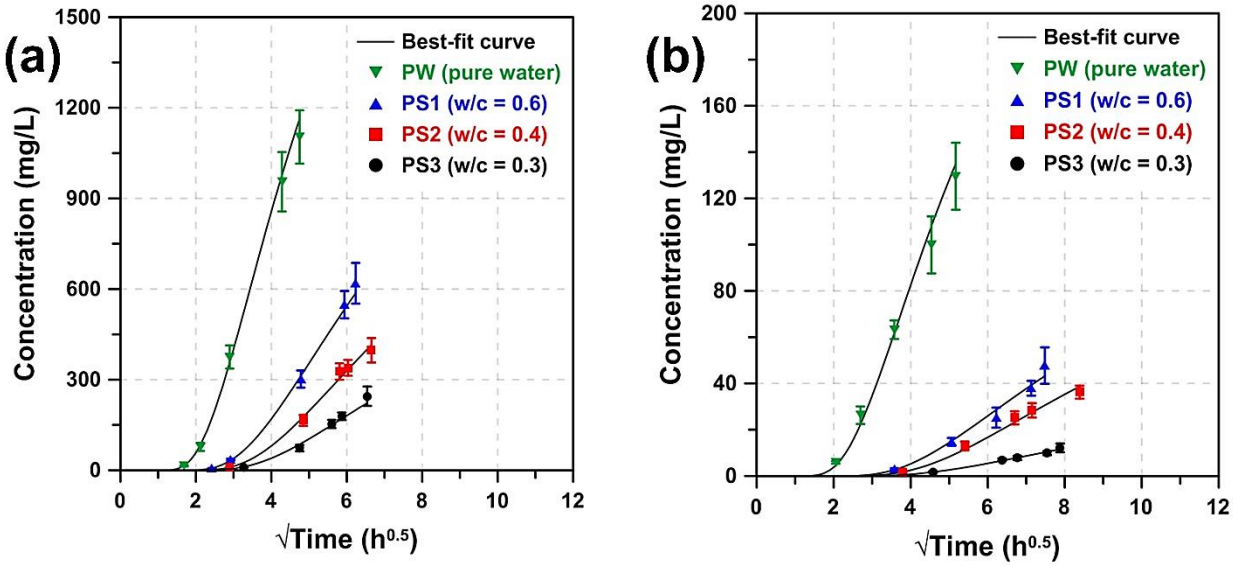

Figure 3.5 Measured concentration in the sampling bottle for (a) benzene (b) PCE during liquid diffusion test in different simulated pore solutions. The best-fit curve is obtained through the numerical solution of Equation 3.3. (The error bars show standard deviation)

Using the experimental results shown in Figure 3.5 and following the procedure mentioned in section 3.3.6.2, the estimated diffusivity of VOCs in the simulated pore solutions are provided in Table 3.5. The free diffusion coefficients of benzene and PCE in pore solution have not been previously reported in the literature. The diffusion coefficient of benzene and PCE in pure water at 25 ^{o}C is measured as 1.38×10^{-9} m^2/s and 1.17×10^{-9} m^2/s, respectively, which are 19% and 15% higher than the average values obtained through other experimental methods or modeling (e.g. 1.16×10^{-9} m^2/s and 1.02×10^{-9} m^2/s for benzene and PCE, respectively [53, 54]. The measured values herein are in a good agreement with previous results.

Table 3.5 Free diffusion coefficient of VOCs in the simulated pore solutions.

Solution ID	Description	D_o (10^{-9} m^2/s)	
		Benzene	PCE
PW	Pure water	1.38 ± 0.15	1.17 ± 0.12
PS1	w/c = 0.6	0.63 ± 0.08	0.43 ± 0.08
PS2	w/c = 0.4	0.50 ± 0.04	0.35 ± 0.05
PS3	w/c = 0.3	0.46 ± 0.07	0.33 ± 0.03

In Table 3.1, as w/c of cement paste decreases, the total concentration of ions in the pore solution increases. In Table 3.5, the diffusion coefficient of VOCs in the simulated pore solution corresponding to lower w/c cement pastes is smaller than those of higher w/c pore solution, indicating that the higher the concentration of ions in the aqueous solution, the lower the diffusion coefficient of VOCs. This effect can be partly explained by the Wilke-Chang equation (Equation 3.9) [55].

$$D_{12} = 7.4 \times 10^{-8} \frac{(xM_2)^{0.5} T}{\eta_2 V_1^{0.6}} \quad (3.9)$$

where D_{12} is the diffusion coefficient at infinite dilution of the solute (1) in the solvent (2), x is the association parameter equals 2.6 in water and 1.0 for unassociated liquids, M_2 is the molecular weight of the solvent, T is the absolute temperature, η is the viscosity of the solvent, and V_1 is the solute molar volume at normal boiling point.

According to this correlation (Equation 3.9), the free diffusion coefficient of hydrocarbons in an ionic solution decreases by increasing the viscosity of the solvent. Also, it is known that with increase of ionic concentration, the electrical forces between ions in the solution tend to establish and maintain a preferred rearrangement, increasing its viscosity [56]. This can further be supported by the fact that ions with high charge densities lead to strong electrostatic ordering of nearby water molecules through breaking their hydrogen bonds and therefore, these ions (structure making ions)

strengthen the structure of water [57, 58], causing the diffusion path of hydrocarbon molecules to alter. In this respect, by increasing the ionic concentration of pore solution, as the majority of ions in the pore solution i.e. Ca^{2+}, Na^{+}, OH^{-} are structure making ions, the viscosity of the pore solution is increased giving rise to a decrease in the diffusion coefficient of hydrocarbon molecules as indicated by using Wilke-Chang equation.

The diffusion coefficient of benzene is higher than that of PCE in ionic solutions. This could be connected with the larger molecular size of PCE. Also, the decrease in the diffusion coefficient of PCE is greater than the decline in benzene's diffusion coefficient by increasing the ionic strength of the solution. As an example, at the ionic strength of 1.88 M obtained for the simulated pore solution of cement paste with a w/c ratio of 0.30, D_o of benzene and PCE decreases by 67% and 72%, respectively.

Finally, the estimated values of D_o are employed in estimating the effective diffusion coefficient of VOCs for saturated cement paste samples as described in section 3.3.6.3 and results are reported in section 3.4.5.

3.4.4 Effective diffusion coefficient for saturated cement paste

The results of concentration measurements for benzene and PCE transport are presented in Figures 3.6 and 3.7, respectively. Using the data and solving Equation 3.3 for the boundary and initial conditions considered, the effective diffusion coefficient of benzene and PCE for saturated cement paste samples is given in Table 3.6.

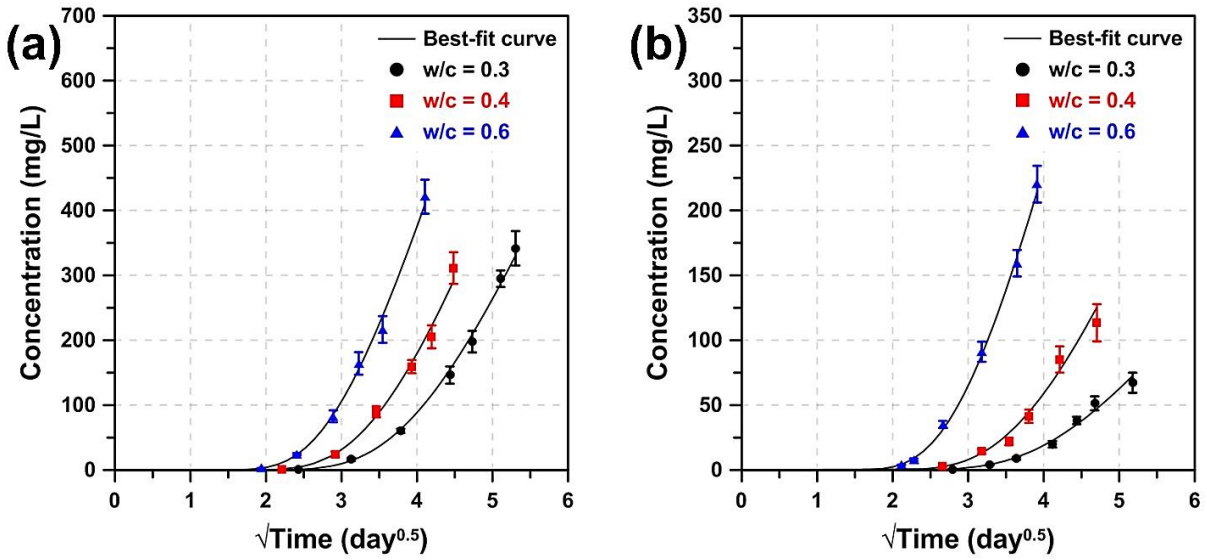

Figure 3.6 Measured concentration of benzene in the sampling bottle during (a) benzene vapor diffusion and (b) benzene liquid diffusion tests on saturated cement paste samples with various w/c. The best-fit curve is obtained through the numerical solution of Equation 3.3. (The error bars show standard deviation)

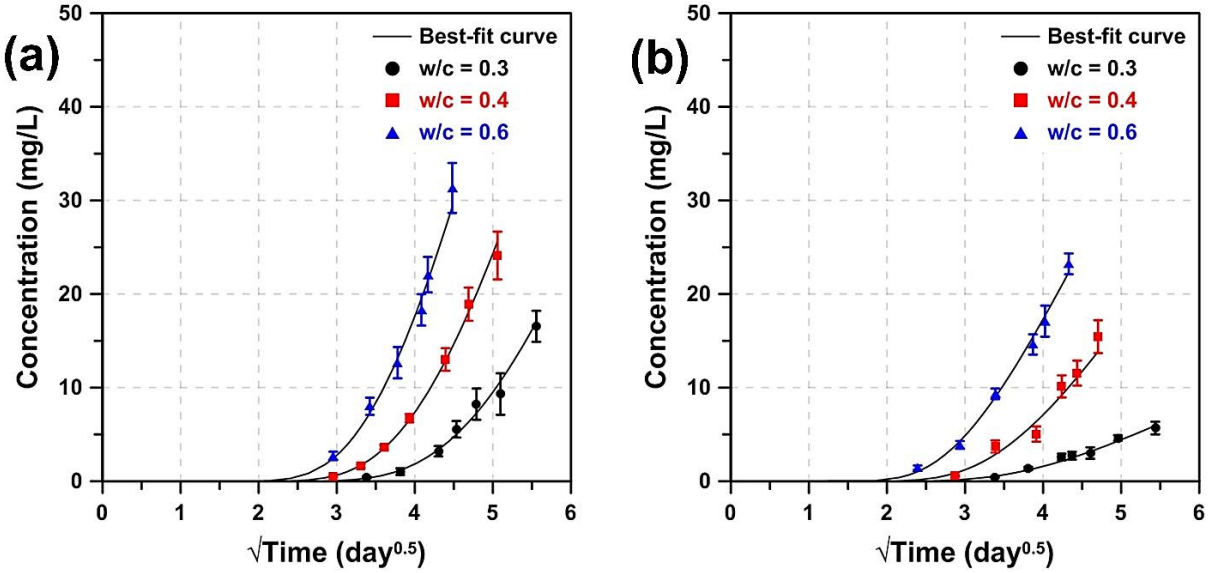

Figure 3.7 Measured concentration of PCE in the sampling bottle during (a) PCE vapor diffusion and (b) PCE liquid diffusion tests on saturated cement paste samples with various w/c. The best-fit curve is obtained through the numerical solution of Equation 3.3. (The error bars show standard deviation)

Table 3.6 Experimentally measured values of the effective diffusion coefficient of VOCs in gas and liquid forms for saturated cement pastes.

w/c	D_e (10^{-12} m^2/s)			
	Benzene		PCE	
	Vapor-liquid	Liquid-liquid	Vapor-liquid	Liquid-liquid
0.30	0.34 ± 0.09	0.36 ± 0.10	0.28 ± 0.06	0.33 ± 0.04
0.40	0.84 ± 0.11	0.98 ± 0.19	0.73 ± 0.18	0.95 ± 0.21
0.60	1.84 ± 0.19	2.28 ± 0.19	1.62 ± 0.23	1.65 ± 0.17

As shown in Table 3.6, by increasing the w/c ratio, the effective VOC diffusion coefficient of the cement paste samples increases. For both benzene and PCE diffusion, the effective diffusion coefficient of VOCs through saturated cement pastes with w/c = 0.40 is 2.5-3.0 times higher than that of cement samples made with w/c = 0.30. This ratio increases to 5.0-6.5 for the cement samples with a w/c of 0.60 compared to that of cement paste with a w/c of 0.30.

This observation can be related to the higher porosity and lower tortuosity of the cement paste with higher w/c as shown in Tables 3.3 and 3.4. Higher porosity and lower tortuosity lead to a higher effective diffusion coefficient through a porous medium as there is less resistance to the diffusion. Also, the free diffusion coefficient of benzene and PCE in the pore solution of cement paste reduces by increasing the ionic strength of the pore solution corresponding to lowering w/c. In addition, the solubility limit of VOCs decreases with decrease of w/c ratio. As such, lower permeable pore volume, less tortuous pore structure, and higher ionic strength of the pore solution (leading to lower D_o) are the main reasons for lower effective diffusion coefficient (D_e) obtained for cement paste with lower w/c.

In the case of VOCs vapor-liquid diffusion through a saturated porous media, it first needs to dissolve in the pore solution and then diffuse through the medium; theoretically, the diffusion of VOCs in vapor-liquid must be the same as their diffusion in liquid-liquid form and as such, the same effective diffusion coefficients are expected. According to Table 3.6, the effective diffusion

coefficient of both benzene and PCE in liquid form is (2-30%) higher than that of VOCs in their solubilized vapor form. However, the scatter of data (as seen in Figures 3.6 and 3.7) is attributed to a few factors. The difference can be resulted from the complex nature of liquid-liquid diffusion as in this case the simulated pore solution in contact with the sample does not exactly represent the pore solution in the matrix. The mismatch between the actual pore solution in the saturated cement paste and the simulated pore solution can cause the transport of species that do not already exist in the simulated pore solution (e.g. SO_4^{2-} and Al^{3+}) and the ions with different concentrations in the actual and the simulated pore solutions could disturb the pure diffusion of VOCs.

From data in Table 3.6, it can be seen that the effective diffusion coefficient of benzene for both cases is higher than that of PCE. This can be due to the larger molecular size of PCE (kinetic diameter of 6.60 Å) than benzene (kinetic diameter of 5.85 Å). Chan et al. [59], has shown that the diffusion coefficient of solutes depends on their size and shape as well as their interaction with the solvent. Since both benzene and PCE are nonpolar and are planar and symmetric, neither interaction with water (which is a polar solvent) nor shape-dependent diffusion is anticipated. Therefore, the difference in benzene and PCE molecular size resulting in the variation of their translation-rotation coupling [60], seems to be the main contributor to the difference.

As mentioned above, the factors affecting the effective diffusion coefficient of VOCs in cement-based materials are pore structure parameters of paste (permeable porosity and tortuosity), pore solution composition, and size of penetrant. However, most of these factors (pore structure parameters and composition of pore solution) are directly related to w/c. Considering this fact and according to Table 3.6, one can say, irrespective of the size of nonpolar VOCs, the effective diffusion coefficient of benzene and PCE in cement-based materials can mainly be influenced by w/c of the paste samples.

3.4.5 Estimation of the effective diffusion coefficient

In order to obtain the fitting parameters of the modified Archie's model, power law model was fitted to the data of D_e/D_o vs. total permeable porosity (φ) as shown in Figure 3.8. The parameter *n* in the modified tortuosity-based model was calculated through minimizing the root mean square error function for the experimentally measured effective diffusion coefficients and the calculated D_e based on the proposed model herein. Table 3.7 shows the fitting parameters of the modified Archie's model and the modified tortuosity-based model.

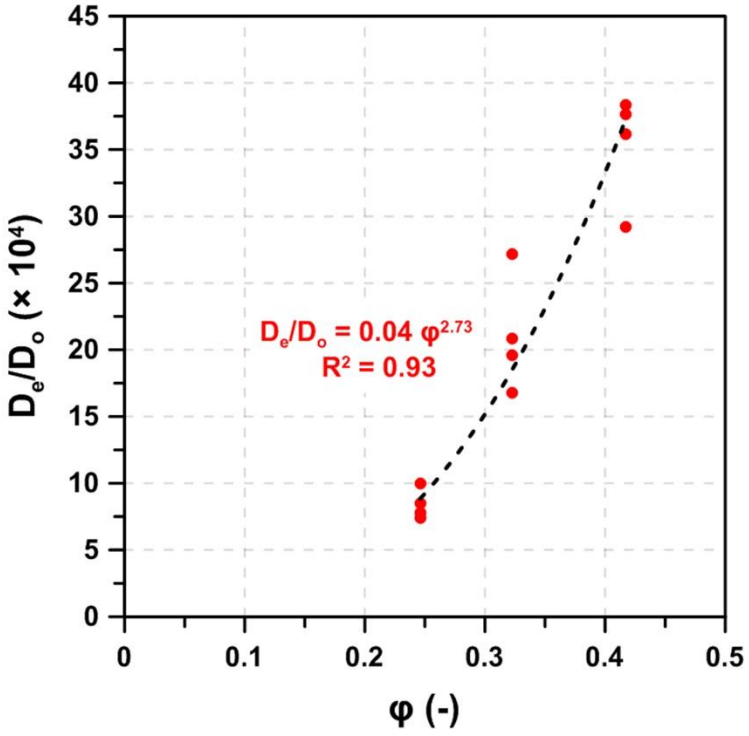

Figure 3.8 Calculating the modified Archie's model parameters.

Table 3.7 Fitting parameters of the empirical models of the effective diffusion coefficient obtained for different forms of benzene and PCE diffusion through saturated cement pastes.

Modified Archie's model		Modified tortuosity-based model
A	c	n
0.04	2.73	2.04

According to Table 3.7, the average value for the parameter n of the modified tortuosity-based model is 1.99 ± 0.05 indicating that this model is similar to the one proposed by Yang et al. [45] shown in Table 3.2.

As stated in section 3.4.4, total permeable porosity (φ), tortuosity (τ), and free diffusion coefficient of VOCs in the pore solution (D_o) are the main contributing factors to the effective diffusivity of VOCs in cement-based materials (D_e). Porosity and free diffusion coefficient in the pore solution directly affect D_e while tortuosity inversely impacts the effective diffusivity. Furthermore, based on section 3.4.3, the free diffusion coefficient of VOCs in the pore solution is inversely influenced by the concentration of structure making ions (mainly Na^+ and OH^-) and the size of VOCs molecules. Considering all these factors indicated above and unit consistency of both sides of the equation, a phenomenological model is developed to estimate the effective diffusivity of VOCs in cement-based materials expressed as follows (Equation 3.10). This model aims at predicting the effective diffusivity of VOCs in cement pastes using pore structure parameters of cement paste and other factors obtained from the literature (free diffusion coefficient of VOCs in pure water and their molar volume) and NIST model (net concentration of structure making ions).

$$D_{e,p} = a \times \frac{\varphi^b}{\tau^c} \times \frac{D_{o,w}}{(C \times V)^d} \tag{3.10}$$

where $D_{e,p}$ is the estimated effective diffusivity of VOCs in cement paste (m^2/s), $D_{o,w}$ is the free diffusion coefficient of VOCs in pure water (m^2/s), C (mol/L) is the total concentration of major structure making ions (Na^+ and OH^-) subtracted from the concentration of major structure breaking

ion (K^+) obtained from the NIST model as described in section 3.3.2, V is the molar volume of VOCs of interest (L/mol). Note that molar volume is utilized instead of kinetic diameter to have unit consistency on both sides of the equation. Also, a, b, c, and d are the constants calculated through minimizing the root mean square error of the predicted diffusivity values ($D_{e,p}$) compared to their corresponding experimental effective diffusion coefficient (D_e).

Using the values of φ and τ from Tables 3.3 and 3.4, respectively, $D_{o,w}$ of 1.16×10^{-9} m^2/s and 1.02×10^{-9} m^2/s, for benzene and PCE, respectively, [53, 54], molar volume of benzene and PCE as 0.096 (L/mol) and 0.128 (L/mol), respectively, computed based on the additive method of Le Bas [53, 61], and calculating C from the data presented in Table 3.1, the constants a, b, c, and d were obtained as 0.077, 0.000, 1.921, and 0.226, respectively. These coefficients indicate that total permeable porosity can be removed from the factors utilized in Equation 3.10 to estimate the effective diffusivity.

In addition, since the formation factor (F) is a parameter taken pore structure characteristics into account such as pore size and volume distribution, their connectivity, and tortuosity, one can use F in place of other pore structure parameters including total permeable pores and tortuosity in the modeling purposes. Moreover, by increasing w/c the formation factor decreases indicating that higher pore volumes, less tortuous and more connected pores would result in higher effective diffusion coefficient of VOCs in cement paste as shown in Table 3.6. As a result, phenomenological model introduced in Equation 3.10 would be modified into Equation 3.11 as follows:

$$D_{e,p} = a \times \frac{1}{F^b} \times \frac{D_{o,w}}{(C \times V)^c} \tag{3.11}$$

Employing the formation factor values listed in Table 3.4 and other factors ($D_{o,w}$, C, and V) mentioned earlier in this section, the constants of the model i.e. a, b, and c are obtained as 0.043, 0.702, and 0.224, respectively.

To compare the effective diffusion coefficients estimated by employing the empirical and phenomenological models and the values obtained experimentally, the results are plotted in Figures 3.9 and 3.10.

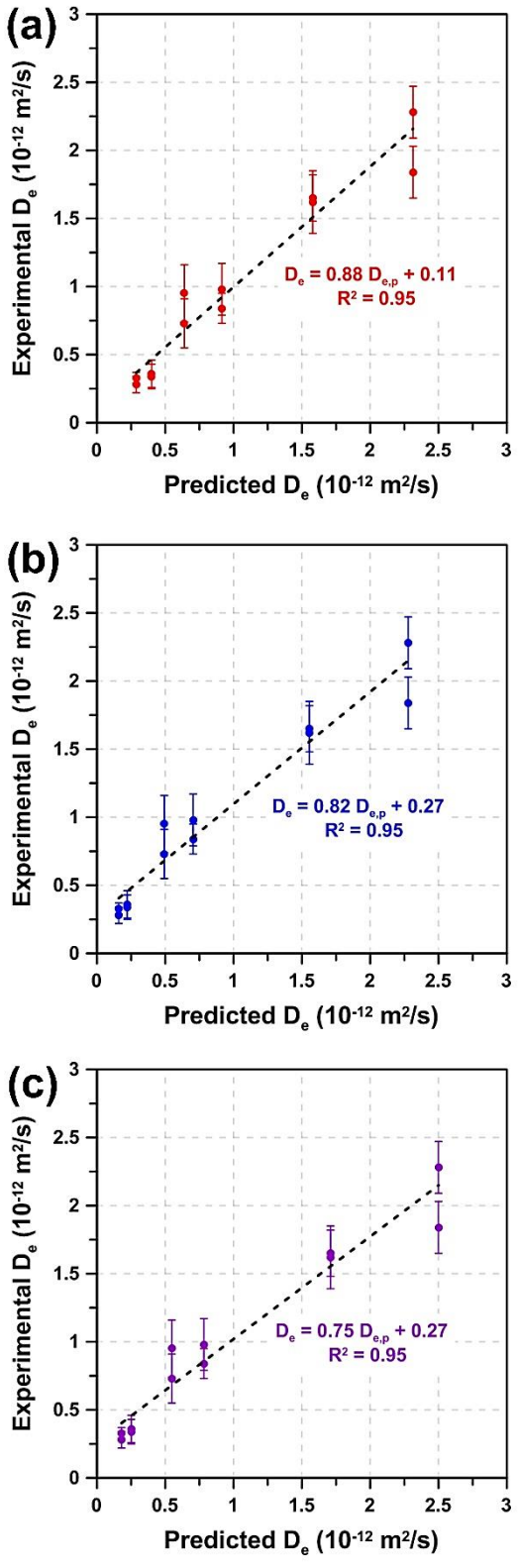

Figure 3.9 Experimentally measured D_e and the values obtained from the empirical models: (a) Modified Archie's model, (b) Modified tortuosity-based model, (c) FF model.

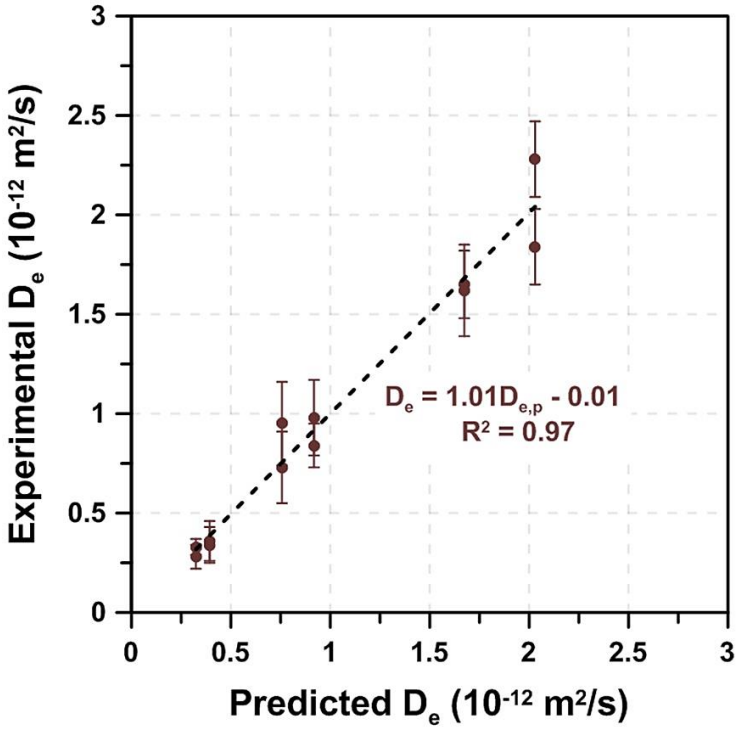

Figure 3.10 Experimentally measured D_e and the values obtained from phenomenological models: Model based on pore structure parameters and model based on formation factor.

According to Figure 3.9, among the empirical models introduced, the modified Archie's model can more precisely predict the values of the effective diffusion coefficient while there is no need to perform additional experiments such as those carried out to find tortuosity. In this regard, the ratio of the effective diffusion coefficients predicted by the modified Archie's model to the value experimentally obtained was found to range from 0.82 to 1.11 while this ratio is 0.55 to 1.36 and 0.59 to 1.21 for the FF model and the modified tortuosity-based model, respectively. The main explanation for the deviation of the outcomes of the empirical models from the experimentally measured values of the effective diffusion coefficient of VOCs can be twofold. First, the values of the coefficient of VOCs free diffusion in the simulated pore solutions are not exactly the same as the diffusion coefficient of VOCs in the actual cement pore solution due to the difference between the composition of the cement pore solution and that of the simulated pore solution. In addition,

as the modified tortuosity-based model and the FF model are both developed for charged species i.e., ions and therefore, employing them to estimate the effective diffusivity of nonpolar species such as benzene and PCE through a porous media (e.g., cement paste) can result in the calculation error.

Regarding the phenomenological models (Figure 3.10), note that both models provide the same prediction results. Also, since the y-intercept is negligible and the slope is very close to 1, both models can properly estimate the effective diffusion coefficient of VOCs in cement pastes. However, as it is theoretically expected that the vapor and liquid phase diffusion of VOCs through saturated cement paste should be quite similar, there is no differentiation between the type of VOCs diffusion in the models developed in this study and therefore, only one value for the effective diffusivity would be achieved using phenomenological models despite the type of diffusing species. Moreover, considering the least root mean square error of approximation, among all the empirical and phenomenological models employed in this study, phenomenological models give the best estimate of the effective diffusivity followed by the modified Archie's model.

3.5 Concluding remarks

This study aims to quantify and estimate the effective diffusion coefficient of two types of nonpolar VOCs i.e., benzene and PCE for the saturated hardened cement paste. Findings of this paper indicate that:

(i) By increasing the ionic strength of the pore solution, the solubility of benzene and PCE is reduced. However, the decrease in the solubility is more pronounced for PCE as compared to benzene. For example, PCE and benzene solubilities in the simulated pore solution with the highest ionic strength (1.88 M) were reduced by 87% and 70%.

(ii) The effective diffusion coefficient of the investigated VOCs (benzene and PCE) increases by decreasing the kinetic diameter of the diffusing species and increasing the w/c ratio of the cement paste samples, however, the effect of the former is very small.

(iii) Regardless of VOCs type, D_e for the cement paste with w/c of 0.40 and 0.60 is 2.5-3.0 and 5.0-6.5 times higher than that of the cement paste with w/c ratio of 0.30, respectively.

(iv) Without regard to the type of hydrocarbon available in the contaminated area, employing concrete materials with finer pore structure is an effective measure to reduce the risk of water contamination. Refining pore structure can be achieved by lowering w/c and/or utilizing reactive supplementary cementitious materials.

(v) Free diffusion coefficient (D_o) of benzene and PCE in the simulated cement paste pore solution was obtained. A sudden drop was detected in the values of diffusion coefficient of VOCs as the ionic strength of the pore solution increases. After such an initial drop, the reduction of D_o is gradual.

(vi) Among the empirical models employed to estimate the effective diffusion coefficient of benzene and PCE for saturated cement paste, the modified Archie's model showed the least estimation error. However, due to the high variation in the results obtained from the empirical models, phenomenological models were then developed considering the major contributing factors to the diffusivity of VOCs in cementitious media. The results indicated the phenomenological models are capable of predicting the effective diffusion coefficient of VOCs in cement paste with higher accuracy.

Chapter 4

Diffusion of Nonpolar VOCs through Unsaturated Cement Paste

4.1 Abstract

Concrete pipes can be located in the contaminated soil or the possibility of soil contamination would expose such pipes to the environmental pollutants. Benzene and tetrachloroethylene (PCE) are among the most prevalent water contaminants in the US. As such, transport of such Volatile Organic Compounds (VOCs) through concrete pipes conveying storm or drainage water would be of immense importance to the public health and the environment. Exposure area in the soil can be saturated or unsaturated. Since the VOCs transport is much faster in their gas state than liquid form, investigating diffusion of VOCs through unsaturated cement-based materials is of great interest.

The aim of this study is to experimentally measure the effective diffusion coefficient (D_e) of benzene and PCE vapors through cement pastes at various degrees of saturation (S). To this end, two water to cement ratios (0.30 and 0.40) and three relative humidities (75.3%, 97.3%, and 100.0%) were considered. In addition, since gas diffusion regimes through diffusive media such as cement paste depends on its pore structure, using composite theory and pore size and volume distribution in the matrix, an effort was made to develop a model to estimate the effective diffusivity of VOCs in unsaturated cement paste exposed to various RHs (≥ 75%). The capability

of the most used empirical models to predict D_e of gas species in unsaturated porous materials was also investigated.

The results show that the effect of RH on D_e is the largest among other influential factors such as water to cement (w/c) ratio and VOCs size. Also, as RH drops, the effect of VOCs size on D_e became more pronounced. Among the composite models introduced in this study to predict the effective diffusivity of VOCs in unsaturated cement paste, parallel and series models provided a boundary that the values of experimentally measured D_e fall within while an alternative composite (AC) model proposed based on a conceptual model of the pore structure of cementitious media showed to estimate the D_e values with higher accuracy compared to parallel and series models. Furthermore, the modified form of Archie's model for unsaturated porous media could best predict the effective diffusivity as compared to other widely used empirical models.

4.2 Introduction

Soil and groundwater contamination can be caused by various sources such as gross spillage of gasoline or leakage from underground storage tanks in the gas stations, or improper disposal of other types of contaminants such as chlorinated solvents mainly used in dry cleaning operations [2].

In the majority of drinking water contamination incidents in the US, benzene (existing in petroleum) and PCE (found in dry cleaning chemicals) have been commonly detected [1-3]. Due to soil or groundwater contamination, buried structures such as concrete pipes can be exposed to various range of contaminants which can penetrate the pipe and pollute the water being transported.

Transport of contaminants such as benzene and PCE (as Volatile Organic Compounds) through concrete pipes can occur while the concrete material is fully or partially saturated with water. Depending on the soil condition surrounding the concrete pipe and the level of water inside it (Figure 4.1), various degrees of saturation (S) can exist within the pipe wall. Degree of saturation is of great importance as it indicates what fraction of pores in the concrete is filled with water and what fraction is empty [62]. This implies that volatile species such as benzene and PCE can diffuse through the concrete matrix in two different forms of gas and or dissolved in pore water. Volatile Organic Compounds (VOCs) can diffuse through empty pores in gas (vapor) form whereas, they penetrate saturated part of the pore structure by first dissolving in the pore solution and then diffuse within the solution.

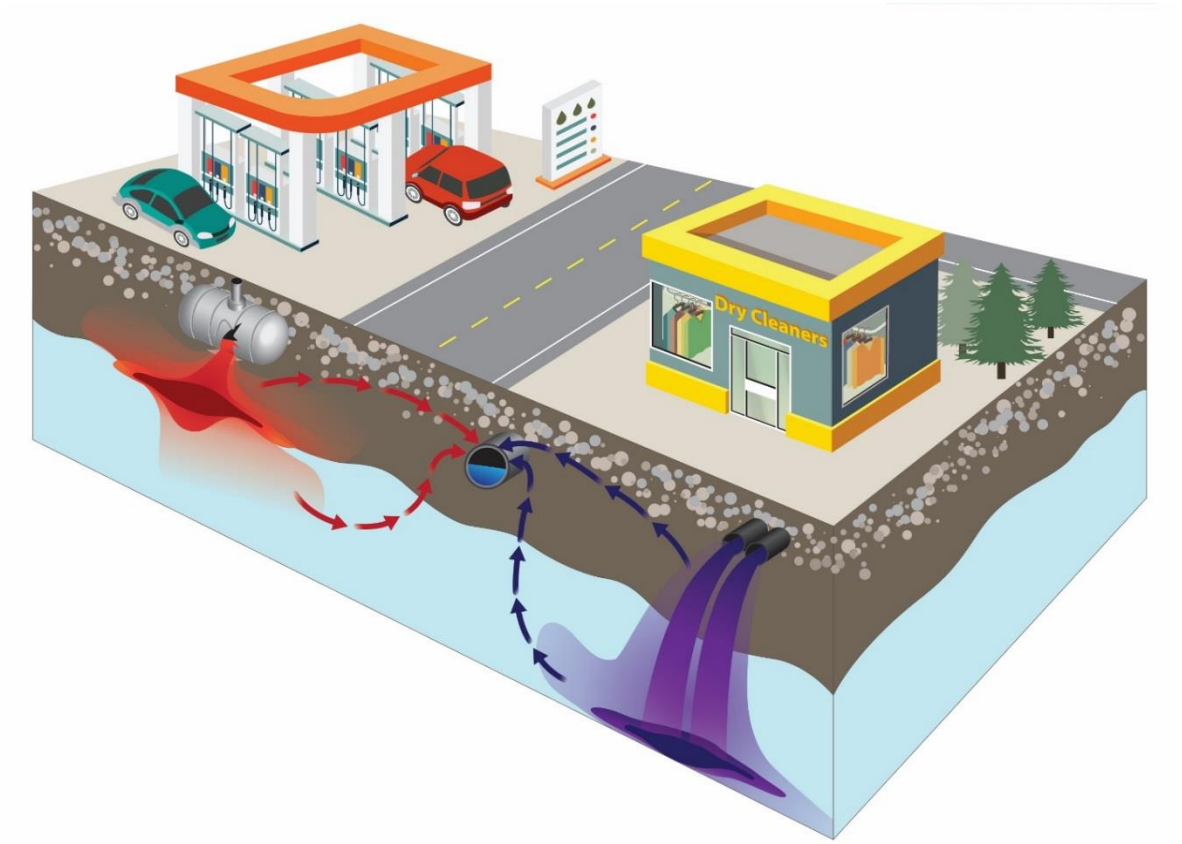

Figure 4.1 Diffusion of VOCs vapor through concrete pipe in unsaturated state.

Since the diffusion coefficient of VOCs vapor in the air is much higher than that of VOCs in the water or aqueous media [12], diffusion in empty pores should dominate the VOCs diffusion process through a partially saturated porous media such as concrete materials. Farajollahi et al. [28], for example, have shown that the water molecules may occupy the microscopic pores in the building materials, and thus, may decrease the rate of diffusion of VOCs through materials, indicating that the effective porosity accessible to gas molecules could be reduced with an increase of water content in porous media.

It is worth mentioning that the majority of the studies concerning the diffusion of VOCs through porous media is limited to the soil and the materials used in the interior parts of buildings and therefore, the focus has been on very low relative humidity (RH) in a range of 20% - 50% [27-29, 63]. However, none of these studies has considered pore size and volume distribution of the porous matrix to distinguish between VOCs transport in gas and liquid phases and their contribution to the total VOCs diffusion through the material. Also, the degree of saturation of the tested samples was not recorded.

According to the study performed by Meininghaus et al. [27], the effective diffusion coefficient of octane and ethyl acetate through aerated concrete conditioned at 45% RH were 7.61 $\times 10^{-7}$ m^2/s and 5.66 $\times 10^{-7}$ m^2/s while these values were 1.04 $\times 10^{-7}$ and 0.51 $\times 10^{-7}$ m^2/s for solid (conventional) concrete. Based on the results, as it is expected that aerated concrete would be more porous than the solid one, by decreasing the porosity the effective diffusivity of VOCs was dropped by a factor of 7-11. However, the mixture proportion and characteristics of the concretes tested have not been reported to reach a more detailed conclusion. In another work by Farajollahi et al. [28], the effect of temperature (15, 23, 31, and 39 ^oC) and RH (0, 20, and 40%) on the effective diffusion coefficient of five types of VOCs (i.e. octane, isopropanol, cyclohexane, ethyl acetate,

and hexane) in ceiling tile was investigated. As results suggested, the diffusion coefficients were found to be positively correlated with the VOC vapor pressure but, there is no specific correlation between the VOCs diffusivity and their boiling points, molecular weights, or polarity. Hexane and cyclohexane showed the highest diffusivity among the VOCs tested while octane had the lowest diffusivity. In addition, their results revealed that temperature and humidity (in the range of typical indoor environments) had a minor effect on the diffusion coefficients of the studied VOCs. Their experiments showed the increase of humidity reduces the diffusion coefficient of VOCs. Although it was indicated that this effect is very small, they hypothesized that moisture may fill up very fine pores in the ceiling tile which reduces the diffusivity of VOCs. De Biase et al. [29], measured the effective diffusion coefficient of a range of VOCs including benzene and PCE through anhydrite screed (called concrete). The temperature was kept at 20 ^{o}C and RH was within the range of 25-40%. The results indicated the effective diffusion coefficient of VOCs in concrete sample was lower than their free diffusivity in air by a factor of 2-1500. This reduction was by a factor of 4 and 88 for benzene and PCE, respectively. However, it should be noted that in addition to the type of VOCs, such a broad change in VOCs diffusion coefficient in concrete sample can be partly attributed to the alteration of RH during the test.

The lack of comprehensive studies on the transport of nonpolar VOCs (benzene and PCE herein) through unsaturated cement-based materials has resulted in different conclusions among various studies; this paper attempts at experimentally and theoretically assessing the effect of pore size and volume of cement paste (as the most porous part of concrete materials) on the effective diffusivity (D_e) of VOCs in unsaturated portland cement-based materials. In addition, utilizing composite theory, several models are developed to relate the pore size and distribution and pore structure parameters of an unsaturated cement paste to the effective diffusion coefficient of VOCs.

Through employing some widely accepted empirical models to predict D_e of gas species in unsaturated porous media, the capability of such models to predict the effective diffusivity of nonpolar VOCs vapor in unsaturated cement paste are discussed.

4.3 Materials and methods

4.3.1 Specimen preparation

Cement paste samples with two water to cement (w/c) ratios of 0.30 and 0.40 were prepared and seal cured for 21 months to ensure a high degree of hydration in the paste samples preventing further changes in their pore structure during the diffusion tests. Portland cement Type I/II in accordance with ASTM C 150 and tap water were used to prepare cement paste samples.

To prepare cement paste samples for diffusion test, discs of 5-9 mm in thickness were cut from cylindrical specimens of 63.5 mm × 250 mm and circumferentially coated with a hydrocarbon-resistant epoxy. Cement paste discs were then preconditioned through vacuum saturation in deaired water for 24 h to ensure complete saturation and removing all air pockets in the samples. Subsequently, the samples were put in sealed chambers maintained at different RH of 75.3% and 97.3% at an ambient temperature of 23 ± 2 ^{o}C for 3-4 months to equilibrate the cement paste discs at the mentioned RH. Relative humidity of 75.3% and 97.3% in the chambers was achieved through using saturated salt solutions of NaCl and K_2SO_4, respectively. All samples were conditioned until the mass change was less than 0.01%/day. In addition, soda lime was used to prevent carbonation in the paste samples during conditioning at each RH. In addition, to condition cement paste discs at 100.0% RH, vacuum saturation was carried out in deaired water for 24 h similar to the preconditioning stage of unsaturated samples mentioned above. The samples were then surface dried using a wet towel before diffusion tests in saturated condition. Note that

measurement of VOCs diffusion in cement paste samples equilibrated at 100.0% RH was performed to compare the results of VOCs diffusion through unsaturated cement paste specimens with the fully saturated ones and determine the effect of degree of saturation on VOCs diffusivity.

4.3.2 Experimental methods

4.3.2.1 Pore structure parameters

To measure total permeable porosity of cement pastes (φ), the method introduced by Bu et al. [33], was adopted. Vacuum saturation was used to saturate the cement paste samples. Subsequently, the samples were dried in an electric oven at 110 ± 5 °C for 24-48 h until achieving a constant weight (weight change of less than 0.1%/h, m_{OD}). Next, samples were vacuum saturated in a desiccator for 4 h. The vacuum pump was then turned off and the samples were left in water for 20 ± 2 h. Afterwards, the cement paste samples were removed from the desiccator and their surfaces were wiped dry with a saturated towel to attain saturated surface dry (SSD) condition (m_{SSD}). The weight of the cement paste sample in water was also measured (m_{SSB}). Finally, the volume ratio of total permeable porosity (φ) was determined using $\varphi = \frac{m_{SSD} - m_{OD}}{m_{SSD} - m_{SSB}}$. Three replicates were tested for each cement paste mixture.

Following the same method for measuring total porosity, degree of saturation (S) of unsaturated cement paste sample was calculated by $S = \frac{m_{RH} - m_{OD}}{m_{SSD} - m_{OD}}$ in which m_{RH} is the sample weight equilibrated at RH of interest for 3-4 months as discussed in section 4.3.1

In porous media, (matrix) tortuosity is used to show how convoluted pores are i.e. the pathways of moving species are. To compute tortuosity (τ), electrical resistivity of cement paste samples and their pore solution were utilized $\tau = \sqrt{\frac{\rho_s \times \varphi}{\rho_o}}$ [46, 47].

where τ is the electrical-based tortuosity, ρ_s is the bulk resistivity of the porous media which is cement paste therein (Ω.m), and ρ_o is the resistivity of the solution existing in the pore structure (Ω.m) estimated for cement paste using the National Institute of Science and Technology model [34]. Further details of calculating tortuosity based on the electrical method is provided in Appendix C. Note that pore structure parameters (φ and τ) are later employed in composite and empirical models for predicting the effective diffusivity of VOCs in unsaturated cement paste (sections 4.3.4.1.3 and 4.3.4.2).

4.3.2.2 Pore size and volume distribution measurement

To examine the pore structure of cement paste samples cured for 21 months, both dynamic water vapor sorption (DWVS) and Mercury Intrusion Porosimetry (MIP) measurements were carried out to obtain a full and more representative pore size and volume distributions of the paste samples.

DWVS is used to experimentally obtain water vapor sorption isotherms of the samples using an automated sorption analyzer (Q5000 SA, TA Instruments, USA). Small flat disks (30–50 mg) of cement paste were cut and submerged in lime-saturated water in a sealed container for about 24 h before placing them in the sorption analyzer. The measurements were performed at 25 ^{o}C. Each test was initiated with the desorption process. The pre-saturated sample was first equilibrated at 97.5% relative humidity (RH) for either 96 h or reaching a stable mass (less than 0.001% mass change within 15 min) whichever took place first [64-66]. Subsequently, the RH was sequentially dropped from 97.5% to 0% RH, in 10% RH increments to 7.5% and then to zero RH. Note that the specimen was held at each RH step until either it reached to mass equilibrium (less than 0.001% mass change within 15 min) or equilibrated for 48 h whichever happened first [64, 65].

Furthermore, MIP was performed employing a PASCAL 440 series instrument. The samples' dimensions were between 3 mm to 5 mm. The relationship between the applied pressure and the pore diameter (with the assumption of cylindrical shape) can be described by the Washburn equation as follows (Equation 4.1) [67], considering that all pores are entirely and equally accessible to mercury:

$$d_p = \frac{-4\gamma cos\theta}{P} \quad (4.1)$$

where d_p is the pore diameter (m), γ is the surface tension of mercury (N/m), h is the contact angle between mercury and solid (^{o}), and P is the applied pressure (N/m^2). The surface tension of mercury and the contact angle between mercury and the pore wall were taken as 0.485 N/m and 140^o, respectively. The maximum applied pressure was 280 MPa, corresponding to a minimum pore diameter of 5 nm according to Washburn equation [67].

According to the International Union of Pure and Applied Chemistry (IUPAC) [68], pores are classified as micropores (< 2 nm), mesopores (2 nm ≤ pore diameter ≤ 50 nm), and macropores (> 50 nm) for porous media. As reported elsewhere [69, 70], DWVS can be employed to obtain the volume of mesopores; however, it can also give the volume of micropores for comparative analysis or modeling. In addition, MIP cannot identify the whole range of very small pores (mesopores and micropores) and is mainly capable of measuring the volume of macropores [69]. As such, since cement paste samples are composed of fine pores significantly affecting their degree of saturation when exposed to RHs lower than 100.0% and to capture a more representative pore size and volume distribution for cement paste samples, a combination of DWVS and MIP tests results was utilized. The method applied to develop combined pore size and volume distributions is discussed in Leech et al. [69]. Also, to translate the results obtained by DWVS test into pore

size and volume distribution, Barrett, Joyner, and Halenda (BJH) method was adopted [71]. It should be pointed out that only cumulative pore volume distribution is needed to estimate the VOCs diffusivity in unsaturated cement pastes as discussed further in section 4.3.4.1.3.

4.3.2.3 VOCs diffusion measurements

To investigate the diffusion of VOCs through cement paste samples at different RHs, a special diffusion cell was designed and prepared in this study as shown in Figure 4.2. This setup enables us to quantify the effective diffusivity of VOCs in both saturated and unsaturated cement-based samples.

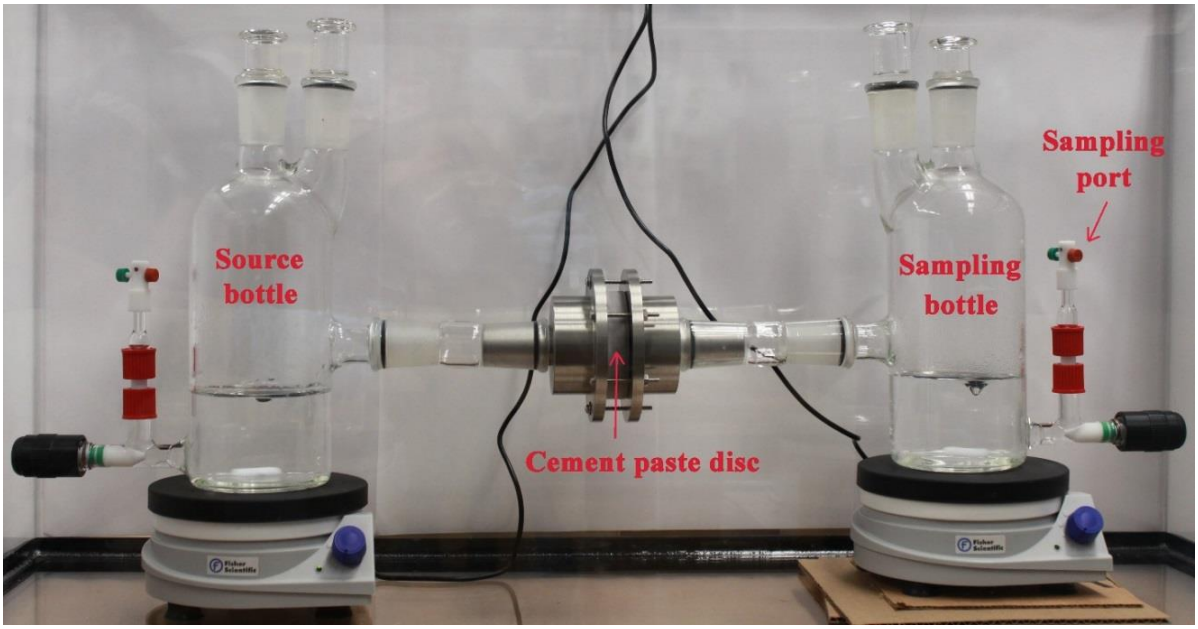

Figure 4.2 Diffusion cell for measuring VOCs vapor transport through saturated/unsaturated cement paste samples.

To perform a diffusion test, coated discs equilibrated at each specific RH were placed between two stainless steel plates connected to the source and sampling bottles. The aqueous

solution in the source bottle (upstream) is always kept at saturation with respect to the VOCs of interest using extra amount of pure benzene or PCE.

In the diffusion test at 100.0% RH, distilled deionized water in both source and sampling bottles (200 mL) were acidified with maleic and ascorbic acids (5 and 0.625 g/L, respectively) following EPA method 524.3 [35], to avoid hydrocarbons degradation due to bacterial growth. In the diffusion experiments at lower RH of 75.3% and 97.3%, corresponding saturated salt solutions (NaCl or K_2SO_4) was added to the source and sampling bottles. No acidification was performed as it is expected that no bacterial growth can occur in such concentrated salt solutions [72, 73]. The entire set up is then placed into a temperature-controlled chamber set at 25 ^oC to minimize the effect of temperature on the diffusion process.

The procedure that was followed for taking samples from the solution in the downstream (sampling) bottle is as follows: Using Hamilton gastight® syringes, at each pre-specified time, two samples of 200 μL and 500 μL for benzene and PCE diffusions, respectively, were taken from the downstream bottle and diluted in a ratio of 1:42.7 with deionized distilled (ASTM type II) water previously acidified with ascorbic and maleic acids (with the same concentrations used for acidifying bottles in the VOCs vapor diffusion test at 100.0% RH) to preserve the samples. Afterwards, second dilution was performed using 300 μL and 1000 μL samples from of the first diluted benzene and PCE vials, respectively, in a ratio of 1:42.7 with deionized distilled water. The samples were then kept in a refrigerator at a temperature of 4 ^oC until the concentration measurement date utilizing a Gas Chromatography–Mass Spectrometry (GC-MS) equipment. The mass (concentration) of benzene or PCE diffused through the cement paste samples was then used to compute the effective diffusivity of VOCs vapors in saturated and unsaturated cement paste samples (section 4.3.3).

4.3.3 Effective diffusion coefficient (D_e) estimation

4.3.3.1 Calculation methodology

In the diffusion tests, cumulated concentration in the sampling bottle over a period of a few hours to one month is used to calculate the effective diffusion coefficient VOCs in saturated and unsaturated cement paste samples using Fick's second law assuming 1-D diffusion (Equation 4.2). As there is no analytical solution for the Equation 4.2 with the boundary and initial conditions considered, a numerical approach based on centered finite difference method with explicit formulations is developed using MATLAB to calculate the effective diffusion coefficients (D_e).

$$\varphi_a \frac{\partial C(x,t)}{\partial t} = D_e \frac{\partial^2 C(x,t)}{\partial x^2} \tag{4.2}$$

$C(x,0) = 0,\ 0 < x \leq L$ (Initial condition)
$C(0,t) = C_o, 0 \leq t$ (Boundary condition)

where φ_a is the air-filled porosity calculated using $\varphi_a = (\frac{100-S}{100})\varphi$, C(x,t) is the concentration of VOCs of interest within the cement paste sample (mg/m^3) quantified at x = L by sampling from the downstream solution, t is the sampling time (s), x is the distance within the sample in the diffusion direction (m), L is the sample thickness (m), D_e is the effective diffusion coefficient of VOCs in saturated/unsaturated cement paste (m^2/s), and C_o is the fixed concentration for benzene or PCE vapor in the upstream which can be obtained through employing Henry's law constant (HLC) for dilute solutions of VOCs (Equation 4.3).

$$H\ (dimensionless) = \frac{c_g}{c_a} \tag{4.3}$$

where H is the water/salt solution-air partitioning coefficient for a dilute aqueous (salt if any) solution of the hydrocarbon of interest, c_g and c_a are the concentrations of hydrocarbon in gas and

aqueous phases, respectively. Note that since the concentrations of benzene and PCE are reasonably low at their solubility (their concentrations are much below 10 g/L [38]), dimensionless HLC can be adopted to relate the concentration of VOCs vapor in the source and sampling bottles to the concentration of hydrocarbon of interest at both sides of the cement paste sample i.e., C_o at x = 0 and C at x = L for VOCs vapor diffusion through saturated and unsaturated cement paste samples. However, as the environmental conditions in both upstream and downstream are the same and it is assumed that the air/solution systems in both bottles are in equilibrium at any time (Henry's law is always being held), instead of using VOCs vapor concentrations in the headspace, quantification of VOCs concentrations in the source and sampling bottles can directly be employed to calculate D_e.

It is worthy of mention that since cement particles and its hydration products contain almost no organic materials such as organic carbon, the sorption of benzene and PCE by cement paste is assumed to be negligible in the calculation of the effective diffusion coefficient [39].

4.3.3.2 Solubility of VOCs in saturated salt solutions

The solubilities of benzene and PCE in saturated salt solutions of NaCl and K_2SO_4 were experimentally measured. 60-mL amber vials were first filled with filtered saturated salt solutions. The filtration was carried out using 0.2 μm nylon syringe filters. The saturated salt solutions were obtained through dissolving analytical grades of salts in deionized water for 4 days using magnetic stirrer. Additional amount of salts was added to the flasks after initial dissolution to achieve complete salt saturation. After introducing filtered saturated salt solutions to the 60-mL vials, pure benzene and PCE were added to the vials at a volume of 1.0 mL and 0.5 mL, respectively. These volumes ensure that there is enough VOCs to saturate the salt solutions. All vials were headspace

free and capped with a Teflon®-lined closure. The vials were kept in a chamber with controlled temperature (25 ^{o}C) for a week to allow VOCs to freely dissolve in the salt solutions. Subsequently, samples of 200 µL and 700 µL were taken from each vial (three replicates) for benzene and PCE, respectively, using Hamilton gastight® syringes and tested with GC-MS.

4.3.4 Estimation of the effective diffusion coefficient of VOCs in unsaturated cement paste

To predict the effective diffusivity of VOCs vapor in unsaturated cementitious media, two different approaches were adopted: model developed based on composite theory and empirical models. Pore structure parameters (total permeable porosity and tortuosity) and pore size and volume distributions of cement paste samples, bulk diffusivity of VOCs in air and water (retrieved from literature), and the RH the porous medium is exposed to are utilized to develop the models. A detailed description of each approach is provided in this section.

4.3.4.1 Model based on composite theory

4.3.4.1.1 Effect of RH on pore saturation of unsaturated porous media

According to Kelvin-Laplace equation (Equation 4.4), for a porous medium consisting of cylindrical pores and equilibrated at a specific RH, Kelvin or capillary pore radius (r_k) is defined as the maximum pore radius that remains saturated due to capillary condensation meaning that pores larger than r_k are considered (partially) empty [62, 74].

$$r_k = \frac{2\sigma V_m}{RTln(RH)} \quad (4.4)$$

where r_k is the Kelvin radius (m) at the equilibrium RH, σ is the surface tension of pore solution which can be considered 0.072284 (N/m) for water, V_m is the molar volume of water (1.8×10^{-5} m^3/mol), R is the universal gas constant (8.3145 N.m/mol.K), and T is the absolute temperate (K).

As stated, pores with radius larger than r_k are partially empty. In other words, there is an adsorbed layer of water in the so-called empty or dry pores. Thickness of this adsorbed layer depends on the RH at which the media is equilibrated. To find the corrected pore radius (r_p), the thickness of the adsorbed layer known as t-curve (t) needs to be added to the capillary pore radius (r_k) giving Equation 4.5. As such, the corrected pore diameter (d_p) can be calculated based on Equation 4.6.

$$r_p = r_k + t \tag{4.5}$$

$$d_p = 2 \times (r_k + t) \tag{4.6}$$

Concerning the thickness of adsorbed water layer, many theoretical models and experimentally obtained values are proposed to achieve t-curve among which the experimental data provided by Hagymassy et al. [75], was used in this study due to its widespread application in cement science [76]. Note that to use data obtained by Hagymassy et al., the average statistical thickness of a monomolecular water layer adsorbed was considered 3 Å [75, 76].

As mentioned above, at each specific RH there exists an adsorbed layer of water in the larger pores that dry out whose thickness depends on the equilibrium RH ranging from a few angstroms to about two nanometers [62, 70, 75]. This indicates that the assumption of having empty pores larger than the r_k is not accurate; however, for the ease of modeling purpose, it is assumed that the effect of this adsorbed layer is negligible as it is very small compared to the pore

diameter especially larger pores which have considerable effect on gas diffusion in unsaturated materials [77].

As discussed in section 4.3.2.3, two RHs were chosen to condition unsaturated cement paste samples. Using Equations 4.4 to 4.6, the maximum diameter of pores considered fully saturated at 75.3% and 97.3% RH are 8.7 nm and 79.5 nm, respectively. These pores that divide the saturated and dry regions in the pore structure called separating pores hereafter.

4.3.4.1.2 Modes of VOCs transport in cementitious media

Diffusion in a porous media occurs due to the existence of concentration or partial pressure gradient for any diffusing species [78]. In a saturated porous system, the only diffusion mode is the ordinary diffusion happening based on the concentration gradient of penetrant in the liquid phase which follows Fickian mechanism. On the other hand, in a dry porous media or dry portion of unsaturated matrix, among different modes of gas/vapor transport, those based on concentration difference are molecular (ordinary or bulk), Knudsen, and surface diffusions [78, 79].

The contribution of each mode of gas transport in a dry porous medium depends on the pore size or the Knudsen number (Kn) which is defined according to Equation 4.7.

$$Kn = \frac{\lambda}{l} \tag{4.7}$$

where λ is the mean free path of gas molecules and l is characteristics length scale of the medium which is the pore diameter if the pores are assumed to be cylindrical [79, 80]. Also, mean free path of any gas molecule can be calculated through Equation 4.8 [81].

$$\lambda = \frac{k_B T}{\sqrt{2}\,\pi\, {d_g}^2\, p} \tag{4.8}$$

where k_B is the Boltzmann constant (J/K), T is the temperature (K), d_g is the diameter of gas the molecule (m), and p is the gas pressure which is atmospheric pressure in our case (pa).

Molecular diffusion happens in pores where molecule-molecule collisions become dominant compared to molecule-pore wall collisions [79]. This is the case when the gas mean free path (λ) is much smaller than the pore diameter (d) i.e. $Kn << 1$ (typically < 0.1) [82, 83]. As such, molecular or continuum regime (within which Fickian diffusion exits) occurs when pore size is large enough compared to the mean free path of gas molecules. On the other hand, if the Knudsen number is large i.e. $Kn >> 1$ (typically > 10), Knudsen diffusion dominates the transport regime in the pores indicating that the pore size is much smaller than the mean free path of molecules and thus, gas molecules collide more frequently with the pore walls than with each other [79, 82, 83].

According to the above-mentioned, molecular diffusion is dominant in larger pores whereas Knudsen diffusion predominates in very small pores. Between the regions in which either molecular or Knudsen mechanisms is prevailing, there exists an intermediate region with a transition diffusion regime for which $0.1 \leq Kn \leq 10$. In the transition regime, both diffusion mechanisms i.e. molecular and Knudsen affect the transport of gas species.

Note that surface diffusion is disregarded in this study since its contribution to the overall transport cannot be accurately determined due to its complex nature as indicated by Sercombe et al. [79]. In addition, surface diffusion is the determining mode of gas transport within the very fine pores in the order of a few nanometers [84], meaning that it usually coexists with Knudsen diffusion in the very small pores region. Since the selected RHs are 75.3% and 97.3% resulting in separating pores of 8.7 nm and 79.5 nm in diameter, respectively, and maximum pore diameters of Knudsen region for benzene and PCE are 2.7 nm and 2.1 nm, respectively, Knudsen regime cannot exist within the cement paste matrix equilibrated at the selected RHs mentioned above due

to the saturation of all pores below pore size of 8.7 nm and 79.5 nm in diameter for 75.3% RH and 97.3% RH, respectively.

4.3.4.1.3 Composite model

At the macroscopic scale, cement paste is composed of solid phase (hydrated and anhydrate phases) and empty spaces dispersed within the solid phase. Considering that mass transport cannot happen in the solid phase, the empty space or pore structure is the only way for diffusing species to pass through the cement paste. As such, to model the transport of any penetrant in cement paste, its matrix can be simulated by a two-phase composite i.e. solid phase and pore phase. However, the configuration of these phases in the matrix can be very different from one case to another and sometimes can be very complex. To avoid complication, two simpler cases are considered based on composite theory: parallel and series models (Figure 4.3) [85]. Nonetheless, the arrangement of phases in series (Figure 4.3b) would result in the full blockage of transport of penetrants in the matrix as the solid phase does not allow any mass transport within itself and therefore, the only possible case is the parallel model. As a result, employing the law of mixtures the diffusivity for the simplified matrix simulated by parallel model (D_M) can be calculated through Equation 4.9. Note that since the diffusivity of VOCs in solid phase is considered negligible (~ 0), the matrix diffusivity calculation can be simplified by removing the term containing D_I.

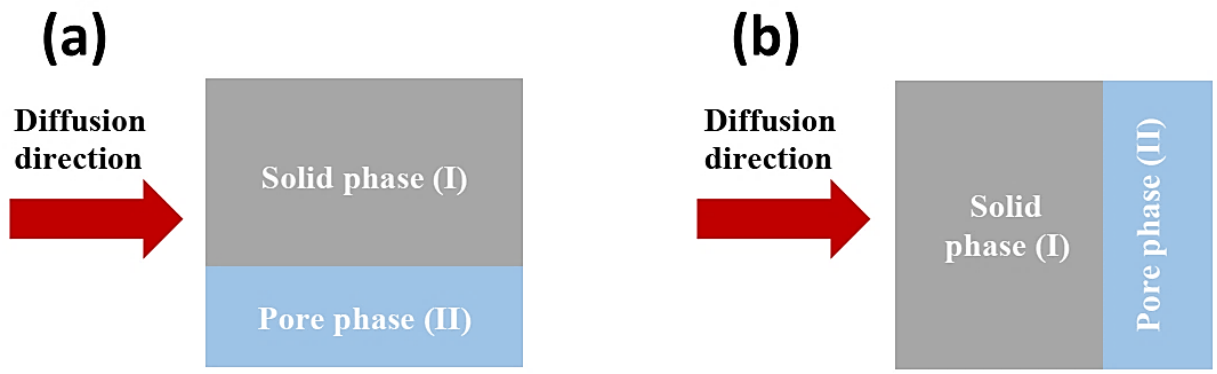

Figure 4.3 Configuration of phases in a simulated cement paste (a) Parallel model (b) Series model.

$$D_M = \varphi_I D_I + \varphi_{II} D_{II} \rightarrow D_M = \varphi_{II} D_{II} \quad (4.9)$$

where φ_I and φ_{II} are the volume fraction of the solid phase and the pore phase (total porosity) in the cement paste specimen, respectively. Also, D_I (~ 0) and D_{II} are the diffusivity of VOCs in the solid and pore phases, respectively.

To take the contribution of each mode of transport into account in a saturated or unsaturated matrix, the pore phase needs to be divided into different segments in each of which a specific diffusion regime is dominant. Similar to the modeling cement paste matrix, two simpler cases can be considered for modeling pore phase: series model and parallel model (Figure 4.4). Since the diffusion of VOCs in their gas form is much faster than theirs in liquid form moving in an aqueous solution, one can say the saturated portion of pore phase is the limiting factor in the transport of VOCs in cement-based materials. Thus, parallel and series models are the extremes of VOCs transport in the pore phase in terms of diffusion meaning that the arrangement of saturated and dry segments in series results in the lowest matrix diffusivity whereas VOCs would have the fastest diffusion once the segments are in parallel. Again, applying the law of mixtures to the pore phase results in the Equations 4.10 and 4.11 for parallel and series models of pore system, respectively.

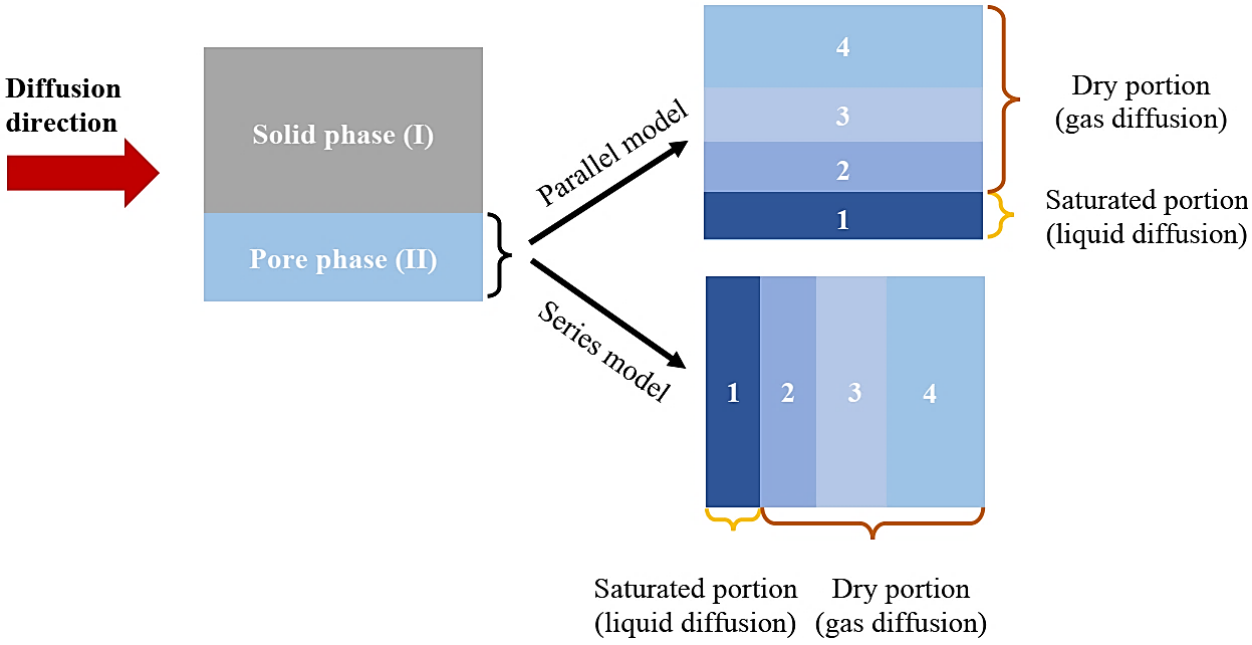

Figure 4.4 Parallel and series models for simulating pore phase of an unsaturated cement paste.

$$D_{II} = \sum_{i=1}^{4} \varphi_i D_i \tag{4.10}$$

$$\frac{1}{D_{II}} = \sum_{i=1}^{4} \frac{\varphi_i}{D_i} \tag{4.11}$$

where φ_i and D_i are the volume fraction of segment i in the pore phase (representing liquid, Knudsen, transition, and molecular diffusion regions herein) and the diffusivity of VOCs of interest in the segment i, respectively. Note that φ_i can be obtained using cumulative pore size and volume distribution curve. However, the cumulative pore size and volume distribution should be normalized to the total pore volume of the matrix to obtain the volume fraction of each segment in the pore phase.

By combining Equations 4.10 and 4.11 with Equation 4.9, the matrix diffusivity of VOCs of interest in the simulated cement paste matrix can be obtained for parallel and series models of pore structure, respectively, as follows (Equations 4.12 and 4.13):

$$D_M = \varphi_{II} \sum_{i=1}^{4} \varphi_i D_i \quad (4.12)$$

$$D_M = \frac{\varphi_{II}}{\sum_{i=1}^{4} \frac{\varphi_i}{D_i}} \quad (4.13)$$

Cement paste pore structure does not consist of straight pores; instead, the pores are tortuous within the matrix affecting the transport of species by increasing their path length. To account for the effect of increased pore lengths due to winding pore paths, tortuosity (τ) factor needs to be applied in the modeling of porous media [86]. As such, the effective diffusivity of the cement paste (D_e) can be obtained through Equation 4.14.

$$D_e = \frac{D_M}{\tau} \quad (4.14)$$

where τ is the tortuosity of the matrix experimentally measured for cement paste samples in this study (section 4.3.2.1).

4.3.4.2 Empirical models

To estimate the effective diffusivities of gas species in unsaturated porous media such as soil or cement-based materials, several empirical models have been introduced. Table 4.1 presents models commonly utilized to connect the effective diffusivity of gas species in an unsaturated porous medium with its pore structure parameters such as total permeable porosity and tortuosity. In addition, these empirical models consider the degree of saturation (S) of the medium and the free bulk diffusivity of gas species in air (D_o).

Table 4.1 Empirical models for the effective diffusivity of non-reactive gas species in unsaturated porous media using pore structure parameters, degree of saturation (S), and free bulk diffusion coefficient of gas species in air (D_o).

Model ID	Reference	Model (general form)	Pore structure parameter	Other parameters	Fitting parameter(s)
EM1	Currie [87], Grable and Siemer [88], Lai et al. [89], Fujikawa and Miyazaki [90]	$D_e = A{\varphi_a}^B D_o$	φ	S, D_o	A, B
EM2	Millington [91], Millington and Quirk [92], Sallam et al. [93], Xu et al., [94], Fujikawa and Miyazaki [90]	$D_e = {\varphi_a}^C \varphi^D D_o$	φ	S, D_o	C, D
EM3	Thiery et al. [95], Boumaaza et al. [77]	$D_e = \varphi^E (\frac{100 - S}{100})^F D_o$	φ	S, D_o	E, F
EM4	Benavente and Pla [96]	$D_e = \frac{\varphi_a}{\tau} D_o$	φ & τ	S, D_o	-
EM5	Modified tortuosity-based model	$D_e = \frac{\varphi_a}{\tau^n} D_o$	φ & τ	S, D_o	n

φ: Volume ratio of total permeable porosity
φ_a: Air-filled porosity (volume ratio of dry pores)
τ: Tortuosity
S: Degree of saturation (%)
D_o: Free bulk diffusivity of gas species in air (m^2/s)

In Table 4.1, most models use φ_a which is air-filled porosity of the material indicating that in gas diffusion through a partially saturated porous medium the dry portion of the matrix controls the total transport mechanism. Furthermore, total permeable porosity (φ) and tortuosity (τ) are the two major parameters utilized in the models to represent the pore structure of porous media. The methods to measure the total permeable porosity and tortuosity are discussed in section 4.3.2.1. Degree of saturation (S) was experimentally measured, and the results are presented in section 4.4.1. Also, the values of free bulk diffusion coefficient of VOCs vapor in air (D_o) employed in

the calculations were obtained from literature as 9.3×10^{-6} m^2/s and 7.6×10^{-6} m^2/s for benzene and PCE, respectively [54, 97].

4.4 Results and discussion

4.4.1 Effective diffusion coefficient for unsaturated cement paste

To calculate the effective diffusion coefficient of VOCs in the saturated and unsaturated cement paste samples using Equation 4.2, the values of C_o, S, and φ must first to be obtained. The results of VOCs solubility measurements in pure water and the saturated salt solutions of NaCl and K_2SO_4 are shown in Table 4.2. According to Price [98], the solubility of benzene in saturated salt solution of NaCl at 25 ^oC is reported to be 134 ± 5 mg/L which is very close to the value measured in the current study (130 ± 4 mg/L).

Table 4.2 Solubility of benzene and PCE in deionized water and saturated salt solutions used in this study at 25 ^oC.

Solution	VOCs solubility (mg/L)	
	Benzene	PCE
Deionized water	1921 ± 144	222 ± 21
Saturated K_2SO_4	881 ± 26	82 ± 5
Saturated NaCl	130 ± 4	13 ± 1

The values of degree of saturation (S) for unsaturated cement pastes obtained through direct experimental measurements is presented in Table 4.3.

Table 4.3 Degree of saturation of cement paste samples conditioned at various RHs adopted in this study.

RH (%)	w/c ratio	
	0.30	0.40
75.3	84.45 ± 1.81	77.16 ± 3.02
97.3	95.12 ± 3.86	90.89 ± 2.93

Table 4.4 shows the results of total permeable porosity and electrical resistivity measurements. Using tortuosity formula (section 4.3.2.1) and the results for electrical resistivity of the cement paste samples, and their corresponding simulated pore solutions, tortuosity of the cement paste matrices are given in Table 4.4. More details on the calculation of tortuosity are provided in Appendix C.

Table 4.4 Total permeable porosity, tortuosity, and electrical resistivity of the cement paste samples (ρ_s) and their simulated pore solutions (ρ_o).

w/c	φ	τ	ρ_s (Ω.m)	ρ_o (Ω.m)
0.30	0.248	20.82	55.92	0.032
0.40	0.324	13.63	28.11	0.049

Using the data in Tables 4.2 to 4.4, VOCs concentration measurements illustrated in Figures 4.5 to 4.7, and Equation 4.2, the effective diffusion coefficients of VOCs in cement paste samples were estimated as presented in Table 4.5.

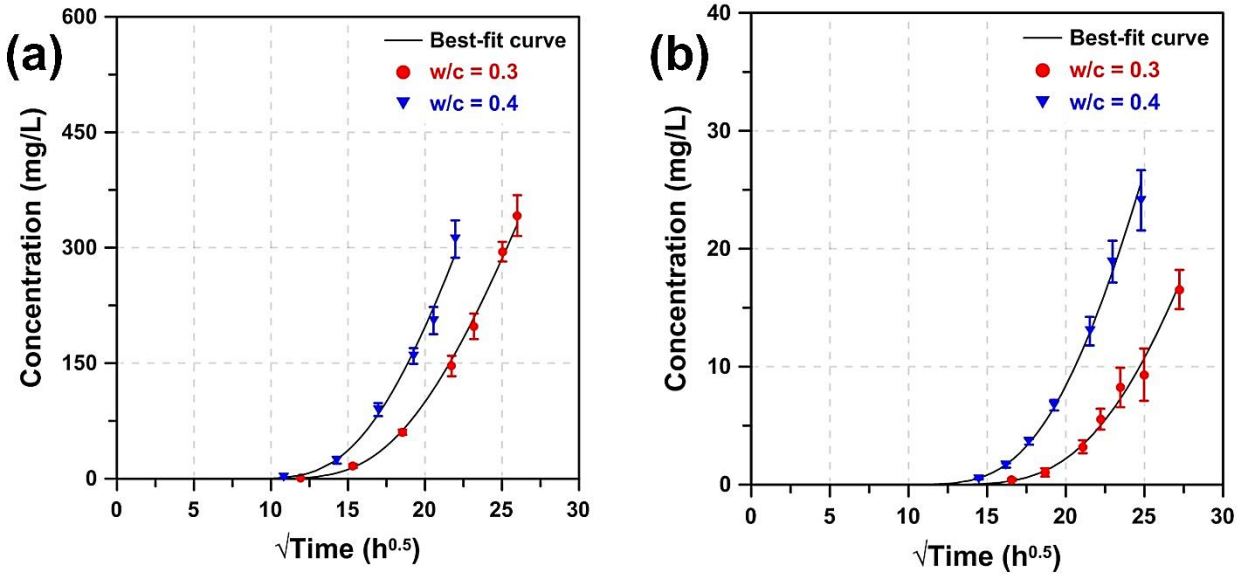

Figure 4.5 Measured concentration of VOC in the sampling bottle during (a) benzene vapor diffusion (b) PCE vapor diffusion tests at 100.0% RH. The best-fit curve is obtained through the numerical solution of Equation 4.2. (The error bars show standard deviation)

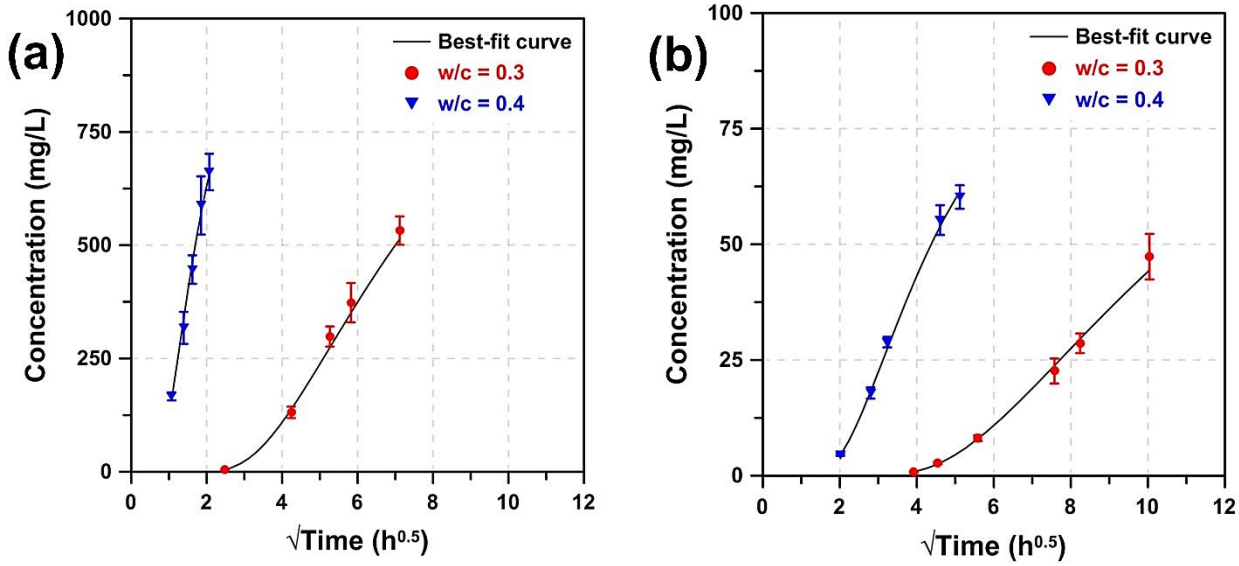

Figure 4.6 Measured concentration of VOC in the sampling bottle during (a) benzene vapor diffusion (b) PCE vapor diffusion tests at 97.3% RH. The best-fit curve is obtained through the numerical solution of Equation 4.2. (The error bars show standard deviation)

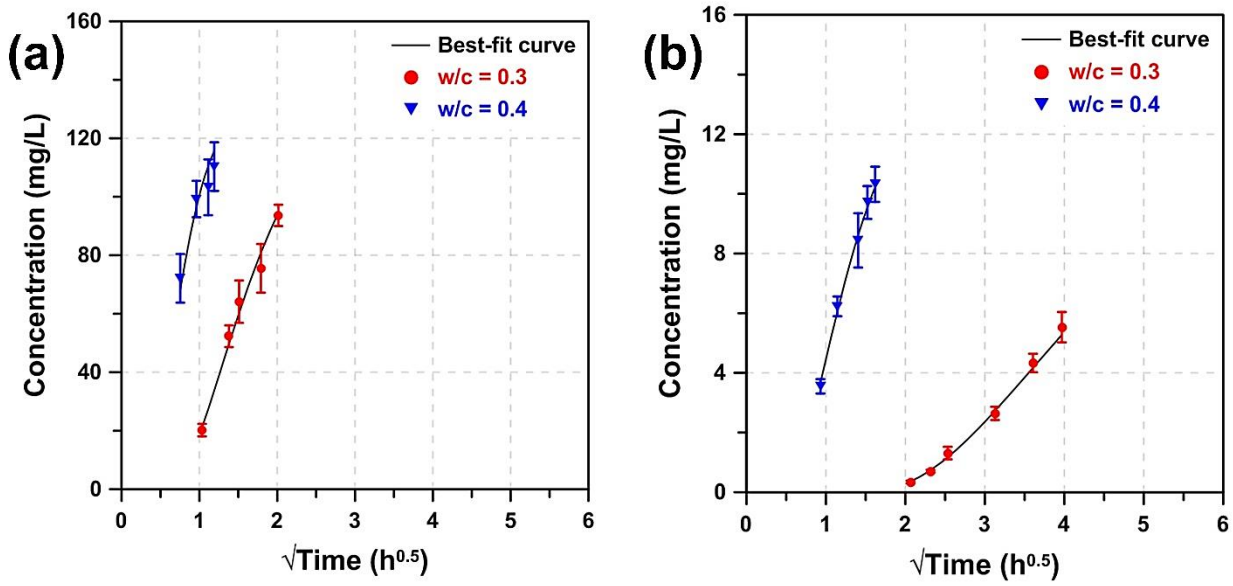

Figure 4.7 Measured concentration of VOC in the sampling bottle during (a) benzene vapor diffusion (b) PCE vapor diffusion tests at 75.3% RH. The best-fit curve is obtained through the numerical solution of Equation 4.2. (The error bars show standard deviation)

Table 4.5 Effective diffusion coefficient of benzene and PCE vapors in saturated and unsaturated cement paste samples with various w/c ratios.

RH (%)	D_e (m^2/s)			
	Benzene		PCE	
	w/c = 0.30	w/c = 0.40	w/c = 0.30	w/c = 0.40
100.0	$(3.41 \pm 0.91) \times 10^{-13}$	$(8.44 \pm 1.12) \times 10^{-13}$	$(2.82 \pm 0.62) \times 10^{-13}$	$(7.31 \pm 1.84) \times 10^{-13}$
97.3	$(9.88 \pm 0.85) \times 10^{-11}$	$(2.01 \pm 0.33) \times 10^{-9}$	$(4.21 \pm 0.69) \times 10^{-11}$	$(3.03 \pm 0.87) \times 10^{-10}$
75.3	$(2.12 \pm 0.44) \times 10^{-9}$	$(1.05 \pm 0.38) \times 10^{-8}$	$(2.63 \pm 0.76) \times 10^{-10}$	$(3.83 \pm 1.02) \times 10^{-9}$

As shown in Table 4.5, the factors influencing the effective diffusivity of VOCs in saturated/unsaturated cement paste include w/c, RH of the environment, and VOC size. Note that the effect of age was eliminated from the controlling factors as the cement paste samples possessed a high degree of hydration at the time of diffusion test. In addition, since the degree of saturation is controlled by w/c ratio and RH of the porous media, it is not included in the factors dominating the effective diffusivity of VOCs in this study. Also, based on the results given in Table 4.5, the

impact of RH on the effective diffusion coefficient of VOCs in unsaturated cement pastes is much greater than that of w/c ratio and VOCs size.

According to Table 4.5, regardless of VOC type, decreasing w/c ratio and increasing RH result in a reduction of the effective diffusion coefficient. Lowering RH led to an increase in the effective diffusivity by about three to five order of magnitudes depending on the w/c ratio and type of VOCs. In this respect, the higher w/c or the lower size of VOCs, the more increase in the effective diffusivity. As can be inferred from the results in Table 4.5, the main reason for these findings would be the faster diffusion of gas species than diffusion of their dissolved form in water (pore solution in cementitious media). The free bulk diffusion coefficients of benzene and PCE vapor in air (D_o) at 25 ^oC are reported as 9.30×10^{-6} m^2/s and 7.64×10^{-6} m^2/s, respectively, whereas their liquid form diffusivities in pure water at 25 ^oC are 1.16×10^{-9} m^2/s and 1.02×10^{-9} m^2/s, respectively, [53, 54, 97], indicating that benzene and PCE diffusion in gas form is of three order of magnitude faster than their diffusion in liquid form while dissolved in water. Also, another reason could be the higher and coarser (discussed in section 4.4.2.1) pore volume as well as less tortuous pore structure (lower tortuosity) in the cement paste with higher w/c ratio.

Besides, for all w/c ratios and RHs, the effective diffusion coefficient of benzene is higher than that of PCE. This difference is more obvious as RH drops especially for cement paste with w/c of 0.30. For instance, by decreasing RH from 100.0% to 75.3% for paste samples with w/c of 0.30, the ratio of the effective diffusion coefficient of benzene to PCE increases from 1.21 to 8.06 while this ratio increases from 1.15 to 2.74 for cement pastes with w/c of 0.40. Higher effective diffusivity of benzene than PCE can be attributed to the smaller molecular size of benzene compared to that of PCE (kinetic diameter of 5.85 Å vs. 6.60 Å). Furthermore, finer pore structure of cement paste with lower w/c can play a key role in increasing the ratio of benzene to PCE

diffusivities by causing the diffusion of larger molecules more difficult to happen and as a result, while more pores in the matrix are accessible to VOC vapor as RH drops, the diffusion of benzene takes place at a higher rate than that of PCE.

4.4.2. Estimation of the effective diffusivity

4.4.2.1 Composite model

To specify pore range for different transport regimes i.e. molecular, transitional, and Knudsen for vapor species and molecular for liquid VOCs, VOCs mean free path need to be first calculated. Using Equation 4.8 and considering a temperature of 25 ^{o}C and kinetic diameters of 5.85 Å and 6.60 Å for benzene and PCE [99-101], respectively, result in the mean free path of 26.7 nm and 21.0 nm for benzene and PCE molecules, respectively.

Kn can be used to determine the pore range affected by each diffusion mechanism in a porous media. By employing Equation 4.7 and the mean free path of benzene and PCE calculated above, Table 4.6 shows the various regions of pore structure under different gas diffusion regimes for benzene and PCE. Note that in these cases, the porous medium is fully dried and thus, gas diffusion happens within the whole matrix.

In addition, according to section 4.3.4.1, the separating pore diameters for 75.3% and 97.3% RHs are 8.7 nm and 79.5 nm, respectively. This results in two different modes of transport i.e. gas and liquid happening in dry and saturated regions, respectively, as given in Table 4.6. Combining conditions in Table 4.6 leads to various diffusion regimes of benzene and PCE as shown in Table 4.7 for 75.3% and 97.3% RHs. According to Table 4.7 and as discussed in section 4.3.4.1.2, Knudsen diffusion region does not exist for benzene and PCE vapor molecules at the

RHs adopted in this study. As such, the main modes of gas (VOCs vapor) transport are transition and molecular diffusions.

Table 4.6 Various gas diffusion regimes existing in a fully dry porous media for benzene and PCE and the effect of RH on the distribution regions of saturated and dry pores.

Condition	Diffusion regime/mode	Effective pore range (diameter in nm)
Benzene vapor diffusion	Knudsen	0 – 2.7
	Transition	2.7 – 267.0
	Molecular	> 267.0
PCE vapor diffusion	Knudsen	0 – 2.1
	Transition	2.1 – 210.0
	Molecular	> 210.0
75.3% RH	Liquid	0 – 8.7
	Gas	> 8.7
97.3% RH	Liquid	0 – 79.5
	Gas	> 79.5

Table 4.7 Diffusion regimes for benzene and PCE in a porous medium equilibrated at 75.3% and 97.3% RHs.

RH (%)	VOCs type	Diffusion mode	Diffusion regime	Effective pore range (diameter in nm)
75.3	Benzene	Liquid	Liquid	0.0 – 8.7
		Gas (vapor)	Transition	8.7 – 267.0
			Molecular	> 267.0
	PCE	Liquid	Liquid	0.0 – 8.7
		Gas (vapor)	Transition	8.7 – 210.0
			Molecular	> 210.0
97.3	Benzene	Liquid	Liquid	0.0 – 79.5
		Gas (vapor)	Transition	79.5 – 267.0
			Molecular	> 267.0
	PCE	Liquid	Liquid	0.0 – 79.5
		Gas (vapor)	Transition	79.5 – 210.0
			Molecular	> 210.0

The diffusivity of VOCs (benzene and PCE) in their vapor (in air) and liquid (in water) forms are given in section 4.4.1. However, the diffusion coefficient of these species in the transition regime is not yet known. According to Bosanquet equation (Equation 4.15), the diffusion coefficient of gas species in the transition regime can be calculated [102].

$$D_T = \left(\frac{1}{D_{iK}} + \frac{1}{D_o}\right)^{-1} \quad (4.15)$$

where D_T is the diffusivity of the gas species *i* in the transition regime, D_{iK} is the Knudsen diffusion in pore i, and D_o is the free bulk diffusivity of the gas species in air which is known for benzene and PCE. As such, D_{iK} is required to be computed to find D_T and employ it in the composite models. Knudsen diffusion coefficient for any gas species is estimated using Equation 4.16 [103, 104].

$$D_{iK} = \frac{d_p}{3}\sqrt{\frac{8RT}{\pi M_i}} \quad (4.16)$$

where d_p (m) is the characteristic length scale of the medium which is the pore diameter assuming that the pores are cylindrical [79, 80], R is the universal gas constant (8.3145 $m^3.Pa.K^{-1}.mol^{-1}$), T is the absolute temperature (K), and M_i the molar weight of gas species *i* (g/mol). It should be pointed out that Knudsen diffusivity for the species *i* is dependent on the pore diameter in which transition regime exists. As shown in Table 4.7, the domain of the region in which transition regime occurs is influenced by the RH and type of diffusing species (benzene or PCE herein). As a result, D_{iK} for each case in Table 4.7 should be separately calculated by weighted averaging the Knudsen diffusivity values for the pores located in the transition diffusion region. For this purpose, the cumulative pore size and volume distribution data (Figure 4.8) are used to obtain D_{iK} for transition region in each diffusion case in Table 4.7 and the results of D_T calculation are given in Table 4.8. Note that although the combined cumulative pore size and volume distribution curves for both cement pastes with w/c ratios of 0.30 and 0.40 are not smooth at the overlap of DWVS and MIP tests results, it would not affect the calculations made in this section as the purpose of using cumulative pore size and volume distributions is solely to find the volume fractions of various diffusion regions.

Since the pore size and distributions of cement pastes with different w/c ratios are not similar, for each w/c ratio there are four different cases of transition region as presented in Table 4.8. In other words, unlike free bulk diffusion of gas species in air and water which are assumed to be constant at any specific environmental conditions (pressure and temperature), the Knudsen diffusivity depends on the pore structure (size and volume of pores in the matrix) of the diffusive media. Another point is that it is assumed to have a single diffusing gas species in all diffusion regimes mentioned above to avoid interacting effects of gas species on their transport. This assumption is reasonable in this study as in the diffusion tests the setup was designed in a way that only a single VOC diffuses in the cement paste samples in each test.

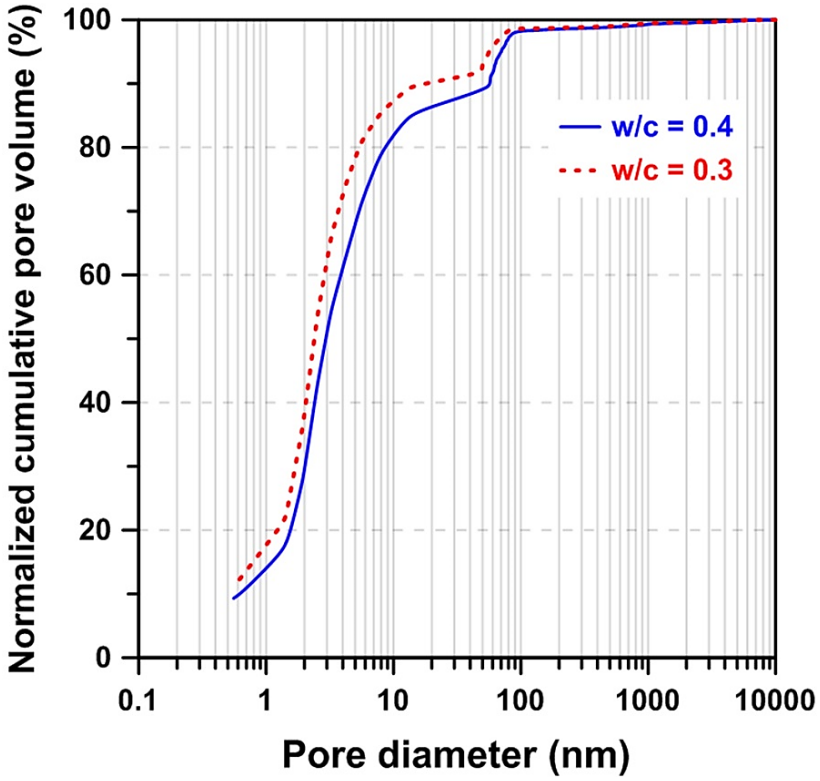

Figure 4.8 Combined cumulative pore size and volume distributions of cement pastes with w/c of 0.30 and 0.40. (Note that the pore volume was normalized to the total permeable pore volume of each sample).

Table 4.8 Diffusivity of benzene and PCE in transition regime for various RH and w/c ratios.

RH (%)	D_T (10^{-6} m^2/s)			
	Benzene		PCE	
	w/c = 0.30	w/c = 0.40	w/c = 0.30	w/c = 0.40
97.3	5.51	5.51	3.89	3.89
75.3	4.40	4.57	3.07	3.18

To develop composite models for predicting the effective diffusivity of VOCs in saturated and unsaturated cement paste samples, parallel and series models (Figure 4.4) were first chosen. To apply Equations 4.12 to 4.14, the volume fraction of each diffusion region is needed to be calculated. As such, combined cumulative pore size and volume distributions of cement paste samples (Figure 4.8) are employed to estimate the contribution of each region in the pore structure. The results of volume fraction estimations for various diffusion regions (given in Table 4.7) are presented in Table 4.9. Using pore structure parameters presented in Table 4.4, the volume fraction values given in Table 4.9, and Equations 4.12 to 4.14, the effective diffusion coefficients predicted by parallel and series models are shown in Figures 4.9a and 4.9b for benzene and PCE diffusions, respectively. As seen in Figure 4.9, parallel and series models provide a range that covers the changes in D_e over the range of degree of saturation studied in the current work.

Table 4.9 Volume fractions of regions with various liquid and gas diffusion regimes for benzene and PCE diffusion in unsaturated cement paste matrix.

Diffusion regime		Benzene				PCE			
		75.3% RH		97.3% RH		75.3% RH		97.3% RH	
		w/c = 0.30	w/c = 0.40	w/c = 0.30	w/c = 0.40	w/c = 0.30	w/c = 0.40	w/c = 0.30	w/c = 0.40
Liquid		0.8604	0.7970	0.9820	0.9702	0.8604	0.7970	0.9820	0.9702
Gas	Transition	0.1276	0.1893	0.0060	0.0161	0.1272	0.1888	0.0056	0.0156
	Molecular	0.0120	0.0137	0.0120	0.0137	0.0124	0.0142	0.0124	0.0142

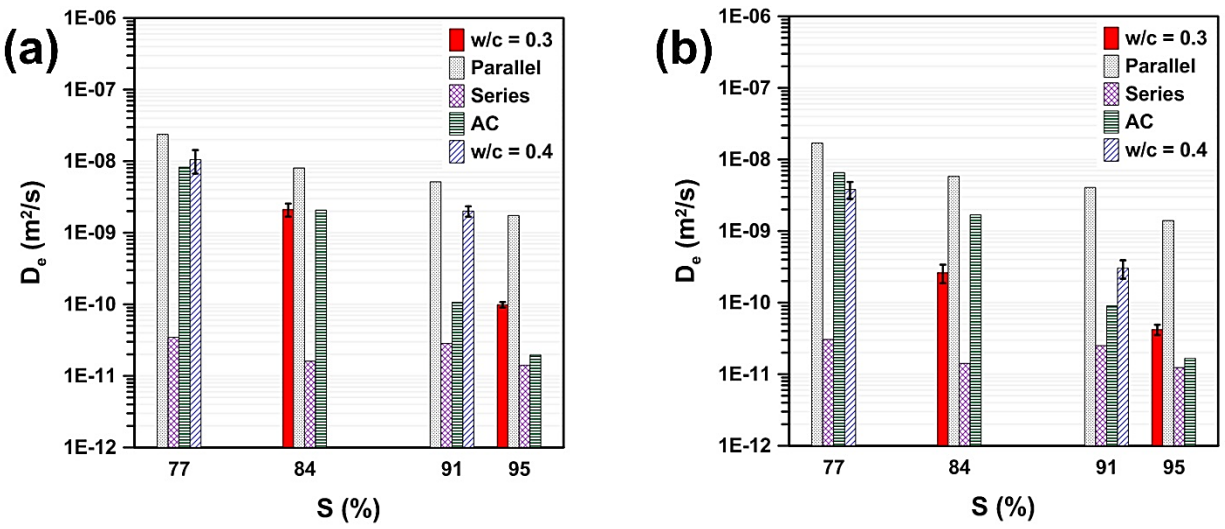

Figure 4.9 Comparison of the experimentally measured D_e of (a) benzene and (b) PCE in unsaturated cement paste with the effective diffusivity predicted by composite models at various degree of saturations.

As observed in Figure 4.9, parallel and series models could only provide a range within which the values of experimentally measured D_e can change. Also, as expected, series model provides the lower boundary since the saturated region has a limiting effect on the diffusivity in the matrix. On the contrary, the effect of liquid region is negligible when the segments of different diffusion regions are in parallel and as such, parallel model gives the upper boundary of D_e. Considering these findings, to further improve the parallel and series composite models in a way that it shows a better estimate of the effective diffusivity, an alternative composite (AC) model is proposed based on the geometry of pores in cement pastes.

For a cement-based sample exposed to the environment at its both sides and equilibrated at a RH lower than 100.0% similar to the unsaturated cement paste samples tested in this study, large pores will be dried out first followed by smaller pores depending on the RH based on Kelvin-Laplace relationship (as discussed in section 4.3.4.1.1). As such, one can say there would be

molecular VOCs vapor diffusion in the large empty pores while in the smaller dry pores there exits transition diffusion (a combination of Knudsen and molecular VOCs vapor diffusions). Also, since very fine pores are the last ones to be dried out, they are fully saturated at the RHs adopted in the current research work. Considering the aforementioned concepts and knowing that a large portion of pores is occupied by the pore solution (water herein) as shown in Table 4.9, Figure 4.10 illustrates the physical interpretation of the alternative composite model. In Figure 4.10, in accordance with the volume fractions given in Table 4.9, the majority of pores are filled with water while a small portion of pore phase is occupied by fully dried small and large pores representing the regions for transition and molecular gas diffusion regimes, respectively.

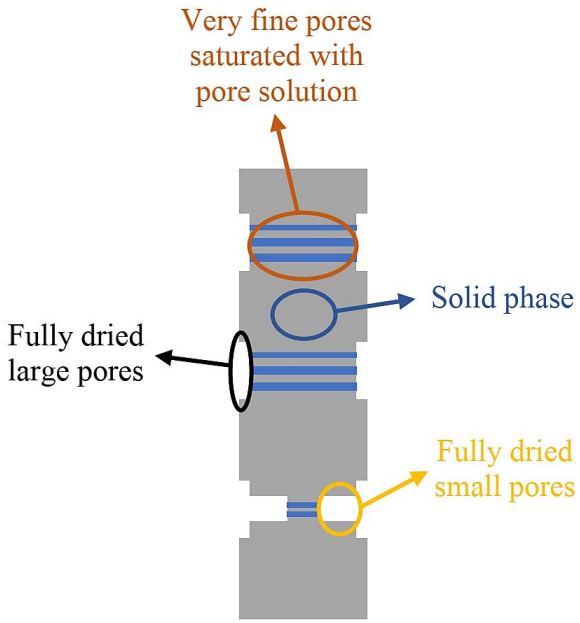

Figure 4.10 Physical interpretation for AC model proposed in this study.

Using the conceptual model proposed for AC (Figure 4.10), it can be inferred that, in the pore phase, part of saturated region is in parallel with the transition regime region both of which

are in series with the region there exists molecular gas diffusion in. In addition, a portion of saturated region is in series with the region of the transition regime. This interpretation of the conceptual model would result in the alternative composite model (AC) shown in Figure 4.11. However, the volume fraction of the liquid (saturated) segment (segment 5) which is in series with the segment of the transition diffusion regime (segment 2) is not known and will be obtained through minimizing the root mean square error of the predicted D_e values compared to the experimental data of D_e.

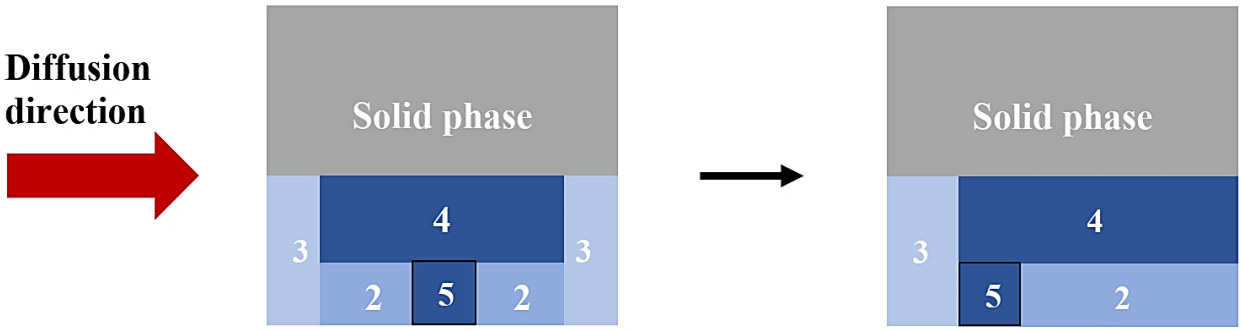

Figure 4.11 Schematic illustration of the alternative composite (AC) model. (Note that the volumes in the picture do not represent the actual volume fractions obtained using cumulative pore size and volume distribution curve).

Note that segment 5 is part of the whole saturated (liquid) region (segment 1 in parallel/series model) already exists in the pore structure and thus, Equation 4.17 gives a relationship between the volume fractions of segments 1 and 5 in the pore phase. This assumption results in a relationship between the volume fractions of the two saturated (liquid) segments (segments 4 and 5) obtained through splitting segment 1 (Equation 4.18).

$$\varphi_5 = \alpha\varphi_1 \tag{4.17}$$

$$\varphi_1 = \varphi_4 + \varphi_5 \rightarrow \varphi_4 = (1-\alpha)\varphi_1 \quad (4.18)$$

where φ_1 is the total volume fraction of saturated (liquid) region in the pore phase shown in Table 4.9 for various diffusion cases, φ_4 is the volume fraction of the saturated phase which is in parallel with the transition diffusion regime segment (segment 2) and φ_5 is the volume fraction of the saturated (liquid) segment which is in series with the segment 2.

By applying law of mixtures to the phase configurations in AC model and utilizing Equations 4.14, 4. 17, and 4.18, D_e can be estimated through Equation 4.19.

$$D_e = \frac{\varphi}{\tau}\left[\frac{(\varphi_1+\varphi_2)^2}{(1-\alpha)\varphi_1 D_1+(\alpha\varphi_1+\varphi_2)^2\left(\frac{\alpha\varphi_1}{D_1}+\frac{\varphi_2}{D_2}\right)^{-1}}+\frac{\varphi_3}{D_3}\right]^{-1} \quad (4.19)$$

where φ_i is the volume fraction of each region already defined in parallel/series composite model (Table 4.9) and D_i is the diffusivity of VOCs in the diffusion regime which is dominant in each specific region.

Utilizing Equation 4.19 and carrying out the minimization of the root mean square error of the predicted D_e values compared to the experimentally measured D_e results, the coefficient α for calculating the volume fraction of segment 5 (φ_5) is calculated as 9.2×10^{-5}. According to Figure 4.9, AC model could provide a good estimate of D_e values compared to parallel and series models.

It is worth mentioning that the values of D_e obtained from various composite models for saturated cement paste samples are all the same due to the existence of only one diffusion regime (liquid) in the whole pore phase ($\varphi_1 = 1$). Furthermore, even though none of the composite models could accurately predict the effective diffusivity of benzene and PCE in saturated cement paste samples, by applying $n = 2$ as the exponent of tortuosity (τ^2) the results do more perfectly match the experimental data as shown in Table 4.10. This observation implies that the impact of tortuosity on liquid diffusion in saturated porous media is more pronounced compared to its influence on gas

diffusion in unsaturated materials. These findings are in good agreement with the empirical models based on tortuosity introduced to predict the diffusion of species in saturated cement-based materials [45].

Table 4.10 Experimentally measured values of D_e vs. the predicted D_e obtained from composite models for saturated cement paste samples (100.0% RH) by employing $n = 2$ as tortuosity's exponent.

D_e (10^{-13} m^2/s)	Benzene		PCE	
	w/c = 0.30	w/c = 0.40	w/c = 0.30	w/c = 0.40
Experimental	3.41	8.44	2.82	7.31
Predicted	6.64	20.23	5.84	17.79

4.4.2.2 Empirical models

As discussed in section 4.3.4.2, employing the empirical models presented in Table 4.1 and the values of D_o (section 4.3.4.2), S (Table 4.3), φ, and τ (Table 4.4), the predicted effective diffusivity of VOCs in unsaturated cement paste samples are shown in Figures 4.12a and 4.12b for benzene and PCE diffusion cases, respectively.

According to Figure 4.12 and considering the least root mean square error of approximation, EM1 (which is a modified form of the well-known Archie's model for diffusion of gas species in unsaturated porous media), EM2 (the model includes both total and air-filled porosities) and EM3 (the model involves total porosity and degree of saturation) models provide the best estimate of the effective diffusion coefficient; nonetheless, none of these models could properly predict the order of magnitude of all the effective diffusion coefficients obtained through experimental tests.

Note that both EM2 and EM3 models provided the same results as they can be converted into each other by selecting the appropriate fitting parameters achieved by optimizing both models to fit the experimental data. Thus, in Figure 4.12, EM2/EM3 model is shown.

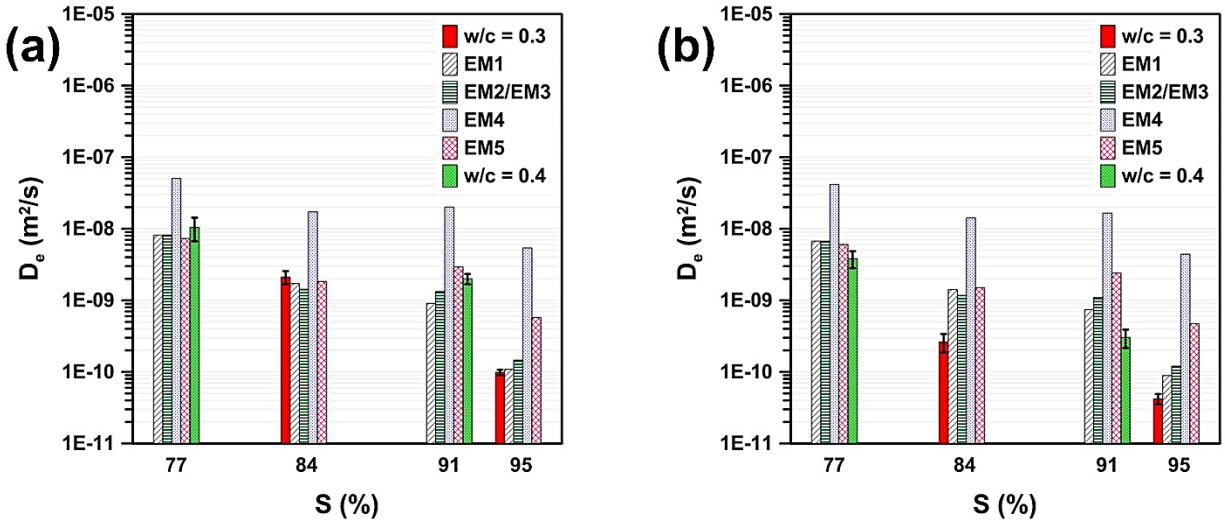

Figure 4.12 Comparison of the experimentally measured D_e of (a) benzene and (b) PCE in unsaturated cement paste with the effective diffusivity predicted by empirical models at various degree of saturations.

Furthermore, the fitting parameters of EM1, EM2, EM3, and EM5 models were achieved through minimizing the root mean square error of the predicted diffusivity values in comparison with their corresponding experimental effective diffusion coefficient and the results are given in Table 4.11. According to Table 4.11, the value of *n* in EM5 (modified tortuosity-based) model was obtained as 1.74 indicating the larger effect of tortuosity on the effective diffusivity of VOCs in unsaturated cement paste samples as compared with tortuosity's exponent in EM4 model which is a widely-accepted empirical model for predicting the effective diffusion coefficient of gas species in unsaturated porous media such as soil and cement-based materials. This is also the main reason

why EM4 model gives the furthest results from the diffusivity values measured experimentally. Also, it is interesting to mention that as discussed in section 4.4.2.1, the value of $n = 2$ is used as tortuosity's exponent in the empirical models developed for predicting D_e in saturated porous media [45] and thus, the results obtained in this study indicate that the effect of tortuosity in gas diffusion in unsaturated porous material is almost similar to its impact on the diffusion in saturated diffusive media. Note that empirical models are developed solely for gas diffusion in unsaturated porous media and that is why they were not utilized to predict the results obtained for 100.0% RH.

Table 4.11 Fitting parameters of the empirical models for predicting the effective diffusion coefficient of VOCs in unsaturated cement paste.

EM1		EM2		EM3		EM5
A	B	C	D	E	F	n
0.43	2.38	1.96	1.71	3.67	1.96	1.74

4.5 Concluding remarks

The current study aims to experimentally and theoretically estimate the effective diffusion coefficient of the vapor of benzene and PCE as two of major water pollutants in unsaturated cement paste. VOCs vapor diffusion through saturated cement paste (100.0% RH) was also measured for comparison purposes.

The results indicate that by increasing the RH or lowering the w/c ratio, the effective diffusion coefficient of VOCs is decreased. In addition, VOCs type would affect the effective diffusivity of VOCs in saturated/unsaturated cementitious media; the larger the VOCs, the lower the effective diffusion coefficient .However, the effect of RH is much larger than that of w/c ratio and VOCs size as evidenced by the experimental data. In this respect, through reducing RH from 100.0% to 75.3%, the effective diffusivity of VOCs vapor was increased by three to five order

magnitudes depending on the w/c ratio whereas, the effect of w/c on D_e was of one to two order of magnitudes in unsaturated cement paste samples.

To predict the effective diffusion coefficient of benzene and PCE in unsaturated cement pastes, various composite and empirical models were used and modified to achieve the best estimate within the range of RH studied (75.3% to 100.0%).

To develop models based on the composite theory, a modified pore size and volume distribution for cement pastes was constructed by combining the data obtained from DWVS and MIP tests. Parallel and series models give the boundary of changes in D_e value and thus, an alternative composite (AC) model was proposed to represent the cement paste matrix and enhance the accuracy of the prediction of VOCs effective diffusivity by employing pore structure parameters and pore size and volume distribution on the basis of coexistence of various regimes of gas and liquid diffusions in the pore phase of an unsaturated cement-based material.

Through minimizing the root mean square error of the predicted values of D_e with respect to those experimentally obtained, an attempt was made to find the fitting parameters of the empirical models for the case of benzene and PCE vapors diffusion through unsaturated cement paste samples. The empirical models were then compared based on providing the least root mean square error of prediction. Among the empirical models, the modified form of Archie's model for diffusion of gas species in unsaturated porous media (EM1) accompanied by EM2/EM3 models showed the best prediction performance. In addition, the modified tortuosity-based model (EM5) could better predict D_e in comparison with the tortuosity-based model (EM4) commonly used in estimating the effective diffusivity in unsaturated porous media. The exponent of tortuosity (n) was obtained as 1.74 for EM5 indicating that the effect of tortuosity on D_e should be more highlighted.

Chapter 5

Summary and Concluding Remarks

The present thesis was aimed at i) quantifying the effect of two major water contaminants (benzene and PCE herein) on mechanical degradation of PVC pipe and rubber gaskets in terms of developing a tensile strength degradation model, ii) measuring the effective diffusivity of benzene and PCE in saturated and unsaturated cement pastes, and iii) modifying the existing empirical models and introducing new models by incorporating the factors dominating VOCs diffusion in cement-based materials as well as employing composite theory.

In chapter 2, the degradation of mechanical properties of PVC pipe and three types of rubber gaskets including chloroprene rubber, nitrile butadiene rubber (NBR), and fluoroelastomer rubber due to their exposure to water contaminated with benzene or PCE was investigated in terms of tensile strength loss. To speed up the degradation and capture the changes in tensile strength over a wider range of temperature, an accelerated aging method was adopted at an elevated temperature of 20 ^{o}C, 40 ^{o}C, and 60 ^{o}C. Using the data from the tension test on aged and unaged samples, WLF method was then employed to develop a model capable of predicting tensile strength degradation of PVC and rubber gaskets over time at any temperature of interest within the range used in aging (20 ^{o}C herein). Furthermore, the developed model for PVC was successfully utilized to introduce a new method to indirectly estimate the rate of thickness loss of PVC pipe wall by tensile strength measurements during aging process.

In chapter 3, the transport of benzene and PCE in the forms of vapor and liquid through saturated cement paste samples was assessed. Various cement paste samples with w/c of 0.30, 0.40, and 0.60 were tested to investigate the effect of pore structure characteristics on the effective diffusivity of VOCs. Diffusion test results indicate that the effective diffusion coefficient of benzene and PCE increases by decreasing their kinetic diameter and increasing the w/c ratio of the cement-based materials, nonetheless, the former's contribution is negligible compared to w/c ratio. In addition, it was shown that solubility and free bulk diffusivity of VOCs drops as the ionic strength of cement paste pore solution increases (representing lowering w/c ratio or increasing the age of cement-based materials). To estimate the effective diffusivity of VOCs in saturated cement paste, empirical models were modified among which the modified Archie's model could best estimate the effective diffusivity data. Also, phenomenological models developed by incorporating the factors affecting the effective diffusivity of VOCs in saturated cement paste were able to accurately predict D_e.

In chapter 4, benzene and PCE vapor diffusion in unsaturated cement paste samples were studied and compared with the saturated samples. Results show that by increasing the RH or decreasing the w/c ratio of unsaturated cement paste samples, the effective diffusion coefficient of VOCs decreases. The influence of RH is, however, larger than that of w/c ratio and VOCs size. Furthermore, to predict the effective diffusivity of VOCs in unsaturated cement pastes, using composite theory, composite models (parallel and series) representing the microstructure of cement pastes were developed considering various diffusion regimes in the pore structure which itself depends on the pore size and volume distribution in the matrix and physical characteristics of diffusing species (VOCs herein). The parallel and series composite models were then further modified based on a conceptual model simulating the pore phase of cement-based matrices to

achieve the most representing model for VOCs diffusion in unsaturated cement paste samples. Finally, some widely used empirical models were used to predict the effective diffusivity of VOCs and were modified to improve their accuracy. Among empirical models studied, the modified form of Archie's model for unsaturated porous media showed the best estimation results as confirmed by its least root mean square error of the prediction values.

Note that although this study focuses on cement paste to investigate the fundamentals of diffusion in cementitious media, the results can be employed to estimate the diffusivity of benzene and PCE in concrete materials by using composite theory and considering that aggregates are impermeable due to their negligible porosity. This way, the outcomes of the current study can be extended to the actual cases in which concrete pipes of different mix proportions are utilized.

REFERENCES

[1] T.M. Holsen, J.K. Park, D. Jenkins, and R.E. Selleck. Contamination of potable water by permeation of plastic pipe. *Journal of American Water Works Association*, 1991, 83(8):53–56.

[2] AWWA. *Permeation and Leaching*. Environmental Protection Agency (EPA), 2002.

[3] D.H. Koo. *Assessment and Calculation of BTEX Permeation through HDPE Water Pipe.* School of Engineering and Technology. Purdue University Indianapolis, 2012.

[4] F. Mao. *Permeation of Hydrocarbons through Polyvinyl Chloride (PVC) and Polyethylene (PE) Pipes and Pipe Gaskets*. Iowa State University, 2008.

[5] A.J. Whelton, and T. Nguyen. Contaminant migration from polymeric pipes used in buried potable water distribution systems: A review. *Critical Reviews in Environmental Science and Technology*, 2013, 43:679–751.

[6] S. Burn, P. Davis, T. Schiller, B. Tiganis, G. Tjandraatmadja, M. Cardy, S. Gould, P. Sadler, and A.J. Whittle. *Long-Term Performance Prediction for PVC Pipes*. Water Research Foundation (AwwaRF), 2005.

[7] A.R. Berens, Prediction of organic chemical permeation through PVC pipe. *Journal American Water Works Association*, 1985. 77(11):57–64.

[8] M.W. Vonk, *Permeation of Organic Compounds through Pipe Materials*. Publication No. 85. KIWA, 1985.

[9] J.K. Park, L. Bontoux, T.M. Holsen, D. Jenkins, and R.E. Selleck. Permeation of polybutylene pipe and gasket material by organic chemicals. *Journal of American Water Works Association*, 1991. 83(10):71–78.

[10] C.L. Cheng, J.A. Gaunt, F. Mao, and S.K. Ong. Permeation of gasoline through DI pipe gaskets in water mains. *Journal of American Water Works Association*, 2012. 104(4):73,74.

[11] F.P. Reding, E.R. Walter, and F.J. Welch. Glass transition and melting point of Poly(vinyl Chloride). *Journal of Polymer Science*, 1962. 56:225–231.

[12] R.K. Rowe, T. Mukunoki, and H.P. Sangam. BTEX diffusion and sorption for a geosynthetic clay liner at two temperatures. *Journal of Geotechnical and Geoenvironmental Engineering*, 2005. 131(10):1211–1221.

[13] R.P. Brown, *Practical Guide to the Assessment of the Useful Life of Rubbers*. Rapra Technology Ltd., 2001.

[14] N.L. Thomas, and A.H. Windle. Theory of case II diffusion. *Polymer*, 1982. 23(4):529–542.

[15] T.M. Aminabhavi, and H.G. Naik. Chemical compatibility testing of geomembranes sorption/desorption, diffusion and swelling phenomena. *Geomembranes and Geotextiles*, 1998. 16 (6):333–354.

[16] M. Saleem, A.A. Asfour, D. De Kee, and B. Harison. Diffusion of organic penetrant through low density polyethylene (LDPE) films: effect of size and shape of the penetrant molecules. *Journal of Applied Polymer Science*, 1989. 37(3):617–625.

[17] J.H. Jensen, and J.C. Kromann. The molecule calculator: A web application for fast quantum mechanics-based estimation of molecular properties. *Journal of Chemical Education*, 2013. 90(8):1093–1095.

[18] F. Mao, J.A. Gaunt, and S.K. Ong. Permeation of organic contaminants through PVC pipes. *Journal of American Water Works Association*, 2009. 101(5):128–136.

[19] X. Guo, C. Chen, and J. Wang. Sorption of sulfamethoxazole onto six types of microplastics. *Chemosphere*, 2019. 228:300–308.

[20] B. Wu, C.M. Taylor, D.R.U. Knappe, M.A. Nanny, and M.A. Barlaz. Factors controlling alkylbenzene sorption to municipal solid waste. *Environmental Science and Technology*, 2001. 35(22):4569–4576.

[21] V. Le Saux, P.Y. Le Gac, Y. Marco, and S. Calloch. Limits in the validity of Arrhenius predictions for field ageing of a silica filled polychloroprene in a marine environment. *Polymer Degradation and Stability*, 2014. 99:254–261.

[22] F. Mao, J.A. Gaunt, C.L. Cheng, and S.K. Ong. Microscopic visualization technique to predict the permeation of organic solvents through PVC pipes in water distribution systems. *Journal of Environmental Engineering*, 2011. 137(2):137–145.

[23] Crank, J. *The Mathematics of Diffusion*, Clarendon, Oxford, 1975.

[24] Comyn, J. *Polymer Permeability*, Elsevier Applied Science Publishers, Essex, 1985.

[25] T.J. Alfrey, E.F. Gurnee, and W.G. Lloyd. Diffusion in glassy polymers. *Journal of Polymer Science: Part C*, 1966. 12(1):249–261.

[26] A. Peyvandi, and P. Soroushain. Structural performance of dry-cast concrete nanocomposite pipes. *Materials and Structures*, 2015. 48(1):461–470.

[27] R. Meininghaus, L. Gunnarsen, and H.N. Knudsen. Diffusion and sorption of volatile organic compounds in building materials - Impact on indoor air quality. *Environmental Science and Technology*, 2000. 34(15):3101–3108.

[28] Y. Farajollahi, Z. Chen, and F. Haghighat. An experimental study for examining the effects of environmental conditions on diffusion coefficient of VOCs in building materials. *Clean*, 2009. 37(6):436–443.

[29] C. De Biase, S. Loechel, T. Putzmann, M. Bittens, H. Weiss, and B. Daus. Volatile organic compounds effective diffusion coefficients and fluxes estimation through two types of construction material. *Indoor Air*, 2014. 24:272–282.

[30] V.C. Goreham, and C.B. Lake. Diffusion and sorption of volatile organic compounds through soil-cement materials. *Environmental Geotechnics*, 2018. 5(3):134–145.

[31] I. Pane, and W. Hansen. Investigation of blended cement hydration by isothermal calorimetry and thermal analysis. *Cement and Concrete Research*, 2005. 35:1155– 1164.

[32] T.C. Powers, and T.L. Brownyard. *Studies of the physical properties of hardened Portland cement paste*. Bulletin 22. Chicago: Research and Development Laboratories of the Portland Cement Association; 1948.

[33] Y. Bu, R. Spragg, and W.J. Weiss. Comparison of the pore volume in concrete as determined using ASTM C 642 and vacuum saturation. *Advances in Civil Engineering Materials*, 2014. 3(1):308–315.

[34] National Institute of Science and Technology, *Estimation of Pore Solution Conductivity*, NIST Engineering Laboratory/Materials and Structural Systems Division, Gaithersburg, MD, 2017.

[35] B. Prakash, A.D. Zaffiro, M. Zimmerman, D.J. Munch, and B.V. Pepich. *Measurement of Purgeable Organic Compounds in Water by Capillary Column Gas Chromatography/Mass Spectrometry*, Method 524.3, U.S. Environmental Protection Agency, Washington, DC, 2009.

[36] G.H. Robert, F.R. Liewehr, T.B. Buxton, and J.C. McPherson. Apical diffusion of calcium hydroxide in an in vitro model. *Journal of Endodontic*, 2005. 31(1):57–60.

[37] B. Athanassiadis, and L.J. Walsh. Aspects of solvent chemistry for calcium hydroxide medicaments. *Materials*, 2017. 10(10):1219.

[38] J. Staudinger, and P.V. Roberts. A critical compilation of Henry's law constant temperature dependence relations for organic compounds in dilute aqueous solutions. *Chemosphere*, 2001. 44:561–576.

[39] C.B. Lake, G. Arefi, and P.K. Yuet. Examining fly ash as a sorbent for benzene, trichloroethylene, and ethylbenzene in cement-treated soils. *Canadian Geotechnical Journal*,

2013. 50:423–434.

[40] G.E. Archie. The electrical resistivity log as an aid in determining some reservoir characteristics. *Journal of Petroleum Technology*, 1942. 146(1):54–62.

[41] W.O. Winsauer, H.M. Shearin, P.H. Masson, and M. Williams. Resistivity of brine-saturated sands in relation to pore geometry. *Bulletin of American Association of Petroleum Geologists*, 1952. 36:253–277.

[42] P. Grathwohl. *Diffusion in Natural Porous Media: Contaminant Transport, Sorption/Desorption and Dissolution Kinetics*, 1st ed., Kluwer Academic Publishers, Boston, 1998.

[43] M.R.J. Wyllie, and M.B. Spangler. Application of electrical resistivity measurements to problem of fluid flow in porous media. *Bulletin of American Association of Petroleum Geologists*, 1952. 36:359–403.

[44] G. Dogu, and J.M. Smith. A dynamic method for catalyst diffusivities. *AIChE Journal*, 1975. 21:58–61.

[45] P. Yang, G. Sant, and N. Neithalath. A refined, self-consistent Poisson-Nernst-Planck (PNP) model for electrically induced transport of multiple ionic species through concrete. *Cement and Concrete Composites*, 2017. 82:80–94.

[46] P.J. Tumidajski, A.S. Schumacher, S. Perron, P. Gu, and J.J. Beaudoin. On the relationship between porosity and electrical resistivity in cementitious systems. *Cement and Concrete Research*, 1996. 26:539–544.

[47] N. Neithalath, and J. Jain. Relating rapid chloride transport parameters of concretes to microstructural features extracted from electrical impedance. *Cement and Concrete Research*, 2010. 40:1041–1051.

[48] W.J. Weiss, T.J. Barrett, C. Qiao, and H. Todak. Toward a specification for transport properties of concrete based on the formation factor of a sealed specimen. *Advances in Civil Engineering Materials*, 2016. 5(1):179−194.

[49] C. Qiao, M.K. Moradllo, H. Hall, M.T. Ley, and W.J. Weiss. Electrical resistivity and formation factor of air-entrained concrete. *ACI Materials Journal*, 2019. 116(3):85–93.

[50] M.K. Moradllo, C. Qiao, B. Isgor, S. Reese, and W.J. Weiss. Relating formation factor of concrete to water absorption. *ACI Materials Journal*, 2018.115(6):887–898.

[51] P.K. Grover, and R.L. Ryall. Critical appraisal of salting-out and its implications for chemical

and biological sciences. *Chemical Reviews*, 2005. 105:1–10.

[52] S. Endo, A. Pfennigsdorff, and K.U. Goss. Salting-out effect in aqueous NaCl solutions: Trends with size and polarity of solute molecules. *Environmental Science & Technology*, 2012. 46:1496−1503.

[53] B.E. Poling J.M. Prausnitz, J.P. O'Connell, *The Properties of Gases and Liquids*, 5th ed., McGraw-Hill, New York, 2001.

[54] C.L. Yaws. *Handbook of Transport Property Data*, Gulf, Houston, 1995.

[55] C.R. Wilke, and P. Chang. Correlation of diffusion coefficients in dilute solutions. *AIChE Journal*, 1955. 1:264–270.

[56] D.E. Goldsack, and R. Franchetto. The viscosity of concentrated electrolyte solutions. I. Concentration dependence at fixed temperature. *Canadian Journal of Chemistry*, 1977. 55:1062–1072.

[57] J.D. Bernal, and R.H. Fowler. A theory of water and ionic solution, with particular reference to hydrogen and hydroxyl ions. *The Journal of Chemical Physics*, 1933. 1(8):515–548.

[58] K.D. Collins. Charge density-dependent strength of hydration and biological structure. *Biophysical Journal*, 1997. 72:65−76.

[59] T.C. Chan, H.T. Li, and K.Y. Li. Effects of shapes of solute molecules on diffusion: A study of dependences on solute size, solvent, and temperature. *Journal of Physical Chemistry B*, 2015. 119:15718−15728.

[60] R. Vasanthi, S. Bhattacharyya, and B. Bagchi. Anisotropic diffusion of spheroids in liquids: Slow orientational relaxation of the oblates. *Journal of Chemical Physics*, 2002. 116:1092−1096.

[61] G. Le Bas, *The Molecular Volumes of Liquid Chemical Compounds from the Point of View of Kopp*, Longmans, Green and Co., London, 1915.

[62] F. Rajabipour, and J. Weiss. Electrical conductivity of drying cement paste. *Materials and Structures*, 2007. 40:1143–1160.

[63] T. Itakura, D.W. Airey, and C.J. Leo. The diffusion and sorption of volatile organic compounds through kaolinitic clayey soils. *Journal of Contaminant Hydrology*, 2003. 65(3–4):219–243.

[64] R.P. Spragg, J. Castro, W. Li, M. Pour-Ghaz, P.T. Huang, and J. Weiss. Wetting and drying of concrete using aqueous solutions containing deicing salts. *Cement and Concrete*

Composites, 2011. 33(5):535–542.

[65] W. Li, M. Pour-Ghaz, J. Castro, and J. Weiss. Water absorption and critical degree of saturation relating to freeze-thaw damage in concrete pavement joints. *Journal of Materials in Civil Engineering*, 2012. 24(3):299–307.

[66] A. Voss, P. Hosseini, M. Pour-Ghaz, M. Vauhkonen, and A. Seppänen. Three-dimensional electrical capacitance tomography – A tool for characterizing moisture transport properties of cement-based materials. *Materials and Design*, 2019. 181:107967.

[67] E.W. Washburn. Note on a method of determining the distribution of pore sizes in porous materials. *Proceedings of the National Academy of Sciences of the USA*, 1921.7(4):115–116.

[68] IUPAC. Manual of symbols and terminology, appendix 2, Pt.1, colloid and surface chemistry. *Pure and Applied Chemistry*, 1972. 31:578–680.

[69] C. Leech, D. Lockington, and R.D. Hooton. Estimation of water retention curve from mercury intrusion porosimetry and van Genuchten model. *ACI Structural Journal*, 2006. 103(2):291–295.

[70] M. Wu, B. Johannesson, and M. Geiker. Application of water vapor sorption measurements for porosity characterization of hardened cement pastes. *Construction and Building Materials*, 2014. 66:621–633.

[71] E.P. Barrett, L.G. Joyner, and P.P. Halenda. The determination of pore volume and area distributions in porous substances: I. Computations from nitrogen isotherms. *Journal of the American Chemical Society*, 1951. 73:373–380.

[72] K.M. Rath, A. Maheshwari, P. Bengtson, and J. Rousk. Comparative toxicities of salts on microbial processes in soil. *Applied and Environmental Microbiology*, 2016. 82(7):2012–2020.

[73] J. Heinz, J. Schirmack, A. Airo, S.P. Kounaves, and D. Schulze-Makuch. Enhanced microbial survivability in subzero brines. *Astrobiology*, 2018. 18(9):1171–1180.

[74] S. Brunauer, R.S. Mikhail, and E. Bodor. Some remarks about capillary condensation and pore structure analysis. *Journal of Colloid and Interface Science*, 1967. 25 (3):353–358.

[75] J. Hagymassy, S. Brunauer, and R.S. Mikhail. Pore structure analysis by water vapor adsorption: I.t-curves for water vapor. *Journal of Colloid and Interface Science*, 1969. 29(3):485–491.

[76] V. Baroghel-Bouny. Water vapour sorption experiments on hardened cementitious materials

Part I: Essential tool for analysis of hygral behavior and its relation to pore structure. *Cement and Concrete Research*, 2007. 37:414–437.

[77] M. Boumaaza, B. Huet, G. Pham, P. Turcry, A. Ait-Mokhtar, and C. Gehlen. A new test method to determine the gaseous oxygen diffusion coefficient of cement pastes as a function of hydration duration, microstructure, and relative humidity. *Materials and Structures*, 2018. 51:51.

[78] R.B. Bird, W.E. Stewart, and E.N. Lightfoot. *Transport Phenomena*, 2nd ed., John Wiley & Sons, New York, 2007.

[79] J. Sercombe, R. Vidal, C. Gallé, and F. Adenot. Experimental study of gas diffusion in cement paste. *Cement and Concrete Research*, 2007. 37:579–588.

[80] D.M. Tartakovsky, and M. Dentz. Diffusion in porous media: Phenomena and mechanisms. *Transport in Porous Media*, 2019. 130:105–127.

[81] S.Q. Zeng, A. Hunt, and R. Greif. Mean free path and apparent thermal conductivity of a gas in a porous medium. *Journal of Heat Transfer*, 1995. 117:758–761.

[82] T.H. Vu, F. Frizon, and S. Lorente. Architecture for gas transport through cementitious materials. *Journal of Physics D: Applied Physics*, 2009. 42:105501.

[83] C. Liu, Z. Liu, and Y. Zhang. A multi-scale framework for modelling effective gas diffusivity in dry cement paste: Combined effects of surface, Knudsen and molecular diffusion. *Cement and Concrete Research*, 2020. 131:106035.

[84] I.Y. Akkutlu, and E. Fathi. Multiscale gas transport in shales with local kerogen heterogeneities. *SPE Journal*, 2012. 17(4):1002–1011.

[85] N.E. Marcovich, M.M. Reboredo, and M.I. Aranguren. Moisture diffusion in polyester–woodflour composites. *Polymer*, 1999. 40:7313–7320.

[86] S. Barman, H. Rootzén, and D. Bolin. Prediction of diffusive transport through polymer films from characteristics of the pore geometry. *AIChE Journal*, 2019. 65(1):446–457.

[87] J.A. Currie. Gaseous diffusion in porous media. Part 2 - Dry granular materials. *British Journal of Applied Physics*, 1960. 11(8):318–324.

[88] A.R. Grable, and E.G. Siemer. Effect of bulk density, aggregate size and soil water suction on oxygen diffusion, redox potentials and elongation of corn roots. *Soil Science Society of America, Proceedings*, 1968. 32:180–186.

[89] S.H. Lai, J.M. Tiedje, and A.E. Erickson. In situ measurement of gas diffusion coefficient in

soils. *Soil Science Society of America Journal*, 1976. 40(1):3–6.

[90] T. Fujikawa, and T. Miyazaki. Effects of bulk density and soil type on the gas diffusion coefficient in repacked and undisturbed soils. *Soil Science*, 2005. 170(11):892–901.

[91] R.J. Millington. Gas diffusion in porous media. *Science*, 1959. 130(3367):100–102.

[92] R.J. Millington, and J.P. Quirk, *Transport in Porous Media*. In: F.A. Van Baren et al. (eds.) International Congress of Soil Science, 7th, Vol. 1. Madison, WI, pp 97–106, 14-24 August 1960, Elsevier, Amsterdam.

[93] A. Sallam, W.A. Jury, and J. Letey. Measurement of gas diffusion coefficient under relatively low air-filled porosity. *Soil Science Society of America Journal*, 1984. 48(1):3–6.

[94] X. Xu, J.L. Nieber, and S.C. Gupta. Compaction effect on the gas diffusion coefficient in soils. *Soil Science Society of America Journal*, 1992. 56(6):1743–1750.

[95] M. Thiery, G. Villain, P. Dangla, and G. Platret. Investigation of the carbonation front shape on cementitious materials: Effects of the chemical kinetics. *Cement and Concrete Research*, 2007. 37(7):1047–1058.

[96] D. Benavente, and C. Pla. Effect of pore structure and moisture content on gas diffusion and permeability in porous building stones. *Materials and Structures,* 2018. 51:21.

[97] US Environmental Protection Agency (US EPA). *Intermedia transfer factors for contaminants found at hazardous waste sites: Tetrachloroethylene*. Washington, DC, 1994. Available at https://dtsc.ca.gov/wp-content/uploads/sites/31/2018/01/pce.pdf (accessed June 2020).

[98] L.C. Price. Aqueous solubility of petroleum as applied to its origin and primary migration. *American Association of Petroleum Geologists Bulletin*, 1976. 60(2):213–244.

[99] C. Tung, L. Wu, L. Zhang, H. Li, X. Yi, K. Song, M. Xu, Z. Yuan, J. Guan, H. Wang, Y. Ying, and X. Xu. Microreactor-controlled selectivity in organic photochemical reactions. *Pure and Applied Chemistry*, 2000. 72(12):2289–2298.

[100] M.J. Lashaki, M. Fayaz, S. Niknaddaf, and Z. Hashisho. Effect of the adsorbate kinetic diameter on the accuracy of the Dubinin–Radushkevich equation for modeling adsorption of organic vapors on activated carbon. *Journal of Hazardous Materials*, 2012. 241–242:154–163.

[101] A. Bembnowska, R. Pełech, and E. Milchert. Adsorption from aqueous solutions of chlorinated organic compounds onto activated carbons. *Journal of Colloid and Interface Science*, 2003. 265:276–282.

[102] W.G. Pollard, and R.D. Present. On gaseous self-diffusion in long capillary tubes. *Physical Review*, 1948. 73:762.

[103] E.A. Mason, and A.P. Malinauskas, *Gas Transport in Porous Media: The Dusty Gas Model*, Elsevier, Amsterdam, 1983.

[104] W. Kast, and C.R. Hohenthanner. Mass transfer within the gas-phase of porous media. *International Journal of Heat and Mass Transfer*, 2000. 43:807–823.

APPENDICES

Appendix A

Tensile Strength Test Results for Rubber Gaskets and PVC Pipe Samples

Table A1 Actual data of tensile strength measurements on aged CR gasket specimens.

Exposure media	Aging temperature (°F)	Aging duration (week)	Tensile strength (psi)
PCE-saturated aqueous solution	68	1	381 ± 22
		6	341 ± 26
		13	302 ± 19
		30	269 ± 33
	104	1	389 ± 02
		6	318 ± 30
		13	281 ± 05
		30	240 ± 20
	140	1	374 ± 04
		6	290 ± 13
		13	191 ± 17
		30	NA
Benzene-saturated aqueous solution	68	1	364 ± 04
		6	317 ± 11
		13	287 ± 21
		30	205 ± 11
	104	1	354 ± 03
		6	266 ± 16
		13	197 ± 08
		30	148 ± 31
	140	1	331 ± 18
		6	238 ± 18
		13	NA
		30	NA

Table A2 Actual data of tensile strength measurements on aged NBR gasket specimens.

Exposure media	Aging temperature (°F)	Aging duration (week)	Tensile strength (psi)
PCE-saturated aqueous solution	68	1	839 ± 76
		6	805 ± 56
		13	701 ± 04
		30	653 ± 39
	104	1	790 ± 17
		6	725 ± 51
		13	618 ± 20
		30	572 ± 33
	140	1	734 ± 66
		6	697 ± 09
		13	575 ± 28
		30	NA
Benzene-saturated aqueous solution	68	1	700 ± 07
		6	648 ± 45
		13	568 ± 11
		30	488 ± 38
	104	1	650 ± 49
		6	622 ± 50
		13	525 ± 28
		30	449 ± 13
	140	1	643 ± 35
		6	590 ± 03
		13	NA
		30	NA

Table A3 Actual data of tensile strength measurements on aged FKM gasket specimens.

Exposure media	Aging temperature (°F)	Aging duration (week)	Tensile strength (psi)
PCE-saturated aqueous solution	68	1	952 ± 65
		6	898 ± 57
		13	795 ± 32
		30	777 ± 26
	104	1	946 ± 67
		6	887 ± 22
		13	761 ± 30
		30	739 ± 45
	140	1	923 ± 77
		6	871 ± 59
		13	730 ± 25
		30	NA
Benzene-saturated aqueous solution	68	1	928 ± 52
		6	878 ± 69
		13	711 ± 21
		30	641 ± 38
	104	1	903 ± 20
		6	845 ± 17
		13	649 ± 60
		30	558 ± 36
	140	1	857 ± 65
		6	827 ± 16
		13	517 ± 41
		30	NA

Table A4 Actual data of tensile strength measurements on aged PVC specimens.

Exposure media	Aging temperature (°F)	Aging duration (week)	Tensile strength (psi)
PCE-saturated aqueous solution	68	1	6816 ± 076
		6	6788 ± 200
		13	6603 ± 068
		30	6188 ± 291
	104	1	6764 ± 058
		6	6535 ± 141
		13	6361 ± 131
		30	5893 ± 223
	140	1	6730 ± 164
		6	6399 ± 069
		13	6259 ± 023
		25	5538 ± 016
Benzene-saturated aqueous solution	68	1	6845 ± 078
		6	6512 ± 070
		13	6358 ± 032
		30	5231 ± 275
	104	1	6603 ± 066
		6	6390 ± 055
		13	5280 ± 060
		30	1490 ± 245
	140	1	6561 ± 082
		6	6167 ± 089
		13	2761 ± 650
		30	NA

Appendix B

Relationships between Concentrations in the Diffusion Cell

To calculate the effective diffusion coefficient (D_e) of VOCs vapor for saturated cement paste, the concentrations at both ends of the sample are required. Based on the design of diffusion cell, VOCs pre-dissolved in the solution of source bottle evaporates into the air in the headspace following Henry's law. Therefore, as the concentration of VOCs in the deionized distilled water is known which equals the solubility limit of the VOCs of interest in the pure water (for example 1790 mg/L for benzene), using Henry's law constant (air-water partitioning coefficient), one can obtain the concentration of VOCs vapor in the air of the source bottle. In this respect, an average dimensionless HLC for benzene and PCE dissolved in pure water at 25 ^{o}C (HLC_1) is 0.2279 and 0.6470, respectively [1, 2], and can be employed to obtain the concentration of VOCs in the headspace of the source and sampling bottles.

Now, as the cement paste sample is saturated, VOCs vapor needs to dissolve in the pore solution of the sample (at x = 0) and then diffuses through it until reaching the other end of the sample (x = L) at which boundary the VOCs liquid will evaporate and enter the air in the headspace of the sampling bottle. The dissolution and evaporation of VOCs between the sample and air at its both ends follow Henry's law as we are dealing with dilute solutions of VOCs. However, since the composition of the pore solution is different, HLC_2 ($\neq HLC_1$) will be required to find the concentrations of VOCs in the cement paste sample at x = 0 and L which will later be used for calculating D_e. Nonetheless, interesting point is since the solutions in the source and sampling

bottles are the same and the composition of the pore solution within the paste sample is considered to be homogenous, converting both of the concentrations in the source and sampling bottles to the concentrations of VOCs in the paste sample at its both ends (x = 0 and L) will not change the effective diffusion coefficient calculated. As such, as the concentration of VOCs in the source bottle solution is known (1790 mg/L and 206 mg/L, for benzene and PCE, respectively), and the concentration of VOCs in the sampling bottle solution is measured during diffusion test, calculation of D_e is performed using these values and there is no need to measure and use HLC_2.

Figure B1 illustrates a schematic illustration of VOCs vapor diffusion through saturated cement paste samples. In addition, Equations B1 to B6 show the application of Henry's law constant to calculate the concentrations of VOCs in the sample at x = 0 and L.

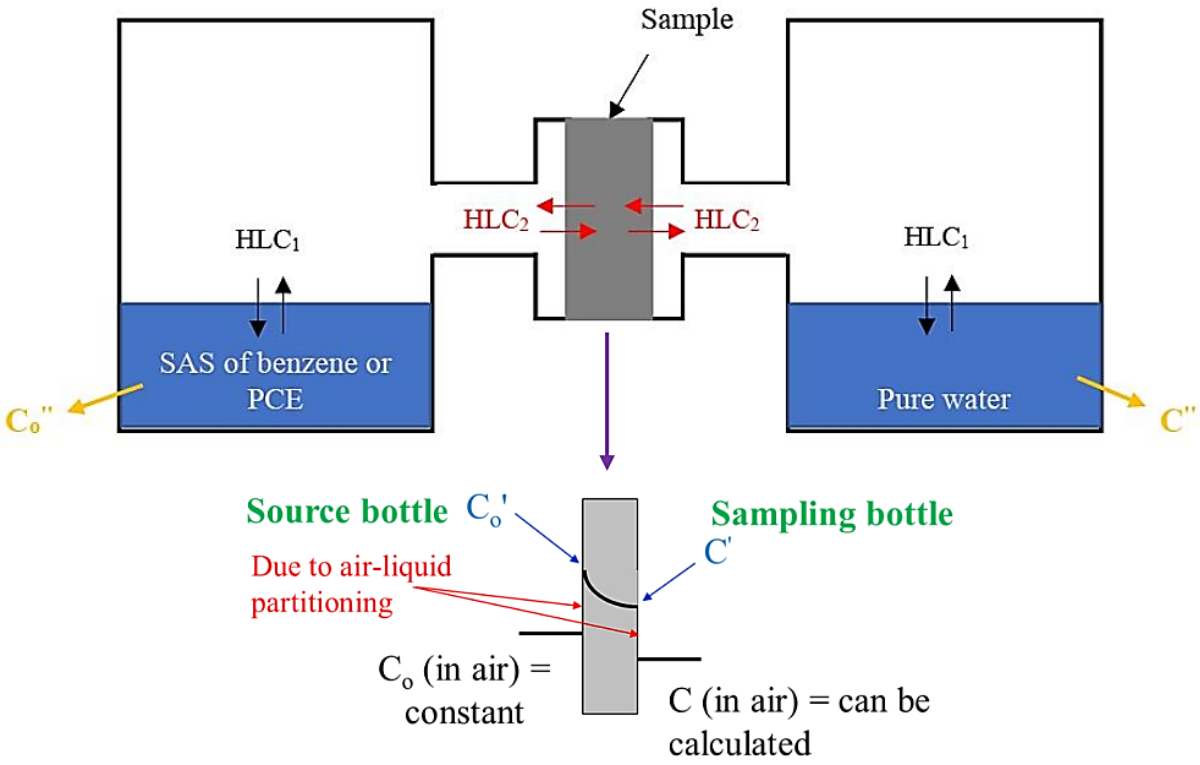

Figure B1 Schematic plot of VOCs vapor diffusion test setup designed for quantifying the effective diffusion coefficient of saturated cement paste (SAS: Saturated Aqueous Solution).

For the source bottle we have:

$$C_o''\ (known) \times\ HLC_1 = C_o \quad \text{(B1)}$$

$$C_o' = \frac{C_o}{HLC_2} \quad \text{(B2)}$$

where C_o'', C_o, and C_o' are VOCs concentrations in the source bottle solution, air in the source bottle, and the cement paste sample at x = 0, respectively. Now, combining Equations B1 and B2 will give:

$$C_o' = C_o'' \times \frac{HLC_1}{HLC_2} \quad \text{(B3)}$$

The same relationships can be written for the sampling bottle:

$$C''\ (measured) \times\ HLC_1 = C \quad \text{(B4)}$$

$$C' = \frac{C}{HLC_2} \quad \text{(B5)}$$

where C", C, and C' are VOCs concentrations in the sampling bottle solution, air in the sampling bottle, and the cement paste sample at x = L, respectively. Now, combining Equations B4 and B5 will result in:

$$C' = C'' \times \frac{HLC_1}{HLC_2} \quad \text{(B6)}$$

In the case of VOCs liquid diffusion (Figure B2), as in both source and sampling bottles the simulated pore solution is used, the concentration of VOCs of interest in the source bottle is different from that in pure water due to ionic strength of the pore solution. As such, solubility of benzene and PCE in each of three simulated pore solutions (C_o) is required to be measured and used in the calculation of D_e. In addition, C is measured for the sampling bottle over time during the diffusion test. In this case, C_o and C will directly be employed in the calculation of the effective diffusion coefficient.

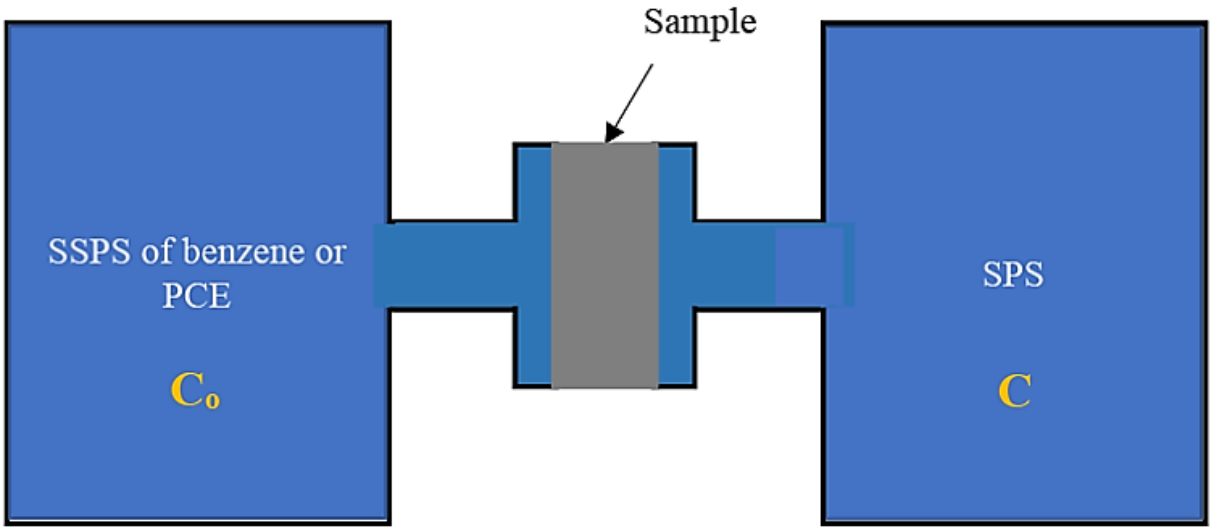

Figure B2 Schematic plot of liquid diffusion of VOCs test setup (SSPS: Saturated Simulated Pore Solution and SPS: Simulated Pore Solution).

References

[1] R. Sander. Compilation of Henry's law constants (version 4.0) for water as solvent. *Atmospheric Chemistry and Physics*, 2015. 15:4399–4981.

[2] J. Staudinger, and P.V. Roberts. A critical compilation of Henry's law constant temperature dependence relations for organic compounds in dilute aqueous solutions. *Chemosphere*, 2001. 44:561–576.

Appendix C

Calculation of Tortuosity

To calculate the tortuosity based on electrical method, Equation C1 was adopted. According to Equation C1, to obtain the tortuosity, the values of total permeable porosity (φ), ρ_s (the resistivity of the cement paste) and ρ_o (the resistivity of the cement paste pore solution) need to be measured.

$$\tau = \sqrt{\frac{\rho_s \times \varphi}{\rho_o}} \tag{C1}$$

To quantify the resistivity of the cement paste samples, Wenner probe array was employed and measurements were performed on cylindrical specimens of 50×150 mm according to the method discussed in AASHTO TP 119-15 [1]. Note that since the cement paste samples were sealed cured for 21-24 months and considering the fact that the cement particles have shown very high degree of hydration, chemical shrinkage voids existing in the microstructure are empty. Thus, the paste samples are not fully saturated as required for the electrical resistivity measurements. Hence, after demolding the samples, they were placed in a container fully filled with their simulated pore solutions to have them saturated. Note that the application of cement paste's simulated pore solution is due to avoiding migration of ions outwards (leaching) especially alkalis already exiting in the pore solution or can be later dissolved in the solution penetrating the pore structure during saturation. In addition, using this method, the need for directly measuring the pore solution resistivity would be eliminated [2]; however, it is not the case in our experiments as the samples are almost dry due to the high degree of hydration of cement particles.

Simulated pore solution for each w/c was prepared using the NIST model [3]. Input to the model include the samples' DOH, their curing method (sealed herein), and the total alkalis content of the cement (Na_2O and K_2O as 0.35% and 0.77%, respectively, by the mass of cement in this study).

Thermogravimetry was carried out at a rate of 10 ^{o}/min up to 1000 ^{o}C in nitrogen atmosphere on cement paste samples (two replicates at each w/c) to quantify the degree of hydration (DOH) of cement particles at the age of 21- or 24-months using Equation C2.

$$DOH = \frac{w_b}{w_{b,\infty}} \times 100 \quad \text{(C2)}$$

where w_b and $w_{b,\infty}$ are chemically bound water (g/g of ignited weight) at the age of interest and the ultimate chemically bound water corresponding to full hydration of cement particles regarded as 0.23 g per 1 g of cement, respectively [4]. According to the thermogravimetric analysis, DOH of cement pastes used in the third part of the study was determined as 80% and 91% for w/c of 0.30 and 0.40, respectively.

NIST model only gives the composition of the ions dominating the pore solution: Na^+, K^+, OH^-. To avoid leaching of calcium hydroxide from cement paste samples during the saturation process for electrical measurements, the calculated concentrations of Na^+, K^+, OH^- were added to saturated calcium hydroxide solution. Thus, the ionic compositions of the simulated pore solutions utilized in the saturation process of cement paste samples employed in electrical resistivity measurements are shown in Table C1 (the data are for the third part of the study). To prepare the simulated pore solutions, ASTM type II water and reagent grade of NaOH, KOH, and $Ca(OH)_2$ were used. The samples were allowed to be in the containers for 4 weeks to ensure complete sample

saturation and solution exchange take place. Afterwards, the samples were removed from the container and surface dried with a wet towel and tested according to AASHTO TP 119-15 [1].

Table C1 Ionic compositions of the simulated pore solutions employed in the saturation of cement paste samples during electrical resistivity measurements (for the third part of this work).

w/c	DOH (%)	Na^+ (M)	K^+ (M)	Ca^{2+} (M)	OH^- (M)	Ionic strength (M)
0.3	80	0.73	1.06	0.02	1.83	1.85
0.4	91	0.44	0.64	0.02	1.12	1.14

To calculate the resistivity of the cement paste pore solutions, a method developed by Snyder et al. [5] was followed. In this regard, electrical resistivity of the pore solution (ρ_o) can be obtained through Equation C3.

$$\rho_o = \frac{1}{\sum_i z_i \lambda_i c_i} \quad \text{(C3)}$$

where z_i (-) is the valence, λ_i is the equivalent conductivity (cm^2 S/mol), and c_i is the concentration (M) of ionic species i in the pore solution. Note that c_i is listed in Table C1 for various ions existing in the simulated pore solutions.

To compute λ_i for each ionic species, Equation C4 is used. λ_i^o is the equivalent conductivity of an ionic species at infinite dilution and is only a function of temperature. Table C2 presents the values of λ_i^o for various ionic species of interest at 25 ^oC.

$$\lambda_i = \frac{\lambda_i^{\,o}}{1 + G_i {I_M}^{0.5}} \quad \text{(C4)}$$

where G_i ($M^{-0.5}$) is an empirical coefficient for the electrical conductivity of solutions at various concentrations whose values are provided in Table C2 for different ions in the simulated pore solutions. Also, I_M is the effective molar ionic strength of the simulated pore solution and can be

calculated by employing Equation C5. The values of the ionic strength of the simulated pore solutions are provided in Table C1.

Table C2 Equivalent conductivity at infinite solution (λ_i^o) and conductivity coefficients (G_i) of the ionic species in the simulated pore solutions at 25 ^oC.

Ionic species	λ_i^o (cm^2 S/mol)	G_i ($M^{-0.5}$)
Na^+	50.1	0.733
K^+	73.5	0.548
Ca^+	29.5	0.771
OH^-	198.0	0.353

$$I_M = \frac{1}{2}\sum_{i=1}^{n} c_i {z_i}^2 \quad \text{(C5)}$$

References

[1] American Association of State and Highway Transportation Officials. *AASHTO TP119 Standard Method of Test for Electrical Resistivity of a Concrete Cylinder Tested in a Uniaxial Resistance Test*, 2015.

[2] J. Tanesi, L. Montanari, and A. Ardani. *Formation Factor Demystified and Its Relationship to Durability*, Washington, DC: Federal Highway Administration, 2019.

[3] National Institute of Science and Technology, *Estimation of Pore Solution Conductivity*, NIST Engineering Laboratory/Materials and Structural Systems Division, Gaithersburg, MD, 2017.

[4] I. Pane, and W. Hansen. Investigation of blended cement hydration by isothermal calorimetry and thermal analysis. *Cement and Concrete Research*, 2005. 35:1155– 1164.

[5] K.A. Snyder, X. Feng, B.D. Keen, and T.O. Mason. Estimating the electrical conductivity of cement paste pore solutions from OH^-, K^+ and Na^+ concentrations. *Cement and Concrete Research*, 2003. 33:793–798.